Università degli Studi di Torino
Doctoral School of the University of Torino
PhD Programme in Chemical and Materials Sciences XXXIV Cycle

Low cost organic and inorganic sorbents to fight water pollution

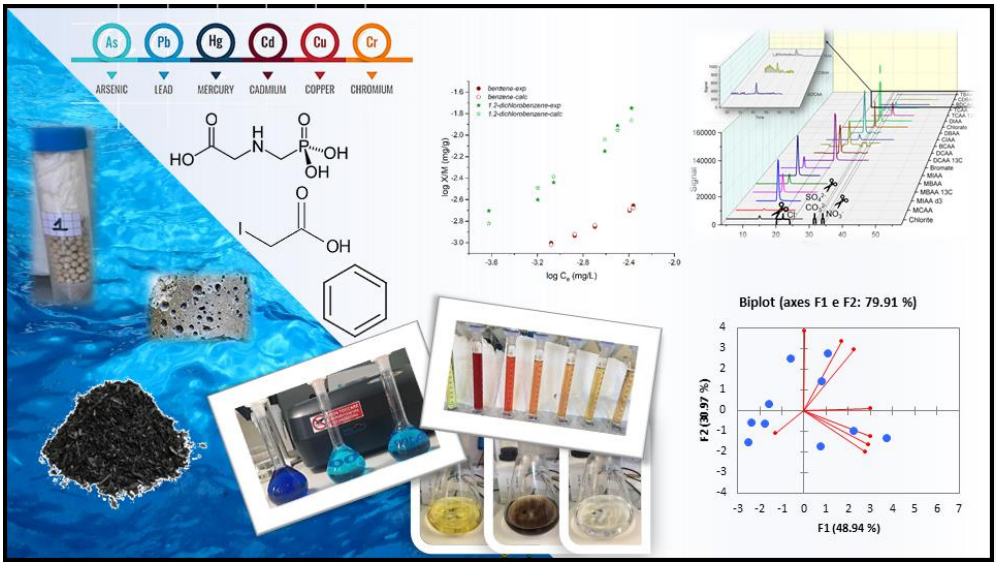

Michele Castiglioni

Supervisor:
Prof. Maria Concetta Bruzzoniti

Università degli Studi di Torino

Doctoral School of the University of Torino

PhD Programme in Chemical and Materials Sciences XXXIV cycle

Low cost organic and inorganic sorbents to fight water pollution

Candidate: **Michele Castiglioni**

Supervisor: Prof. **Maria Concetta Bruzzoniti**

Jury Members:

Prof. **Barbara Onida**
Politecnico di Torino
DISAT (Dipartimento di Scienze Applicate e Tecnologia)

Prof. **Antonio Proto**
Università degli Studi di Salerno
Dipartimento di Chimica e Biologia "Adolfo Zambelli"/DCB

Prof. **Ornella Abollino**
Università degli Studi di Torino
Dipartimento di Scienza e Tecnologia del farmaco

Head of the Doctoral School: Prof. Alberto Rizzuti
PhD Programme Coordinator: Prof. Bartolomeo Civalleri

Torino, 01/12/2021

Summary

1. General Introduction

A recent report from UNESCO states that major problems that humanity is facing in the twenty-first century are related to water quantity and to water quality issues [1]. Indeed, the removal of water contaminants is a demanding but also expensive task [2]. In this regard, in the last decades, several techniques were developed trying to find the right equilibrium between purification efficiency, environmental sustainability and operational costs. Treatment options which are typically considered for the removal of emerging contaminants from drinking water as well as wastewater include adsorption, advanced oxidation processes (AOPs), nanofiltration (NF), and reverse osmosis (RO) membranes [3, 4]. Among them, adsorption techniques are widely used to remove specific classes of pollutants from waters, especially those that are not easily biodegradable such as dyes, organic compounds, pharmaceuticals, pesticides, herbicides. In addition, adsorption does not add undesirable by-products and has been found to be superior to other techniques for wastewater treatment in terms of simplicity of design and operation, and not selective towards pollutants [5]. Among the materials proposed as adsorbents, activated carbons (ACs) have been used for the removal of different types of emerging compounds but their use is sometimes restricted due to high cost, both in term of economic and environmental indicators. Furthermore, even if ACs, when exhausted, can be regenerated for further use, the regeneration process provides a new product with a loss of carbon and a slightly lower adsorption capacity in comparison with the virgin-activated carbon.

These features have resulted in several attempts by various researchers to propose alternative low-cost adsorbents which may replace activated carbons in water pollution control through adsorption technologies, overcoming their

intrinsic economic disadvantages. Among the most promising candidates as alternative adsorbents biochars, as well of tunable silica based mesoporous materials and geopolymers are worth to be investigated and will be briefly introduced hereafter.

1.1 Biochars

Biochar (BC) is a porous, low cost carbon-residue derived from the thermal conversion of biomass wastes under limited oxygen (gasification) or anaerobic (pyrolysis) conditions, which can be used as soil amender [6], feed additive [7], and cosmetics [8].

In agricultural applications BC's high porosity enhances water and nutrients retention, thus promoting their prolonged release for plants, improves the structure of the soil and its mechanical properties [9]. Many studies have already shown a positive impact of the application of biochar on agricultural yields, reducing the need for water and fertilizers [10, 11].

The characteristics of biochar mainly depend on the feedstock and on the production process (i.e. pyrolysis and gasification). Pyrolysis is a process of thermal degradation of an organic material, made in the total absence of the oxidizing agent (oxygen). The characteristics of the final solid product and its yields depend on the operating conditions under which the pyrolysis is carried out, in particular temperature, exposure time and on the type of pyrolyzed material. Gasification, on the other hand, is a thermochemical conversion process in which a carbonaceous material is partially oxidized at a high temperature [12]. Unlike pyrolysis, which takes place in the complete absence of oxygen and requires an external source of heat to reach the operating temperature, gasification involves the use of oxygen (or air) in order to generate the heat necessary for endothermic devolatilization processes of biomass through partial combustion. The gasification process is performed at

temperatures greater than or equal to 800 °C with plant residence times ranging from seconds to hours. The biochar obtained has higher specific surface area (SSA) and porosity than that obtained from the biochar produced by pyrolysis.

As far as Italy is concerned, the use of BC is currently regulated only for agriculture (Legislative Decree n.75, April 29th, 2010, and subsequent amendments and additions), which defines both the characteristics for the classification and the marketing of soil improvers and the characteristics that biochar must possess to be used as a fertilizer.

However, recently, biochar has been also studied as adsorbent for the removal of selected classes of pollutants and emerging contaminants (e.g. haloacetic acids, VOC, plasticizers, pesticides and herbicides) from waters within the potabilization processes [13, 14]. In some instances, sorption and binding affinities of BC towards contaminants were reported comparable or even stronger than commercial AC [15]. Moreover, surface binding affinities can be tuned through biochar production conditions, with benefits in the overall removal process.

1.2 Amorphous porous silica-based materials

Silica-based materials are inorganic solids characterized by both high specific surface areas (200–1500 m^2/g) and a three-dimensional structure made of highly open spaces interconnected to each other via SiO_4 tetrahedra. Their physicochemical characterization gives rise to highly porous structures (up to 1 cm^3/g). Most of them can be easily produced using sol–gel processing, by hydrolysis of silicon alkoxide precursors (e.g., tetramethyoxysilane or tetraethoxysilane) and catalytic polycondensation to produce a macromolecular network of siloxane bonds. The structure of evolving silicates is a consequence of the following typical steps: polymerization, aging, drying,

and heating. An accurate tuning of the synthesis parameters allows to control the micro and mesostructure of the final materials. For example, porosity control can be achieved by the surfactant template route, originating ordered mesoporous materials that possess large uniform pore sizes (1.5–10 nm) and highly ordered nanochannels, and large surface areas (>1000 m^2/g) [16]. The chemical reactivity of silicas is essentially governed by silica surface properties, especially via the weakly acid silanol groups. However, the synthesis of organic-inorganic hybrid materials by the functionalization of materials surface leads to advanced properties that are often difficult to achieve either from totally inorganic or from totally organic materials. Functionalization could be obtained by impregnation of organic or organometallic species within silica matrices, whereas stronger immobilization (organic component strongly attached to the siloxane network via covalent bonds) is usually achieved via co-condensation of alkoxysilane and organosilane reagents. A synergy between organic chemistry and the chemistry of ceramic materials has thus led to the development of numerous novel mesoporous organic-inorganic hybrid materials with controlled characteristics and tailor-made properties.

In Figure 1.1 a schematic pathway for preparing surfactant-templated mesoporous organic-inorganic hybrid materials is represented, illustrating both the formation of the mesoporous silica (A) and its functionalization (B).

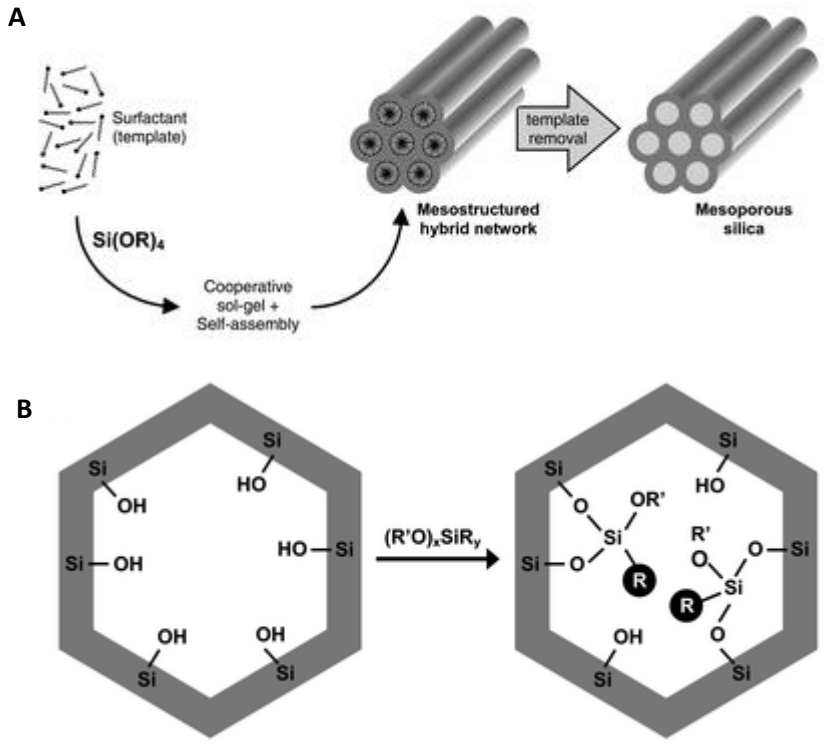

Figure 1.1. A) Schematic pathway for preparing surfactant-templated mesoporous silicas, illustrating a formation mechanism based on a cooperative process. B) post-synthesis grafting strategy applied to produce organically functionalized mesoporous silica

Functionalized silica-based materials are attractive because they combine both the properties of a rigid three-dimensional silica network with the peculiar chemical reactivity of the organic components. Thanks to the versatility of the inorganic chemistry processes (i.e., sol–gel), a wide range of organically-modified silica-based materials have been prepared. An important breakthrough in this field is the use of templating techniques to build regular mesoporous silica architectures on organic templates; these ordered solids can be also designed in the form of organic-inorganic nanocomposites, once functionalized with a large number of suitable

organosilane reagents. If compared to their non-ordered homologues, these mesostructured porous solids offer several advantages, such as:

- good accessibility to active centers (functional groups are likely to be accessible to external reagents) due to highly ordered nanochannels of uniform pore size [17];
- high number of functional groups that can be attached to the (mostly internal) surface of mesoporous silica, as a consequence of very large surface areas [18];
- high mass transport rates inside the porous structure due to the regular spatial arrangement of mesoporous channels of monodisperse dimensions [19];
- good mechanical and hydrothermal stabilities (which however are strongly dependent on mesostructure types and post-synthesis treatments) [19].

Due to their highly organized porosity, high surface area, high pore volume, tailorable pore size, wall thickness, chemical nature and morphology the mesoporous silica are attractive materials for applications in catalysis, adsorption, separation, sensing, drug delivering devices and nanotechnology. Among the above-mentioned applications, the removal of target compounds from water via adsorption has been focused on this work. Indeed, high removal capacities due to large active surface areas and/or high contents of accessible functional groups, and fast uptake processes could be expected, because of rapid mass transport rates in the mesoporous materials. These aspects might be improved by hierarchically organized structures in which (i) the mesopores provide a high level of reactivity (large capacity) through the high specific surface area and (ii) the macropores channels will ensure a fast diffusion. The mechanical stability and non-swelling properties would also enable the porous adsorbents to sustain water flow for extended periods of time. On the other hand, the selectivity of removal of target pollutants can

be tuned by an appropriate functionalization. In this regards, it should be emphasized that the affinity of the organo-functional groups towards target species should be as high as possible to reduce residual pollutant content below the acceptable threshold values defined by existing regulations.
However, the application of porous materials as adsorbents in waters is not always cheap, especially because of the use of rather expensive sacrificial templates (surfactants, block copolymers). This constitutes a real restriction in a wide use of such high-tech adsorbents.
In addition to environmental applications, specifically tuned mesoporous materials could play fundamental roles also in analytical procedures, in order to selectively remove and/or preconcentrate target compounds. In this regard, in the appendix of this thesis, the application of a specifically modified mesoporous silica material, SBA-15, in the removal of sugars interfering in the analysis of micropollutants in food matrices is reported.

1.3 Geopolymers and their application in the removal of glyphosate

Geopolymers (GPs) are aluminosilicate-based materials, defined as polysialates, an abbreviation for silico-oxoaluminates. They are inorganic, covalently bound macromolecules, characterized by -Si-O-Al-O- chains, with Si^{4+} and Al^{3+} coordinated with 4 atoms of oxygen. The empirical formula of geopolymers, is reported below:

$$M_n\{-(SiO_2)_2 - AlO_2\}_n * {}_w H_2O$$

where M is a cation such as K^+, Na^+, or Ca^{2+}; n is the degree of polycondensation and z, silicate monomer, could be 1, 2, or 3 [20].
The silicon/aluminum tetrahedral disposition determines their main characteristics and the final structure [21] (Figure 1.2).

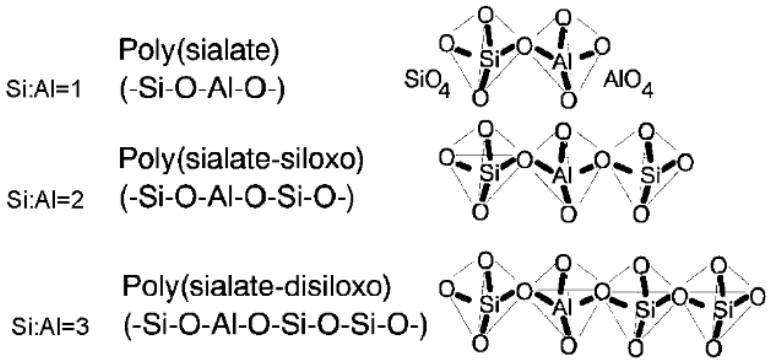

Figure 1.2 - Different structures for geopolymer obtained with one, two or three aluminum atoms

Geopolymers are obtained from the chemical reaction of alumino-silicate oxides with sodium silicate solutions, in an activating, highly alkaline environment (usually NaOH, KOH or $Ca(OH)_2$) [22-24].

The Glukhovsky model divides the synthesis process into three main stages: (a) destruction-coagulation; (b) coagulation-condensation; (c) condensation-crystallization [25] (Figure 1.3).

The dissolution of the solid aluminosilicate occurs by alkaline hydrolysis, thus producing aluminates and silicates; it is important to observe how the hydrolysis of Al and Si occurs preferably on the aluminosilicate surface.

Once released, aluminates and silicates are incorporated into the aqueous phase, which may already contain silicate present in the activating solution, creating a supersaturated aluminosilicate solution. This leads to the formation of a gel, as the oligomers in the aqueous phase agglomerate in large networks by condensation, releasing the water that has been previously used during dissolution. This type of gel structure is commonly called biphasic since the aluminium silicate binder and the water generated two separated phases [26, 27].

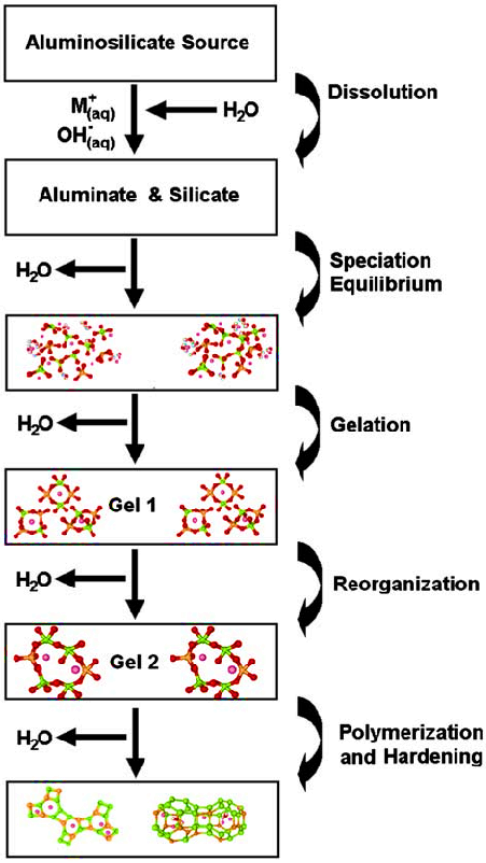

Figure 1.3 - Glukhovsky scheme for geopolymer synthesis

After gelation the system continues to rearrange and reorganize its structure, increasing the connectivity of the gel network, finally resulting in the three-dimensional aluminosilicate network.

As previously described, the synthesis reaction is a complex multi-stage process, and, depending to the reagents applied in each step, GPs with specific properties could be obtained. As an example, in Figure 1.4 a typical reaction scheme to obtain an anion exchange geopolymer is presented. Indeed, the reaction rate and the chemical composition of the final reaction products is strongly affected by several factors, such as physicochemical properties of both the raw materials (i.e. granulometry) and of the activating

solution (i.e. water content or the presence of soluble silicates) [28]. Moreover, the choice of the cation strongly influences the final mechanical properties of the geopolymer [29, 30].

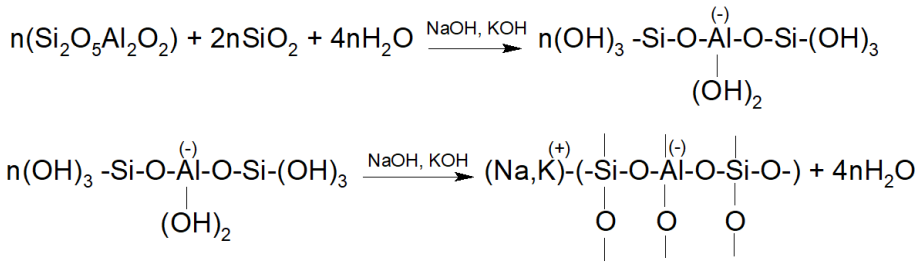

Figure 1.4 - Geopolimerization process for the production of Na, K exchanger geopolymers

In this regards, geopolymers are materials with many excellent properties such as high mechanical strength, resistance to low and high temperatures, resistance to aggressive environments or flame resistance [31]. These properties entitle further investigations on GPs as adsorbent media.

1.4 Aim of the work

Based on the above-mentioned assumptions, the aim of this PhD project was the development, the characterization and the application of new low-cost materials for the removal of pollutants from water. In more detail, biochars, mesoporous silica-based materials and geopolymers are prepared to specifically interact with selective pollutant classes, to drive the effective removal. The above-mentioned materials are tested on target pollutants poorly and/or variably removed by traditional water treatments, testing both ionic and ionizable species, organic and inorganic compounds, with different polarity and molecular weight. If not available, the analytical methods for the determination of the target analytes are also optimized in parallel, in a strict synergy of environmental and analytical chemistry competences.

On these premises, the thesis presents a deep investigation on the use of biochar for water treatment purposes, investigating the physico-chemical and the adsorption characteristics of BCs, as well as their correlations, also from an economic viewpoint. Attention is focused on organic micropollutants of different hydrophilicity and ionic charge, comparing BC performance towards these compounds to that of currently available technological solutions.

As regards the investigation of silica-based materials as adsorbent for water remediation, ordered mesoporous silica of the SBA-15 family functionalized with primary and secondary amino groups is studied for the abatement of the biochemical oxygen demand (BOD_5) in wastewaters derived from food and beverage industry.

Within this thesis geopolymers of tuned composition, even obtained through a 3D printer, are proposed for the removal of metals and herbicides worldwide used (i.e. glyphosate).

Finally, an "a priori" prevention of environmental contamination through suitable substrates capable of releasing controlled amounts of active substances (i.e. herbicides) as well as innovative transversal applications of previously developed materials (i.e. SBA-15 mesoporous silica) in analytical chemistry disciplines (i.e. sample pre-treatment) are also investigated and presented in the Appendix of this thesis.

1.5 References

1. UNESCO. 2021; Available from: https://en.unesco.org/themes/water-security/hydrology/water-scarcity-and-quality.
2. Ismail, W.N.W. and S.U. Mokhtar, *Various Methods for Removal, Treatment, and Detection of Emerging Water Contaminants.* Emerging Contaminants, 2020.
3. Bolong, N., et al., *A review of the effects of emerging contaminants in wastewater and options for their removal.* Desalination, 2009. **239**(1-3): p. 229-246.
4. Rossner, A., S.A. Snyder, and D.R. Knappe, *Removal of emerging contaminants of concern by alternative adsorbents.* Water research, 2009. **43**(15): p. 3787-3796.
5. Tong, D.S., et al., *Adsorption of acid red G dye on octadecyl trimethylammonium montmorillonite.* Applied Clay Science, 2010. **50**(3): p. 427-431.
6. Singh, B., B.P. Singh, and A.L. Cowie, *Characterisation and evaluation of biochars for their application as a soil amendment.* Soil Research, 2010. **48**(7): p. 516-525.
7. McHenry, M.P., *Carbon-based stock feed additives: a research methodology that explores ecologically delivered C biosequestration, alongside live weights, feed use efficiency, soil nutrient retention, and perennial fodder plantations.* Journal of the Science of Food and Agriculture, 2010. **90**(2): p. 183-187.
8. Schmidt, H.-P. and K. Wilson, *55 uses of biochar.* Ithaka Journal, 2012. **1**: p. 286-289.
9. Chan, K.Y. and Z. Xu, *Biochar: nutrient properties and their enhancement*, in *Biochar for environmental management*. 2012, Routledge. p. 99-116.
10. Lehmann, J. and M. Rondon, *Bio-char soil management on highly weathered soils in the humid tropics.* Biological approaches to sustainable soil systems, 2006. **113**(517): p. e530.
11. Vaccari, F., et al., *Biochar as a strategy to sequester carbon and increase yield in durum wheat.* European journal of agronomy, 2011. **34**(4): p. 231-238.
12. Basu, P., *Biomass gasification and pyrolysis: practical design and theory*. 2010: Academic press.
13. Inyang, M. and E. Dickenson, *The potential role of biochar in the removal of organic and microbial contaminants from potable and reuse water: a review.* Chemosphere, 2015. **134**: p. 232-240.
14. Joseph, S., et al., *Developing a biochar classification and test methods.* Biochar for environmental management: science and technology, 2009. **1**: p. 107-126.
15. Ahmad, M., et al., *Biochar as a sorbent for contaminant management in soil and water: A review.* Chemosphere, 2014. **99**: p. 19-33.
16. Kresge, C., et al., *Ordered mesoporous molecular sieves synthesized by a liquid-crystal template mechanism.* nature, 1992. **359**(6397): p. 710-712.
17. Feng, X., et al., *Functionalized monolayers on ordered mesoporous supports.* Science, 1997. **276**(5314): p. 923-926.
18. Olkhovyk, O. and M. Jaroniec, *Ordered mesoporous silicas with 2, 5-dimercapto-1, 3, 4-thiadiazole ligand: High capacity adsorbents for mercury ions.* Adsorption, 2005. **11**(3-4): p. 205-214.
19. Bibby, A. and L. Mercier, *Mercury (II) ion adsorption behavior in thiol-functionalized mesoporous silica microspheres.* Chemistry of materials, 2002. **14**(4): p. 1591-1597.
20. Davidovits, J., *Chemistry and applications.* Saint-Quentin: Institute Geopolymer, 2008.

21. Davidovits, J. *Properties of geopolymer cements*. in *First international conference on alkaline cements and concretes*. 1994. Kiev State Technical University, Ukraine: Scientific Research Institute on ….
22. Škvára, F., *Alkali activated materials or geopolymers.* Ceramics-Silikáty, 2007. **51**(3): p. 173-177.
23. Xu, H. and J. Van Deventer, *The geopolymerisation of alumino-silicate minerals.* International journal of mineral processing, 2000. **59**(3): p. 247-266.
24. Kumar, S., F. Kristály, and G. Mucsi, *Geopolymerisation behaviour of size fractioned fly ash.* Advanced Powder Technology, 2015. **26**(1): p. 24-30.
25. VD, G., *Soil silicater.* Gosstroyizdat, Kiev, 1959.
26. Aiello, R., et al., *Influence of cations on the physicochemical and structural properties of aluminosilicate gel precursors. Part 1. Chemical and thermal properties.* Zeolites, 1991. **11**(8): p. 767-775.
27. Ivanova, I., et al., *Influence of cations on the physicochemical and structural properties of aluminosilicate gel precursors: II. Multinuclear magnetic resonance characterization.* Microporous Materials, 1994. **3**(3): p. 245-257.
28. Xu, H. and J.S. Van Deventer, *Effect of source materials on geopolymerization.* Industrial & engineering chemistry research, 2003. **42**(8): p. 1698-1706.
29. Duxson, P., et al., *Understanding the relationship between geopolymer composition, microstructure and mechanical properties.* Colloids and Surfaces A: Physicochemical and Engineering Aspects, 2005. **269**(1-3): p. 47-58.
30. Rowles, M. and B. O'connor, *Chemical optimisation of the compressive strength of aluminosilicate geopolymers synthesised by sodium silicate activation of metakaolinite.* Journal of materials chemistry, 2003. **13**(5): p. 1161-1165.
31. Duxson, P., et al., *Geopolymer technology: the current state of the art.* Journal of materials science, 2007. **42**(9): p. 2917-2933.

2. Biochars as Tools for Water Treatment

M. Castiglioni, L. Rivoira, I. Ingrando, M. Del Bubba and M.C. Bruzzoniti
Characterization Techniques as Supporting Tools for the Interpretation of Biochar Adsorption Efficiency in Water Treatment: A Critical Review.
(2021) Molecules, 26(16), 5063.

M. Castiglioni, L. Rivoira, I. Ingrando, L. Meucci, R. Binetti, M. Fungi, A. El-Ghadraouic, Z. Bakari, M. Del Bubba, M. C. Bruzzoniti,
Biochars intended for water filtration: a comparative study with activated carbons of their physicochemical properties and removal efficiency towards neutral and anionic organic pollutants.
Chemosphere (2022), 288,132538.

2.1 Introduction

Biochar (BC) is a low-cost solid by-product of thermal conversion of feedstocks of different nature, such as agricultural [1], wood residues [2], manure [3] and sludge [4].

The thermal conversion procedures thus far available to obtain biochar can be grouped into the following technologies, according to the process parameters: fast [5] and slow pyrolysis [6], gasification [7], hydrothermal [8] and flash carbonization [9]. Biochar production mainly relays on the first two technologies. Valuable information for biochars produced by pyro-gasification processes is provided by related literature [10]. It is useful to remind that each of them involves temperature range, heating rate, pressure and residence time different one to the other. Accordingly, these technologies maximize different ratios and characteristics of the final products, i.e. gas (biogas) solid (char) and liquid (tar, oil). More in detail, gasification (700-1500 °C temperature range with residence time from seconds to minutes) methods mainly converts biomass to biogas, fast pyrolysis (400-600 °C temperature range with residence time of seconds) maximizes bio-oil formation, whereas slow pyrolysis (350-800 °C temperature range with residence time from seconds to hours) generally favours the formation of biochar [11].

Over the years, biochar has attracted significant attention in many fields. Indeed, it shows great potential to reduce the environment impact, address

the climate change issue (through CO_2 storage) [12], and establish a circular economy model [13, 14] in many sectors, such as for example agriculture, where it could be used to promote carbon, phosphorus, and nitrogen cycles in soils [15]. The first applications of biochar were aimed at agricultural purposes [16], since biochar addition improves soil properties. As for Italy, the use of biochar as soil amendment as well as technical requirements for this use are disciplined by the DL 75/2010 and further modifications. The *"Standardized Product Definition and Product Testing Guidelines for Biochar That Is Used in Soil"* was recently released by International Biochar Initiative (IBI) to indicate the characteristics that a biochar intended for sale must possess for safe use.

In the last years, studies on biochar were extended also to water purification issues due to the adsorption properties exhibited by this material and to its environmentally low impacts [17].This new interest towards biochar leaded to a progressive increase of publications in this field. The first two reviews on application of biochar for water purification, dated 2014 [11, 18], followed by more recently publications [19, 20], have the merit to present the sorption of organic/inorganic contaminants grouped by classes and to elucidate possible adsorption mechanisms based on the surface chemistry of biochars. The performance of biochar towards selected classes of compounds, mainly nutrients[21], antibiotics[22], metals [23], was the main theme of the reviews subsequently published on water purification by biochar.

The general idea to exploit biochar for water treatment as a potential surrogate of activated carbon (AC), the commercial adsorbent most widely used in the refining tertiary stage of treatment water technologies, has pushed the need of improving sorption characteristics of biochar. These efforts are clearly highlighted by literature and reviews that analyse strategies of surface modification of biochar [24] or production of biochar with the addition of nanoscale-metals [25] to the biomass before thermal conversion.

However, even if BCs are proposed as ACs replacement, only a limited number of studies already published on this topic compare the characterization of BCs with those of a commercial activated carbon, thus making extremely difficult to evidence differences between both substrates.
Differently from what established for the use of biochars in agricultural application, no documents have yet been published by international organizations on biochar characterization for other applications, including water purification. Probably for this reason, despite most of the authors studying the removal of compounds by biochars agree that physicochemical and performance characterization is of a paramount importance to better understand pollutants-BC interactions [26, 27], a lack of homogenous data is observed in the scientific literature.
At the light of the above-mentioned premises, it becomes important to compare biochar and activated carbon as adsorbents for organic micropollutants in water purification. In section 2.2, a deep discussion on the most used techniques for biochars characterization, as well as the adsorption capacities of unmodified BCs and ACs towards the organic compounds more investigated in the literature are presented. In addition, in section 2.3 the application of selected biochars for the removal of emerging contaminants from water is investigated.

2.2 Characterization techniques of biochars intended for the removal of organic contaminants in waters

When studied for water purification purposes, it seems reasonable to compare the adsorption performance and the physicochemical features of biochar with those of activated carbon which is by far most widely used, regulated adsorbent commercially available. Indeed, the overview of the literature currently available on biochar indicates that this is not the approach

followed by authors, as biochar is synthesized and tested per-se for the removal of selected single [28, 29] or mixture [30, 31] of compounds.
To better compare the capabilities of biochar in respect to activated carbon in water filtration, the characterization methods currently available for activated carbon and the ones mainly used for biochar will be hereafter described.

2.2.1 Activated carbon characterization

The characterization of activated carbon is necessary to identify the materials suitable for use in the tertiary treatments of potabilization or wastewater treatment plants
The characterization of activated carbons is obtained through two different main approaches which are based on the determination of (i) adsorption performance and (ii) physicochemical parameters. The first approach allows to determine structure-dependent indices estimated in respect to standardized compounds of proper molecular dimensions that are directly correlated to the adsorption capabilities of the activated carbon itself [32]. The second approach allows to get information about the main structural properties, i.e. morphology, porosity distribution, and about the nature of the chemical groups present in the surface.
Adsorption performance parameters (or performance indices) of activated carbons are strictly regulated when such materials must be applied in drinking water purification processes. Many official documents, which will be here briefly reviewed, indicate the requirements that active carbons should meet when used for water filtration, together with the methods to evaluate such performance indices. Most of these documents were released by the American Society for Testing and Materials International (ASTM), the American Water Works Association (AWWA), the German Institute for Standardization (DIN) and by the International Organization for

Standardization (ISO). Thanks to the work of the European Council of Chemicals Manufacturers' Federation (CEFIC), many of these methods are collected in the so called "Test Methods for Activated Carbon" publication [33].

Experiments to be performed on activated carbons are divided into three groups: physical tests, adsorption tests and chemical/physicochemical tests. In the next part of this work, a brief description of the regulated parameters that need to be tested will be given, along with the documents in which each parameter is defined. These methods are collected in Table 2.1.

Table 2.1 Standard Methods for the characterization of activated carbon.

Test	Method	Reference
	Physical tests	
Bulk density	ASTM D2854, CEFIC	[33, 34]
Absolute density	CEFIC	[33]
Particle density	CEFIC	[33]
Particle size	ASTM D2862, CEFIC	[33, 35]
Pressure drop	CEFIC	[33]
Mechanical strength	ASTM D3802, AWWA B604, CEFIC	[33, 36, 37]
	Adsorption tests and indices	
Adsorption isotherm	ASTM: D3860-98, 5919-96, CEFIC	[33, 38, 39]
Iodine number	AWWA B600-16, EN 12915-1, ASTM D4607-14, CEFIC	[33, 40-42]
Phenol number	CEFIC	[33]
Methylene Blue number	CEFIC	[33]
Molasses number	EPA625171002A	[43]
Tannin number	AWWA B600	[41]
	Chemical tests	
Ashes, water soluble material, and water-	EN 12915-1	[40]

extractable substances (As, Cd, Cr, Hg, Ni, Pb, Sb, Se, CN-, fluoranthene, benzo(b)fluoranthene, benzo(k)fluoranthene, benzo(a)pyrene, benzo(g,h,i)perylene, indeno(1,2,3-cd)pyrene)		
pH	ASTM: D6851-02, D3838-05	[44, 45]

2.2.1.1 Physical tests

Through physical tests, apparent or bulk density, absolute and particle density, particle size, pressure drop, and mechanical strength are determined. Apparent or bulk density (expressed as kg/m^3 on dry basis) is defined as the mass of a unit volume of the sample in air, including both the pore system and the voids between particles. On the opposite, absolute density and particle density (called also He and Hg density, respectively) are defined as the mass of a unit volume of the solid carbon skeleton not accessible to He (for absolute density) or of the carbon particle (for particle density). Both parameters are expressed as g/mL. The above-mentioned density parameters are necessary to evaluate shape and size of activated carbon particles, as well as packing volume, bed porosity and void fraction [46, 47]. Methods to determine bulk density are described in ASTM standard [34], whereas methods to measure bulk density, absolute and particle density, particle size, pressure drop, and mechanical strength are collected by CEFIC standard [33]. Many authors agree that the monitoring of density parameters during the synthesis of activated carbons should be exploited to follow the thermal degradation of the raw precursor material [48, 49].

Particle size (expressed in mm) in activated carbons influences both the adsorption of target compounds and certain mechanical properties, i.e.

hydraulic conductivity and flow speed [50]. Official methods from ASTM [35] and CEFIC require a mechanical separation of particles through sieves. Worth mentioning that particle size, as well as surface morphology and porosity of the adsorbent surface [51], could be also evaluated by using physiochemical techniques, such as Scanning Electron Microscopy (SEM) and Transmission Electron Microscopy (TEM), as detailed in the following sections.

Besides particle size, additional characteristics such as pressure drop, resistance to flow and mechanical strength should be determined. The pressure drop of a gas flow over a packed bed gives information about both the resistance to flow of a gas through the carbon layer; the mechanical strength simulates the resistance to abrasion or friction under real condition [36, 37]. Both particle size and mechanical strength parameters are determined for granular active carbons which are defined by CEFIC as those having 90% of particles larger than 0.18 mm as determined by the above-mentioned particle size test.

2.2.1.2 Adsorption tests

While physical tests are necessary to design drinking water filters (e.g. open gravity types), adsorption tests are needed to evaluate the removal performances of activated carbons. These approaches usually combine the evaluation of the adsorption isotherm of a given adsorbate-adsorbent system and the fitting to a theoretical or empirical model of the adsorption process to estimate the adsorption characteristics of activated carbons. The Freundlich model is suggested by ASTM [38, 39] and CEFIC [33] to determine the adsorptive capacity of activated carbons. It can be expressed by the relation, $X/M=K_F \cdot C_f^{1/n}$, where X/M (mg/g) is the amount of the target pollutant removed per unit mass of carbon, C_f (mg/L) is the residual concentration of the pollutant after treatment and K_F $((mg/g)/(g/m^3)^{1/n})$ and

1/n (adimensional) are constants for a given adsorption system. The same equation is generally used in the linearized logarithmic form.

Adsorption performances of activated carbons are expressed through the determination of selected indices, namely iodine [33, 40, 41], phenol [33], methylene blue [33], molasses [43] and tannin [41] numbers. These parameters give information about the porous structure and the adsorption properties of the activated carbon towards target compounds having similar dimension with the above-mentioned probe molecules.

More in detail, iodine number is defined as the milligrams of iodine adsorbed from an aqueous solution by 1 g of activated carbon when the iodine concentration of the residual filtrate is 0.02 N. Procedures to evaluate this parameter have been proposed both by UNI [52] and by AWWA [37], differing only for the mathematical treatment of the results. In the UNI EN 12902 standard [52], in fact, iodine number is extrapolated from the linear regression model obtained plotting the mg of iodine adsorbed, by three different amounts of carbons, versus the residual iodine concentration, while in the AWWA B600-78 standard, the parameter is obtained introducing a tabulated correction factor, which depends on the residual iodine normality of the filtrate.

When comparing both protocols, the AWWA B600-78 standard is less time consuming, since by one experiment the iodine number could be obtained. However, the correction factor is derived according to the residual concentrations typically obtained by activated carbons. This implies that, as a general consideration, the method cannot be applied to materials with adsorbing capacities very different from those of activated carbon since the residual iodine concentrations would be outside the range of those specified by AWWA. UNI EN 12902, on the other hand, does not require any mathematical treatment and has the advantage of being applicable to a wider range of adsorbent materials of different capacities. However, since UNI EN

12902 requires the determination of an adsorption isotherm, this approach is obviously more time consuming than that described by AWWA, as previously mentioned.

The phenol number is defined as the phenol adsorption for a singular weight unit of carbon when, after adsorption, phenol concentration in solution decreases from 10 to 1 mg/L.

Methylene blue index, which is defined as the methylene blue volume (in mL) of a 1.2 g/L solution adsorbed by a known amount of sorbent (0.1 g) within a prearranged contact time (5 min), was demonstrated to be directly correlated to the specific surface area (SSA) and micropore volume of the adsorbent [53]. Official procedures to evaluate the above-mentioned indices have been detailed by ASTM and Water Research Commission (WRC), respectively [54, 55].

Iodine and phenol indices are usually related to the presence of micropores (<2 nm) and therefore they are considered informative of the effectiveness in removing small-size organic water pollutants. On the other hand, methylene blue index is linked to the abundance of mesopores (2-50 nm) and thus is a useful indicator of adsorption capacities for medium-large sized organic pollutants [56].

Tannin number is defined as the concentration of activated carbon (mg/L) required to reduce the concentration of a standard tannic acid solution from 20 to 2 mg/l. Tannins, a mix of medium and large size molecules, can be adsorbed efficiently by the mesopores and macropores (>50 nm) of the activated carbons. Tannin values of different activated carbon substrates and pore volume of mesopores are linearly correlated [57], and carbons with low tannin number exhibit the highest quality of removing high-molecular-weight impurities.

Molasses number is a measure of the degree of decolorization of a standard molasses solution that has been diluted and standardized against

standardized activated carbon. The molasses number represents the potential pore volume available for larger adsorbing species.

Among the above-mentioned adsorption tests, the iodine index is the only one foreseen by the UNI EN 12915-1 standard for products used for the treatment of water intended for human consumption and for which a specific requirement is set (> 600 mg/g).

An additional adsorption test for activated carbons, also collected in CEFIC report, is the phenazone index. Since not directly linked to the removal of pollutants from waters, but to pharmaceutical purposes [58, 59], phenazone index will not be further detailed.

2.2.1.3 Chemical and physicochemical tests

Chemical tests are foreseen when activated carbon must be used for drinking water filtration in potabilization plants, as they are mainly aimed to assess purity criteria for adsorbents. As an example, according to the EN 12915-1 standard [60], ashes, water-soluble material, and water-extractable substances (As, Cd, Cr, Hg, Ni, Pb, Sb, Se, CN-, fluoranthene, benzo(b)fluoranthene, benzo(k)fluoranthene, benzo(a)pyrene, benzo(g,h,i)perylene, indeno(1,2,3-cd)pyrene) must be evaluated for activated carbons. These substances represent the most probable impurities that may be present in the adsorbent, as a result of both raw material composition [61] and thermal process conditions [62]. Limits are provided for the above-mentioned parameters. As far as water-extractable substances determination is concerned, extraction is performed in a solution containing sodium hydrogen carbonate, calcium chloride and magnesium sulphate [40, 52]. It is important to underline that the presence of other impurities not included in the standard should be notified to users, as defined by the same standard. Worth mentioning that the determination of the aforementioned polycyclic aromatic hydrocarbons (PAHs) and metal content in activated

carbon is foreseen by CEFIC procedure [33] under more drastic conditions, such as cyclohexane extraction and total oxidation, respectively.

Strictly related to operating procedures and start-up operations of the refining stage inside the plant is the pH value of solutions in contact with the adsorbent. The pH conditions strongly influence the duration of the washing procedures of the carbon before its full operability. Inorganic and chemically active groups on carbon surface are responsible for a possible modification of the pH, when the substrate is posed in contact with water. Among the procedures available for the determination of this parameter, the ASTM D6851-02 and D3838-05 standards [44, 45] consider the contact pH and the pH of a boiled water extract, respectively in a 1:10 w/v ratio.

In addition to the techniques presented above, for the characterization of activated carbons, the literature currently available uses other techniques and approaches with the aim of fully understanding surface and bulk chemistry and speculating on possible interactions with the target compounds. As an example, the evaluation of the pH of zero-point charge (PZC), the pH value at which the net charge density of the material is equal to zero, could be important to define the adsorption behaviour of the material towards pollutants of different charge at different pH conditions [63].

Additional information could be obtained also by Boehm's titration, by which the equivalent of surface acidic/basic functionalities (carboxyl, lactone, phenolic groups) per gram of carbon could be obtained [64]. This approach gives a deeper insight on surface chemistry.

Directly connected to the surface charge of the material, cationic exchange capacity (CEC) is defined as the total amount of exchangeable cations of a sorbent [65, 66]. Microscopy (both scanning and transmitting, SEM and TEM), nitrogen adsorption isotherms and Fourier transform infrared spectroscopy (FTIR) are usually applied in order to derive a topographical morphology of

the material, to define particle dimension and porous structure, as well as to study the surface functional groups and structure [67].

An additional characterization of activated carbons is based on the analysis of the elemental composition. From the amount of carbon, oxygen and hydrogen it is possible to get the Van Krevelen diagram, in which the O/C ratio is plotted against the H/C ratio [68]. The above-mentioned graph is used to classify carbons, and its feedstock [69], and to fully understand the evolution of carbon during the heating treatment, thus predicting specific properties of carbon adsorbents (degree of carbonization by H/C ratio, hydrophilicity by O/C ratio, polarity by (O+N)/C ratio) [70].

2.2.2 Biochar characterization

2.2.2.1 Chemical and physicochemical tests

Currently, no official method on the evaluation of performance and characteristics of biochars intended for water filtration has been published. In the absence of indications by regulatory organisms, official procedures previously presented for activated carbons (EN, CEFIC, AWWA standards, see Table 2.1) should be homogenously applied for testing the performances of biochars. This approach would ensure the coherence of the results presented in the literature and the straightforward comparison among the biochars produced and between biochar and activated carbon.

Studies dealing with the removal of contaminants from water using biochar show that biochar is synthesized from different types of feedstock and different thermal process conditions. The extent of adsorption of pollutants is generally correlated with certain properties of the biochar which are specifically measured to characterize the biochar produced.

Table 2.2 collects the main approaches and instrumental techniques used for the characterization of biochar, according to the literature of the last decade

concerning the removal of organic pollutants by biochar. The following are indicative, not exhaustive examples of the characterization of biochars tested for water filtration.

Many authors [71, 72] apply nitrogen adsorption isotherms to provide information about surface area, pore volume and average pore size. We have previously pointed out that the above-mentioned parameters are clearly correlated with the widely discussed adsorption indices for activated carbons, which actually are rarely determined for biochar. Nevertheless, to the best of our knowledge, few studies presented such correlation for biochar [56, 73], differently from what is done for activated carbon [32, 74, 75]. It is worth mentioning that recent literature is now measuring adsorption indices, i.e. iodine index as an indicator of the best adsorption performance of biochars obtained under different process conditions (e.g. heating rate). The iodine and methylene blue indices have been proposed as comparative indicators for the performance of activated carbons and biochars [76].

The physicochemical methods used for the characterization of biochar depend mainly on the objectives of the study in question. However, these methods are used to define the surface properties of biochars and to highlight possible adsorption mechanisms responsible for the biochar-pollutant affinity [71, 77]. Among these methods, FTIR, XPS and XRD are the most frequently applied to characterize surface chemistry.

FTIR spectroscopy is a widespread technique used to investigate the surface chemical functional groups (e.g., aliphatic or aromatic nature) in biochar [78]. Through the FTIR spectrum, vibration bands can be assigned to defined functional groups that allow to speculate on possible interaction mechanisms with the pollutants of interest [11]. Additional information gained from FTIR is the understanding of reactions occurred during thermal treatment steps [70, 79, 80]

XPS analysis provides information about the chemical composition and bonds on the biochar surface to a surface depth <10 nm and about the relative abundance of different species of certain elements on the surface, e.g. different C and N containing groups and bonds (C-C, C-H, C=O, -COOH, N-C, amino acid N, and ammonium-N) on the biochar surface [81, 82].

Structure and phase composition of biochars can be derived by XRD analysis. The information that is gained can be important for determining if successful preparation of modified biochar occurred [77] or to understand the evolution of the thermal process in respect to the starting biomass composition [83].

Van Krevelen plots previously discussed in the activated carbon section are extensively employed in biochar characterization to define biochar composition as a function of the thermal conditions used for biochar production [70, 95, 96].

Table 2.2. Main characterization methods employed for biochar, according to the recent literature.

Test	Ref biochar
Adsorption indices	
Iodine number	[56, 76, 84-86]
Methylene Blue number	[56, 76, 87]
Chemical tests	
Total PAHs	[88]
pH, ash	[56, 87]
Surface and functional groups characterization	
Nitrogen-adsorption isotherm	[30, 56, 71, 89, 90]
FTIR	[56, 87, 90-92]
SEM	[90, 92, 93]

XRD	[56, 90, 91, 93]
Zero point charge	[56, 91, 92, 94]
Boehm's titration	[87]
Cation exchange capacity	[87]
Elemental composition	
H/C, O/C, (O+N)/C (Van Krevelen plots)	[56, 93, 95, 96]
Kinetic and isotherm studies	[56, 97-100]

2.2.2.2 Adsorption tests

The careful study of the current literature provides strong indications that the assessment of the adsorption features of biochars is mainly performed *per-se*, and that the studies in which the adsorption performance of the biochars are simultaneously compared with that of activated carbon are extremely limited. This approach makes it less straightforward to understand the benefits or limitations of using biochar in place of activated carbon. In this regard, research on the use of biochar for water refining should be addressed *a-priori* by always including activated carbon for a direct comparison.

Materials intended for the removal of pollutants from waters are usually described in their retention performance through kinetics and adsorption isotherms [101].

Basically, the optimization of the contact time is essential for further adsorption studies, to ensure the presence of equilibrium conditions within the pollutant-adsorbent (biochar/activated carbon) systems. Additional information provided by kinetics studies is the identification of rate controlling step among (i) transport of the solute molecules from the aqueous phase to the surface of the solid (film or external diffusion); (ii) transfer of solutes from the surface to the intra-particle sites (intra-particle diffusion); (iii) and adsorption of solutes on the interior surfaces of the adsorbent [102]. Pseudo-

first order and pseudo-second order models are the ones mostly computed. However, less often some works thoroughly investigate adsorption performances of BCs through Elovich model [103] (predicting the mass and surface diffusion and the activation/deactivation energy of the system) or through Intra Particle Diffusion and Boyd models [104, 105] (determining the effect of internal and external diffusion on the adsorption mechanism).

Once the equilibrium conditions are identified, adsorption isotherm data are obtained to describe the type of interactions involved between adsorbates and adsorbents and to quantify the extent of the adsorption (i.e. the adsorbent capacity). Correlation of isotherm data by theoretical or empirical equations is useful for practical operation. In fact, a proper understanding and interpretation of adsorption isotherms is crucial for the overall improvement of adsorption mechanism pathways and effective design of adsorption system [106]. Because of its wide applicability, linear regression analysis is frequently used to fit experimental data and to assess adsorption performance in biochar related literature [107, 108]. Langmuir, Freundlich, Tempkin are the most applied models [97-99, 109-113], with few works investigating also Dubinin–Radushkevich [114] and Sips [115] models. Non-linear regression analysis [116], which has also been widely used by a number of researchers in the attempt to minimize the gap between predicted and experimental data, is also applied to biochar studies [117]. The description of the above-mentioned models is out of the scope of the thesis, since further information can be found elsewhere [118, 119].

A careful survey showed that recent publications about adsorption onto BCs dedicate much effort to the study of adsorption kinetics and isotherms; nevertheless, simultaneous studies on both BCs and ACs are only rarely considered for comparison [56, 99, 120], with a consequent lack of information.

2.2.2.3 Adsorption tests in dynamic bench- and pilot-scale conditions

Besides the knowledge of adsorption performances of BCs in batch conditions, the evaluation of kinetic and isotherm models in dynamic conditions by bench- and pilot-scale systems is of paramount importance to simulate real applications of BCs in filtering systems and to achieve Technology Readiness Levels (TRL) higher than an experimental proof of concept.

Despite such premises, only few studies evaluate the retention of pollutants from water matrices on unmodified BCs using small lab-scaled columns [121], and even fewer investigate the adsorption isotherms [122].

In dynamic testing conditions, kinetic models should be replaced by breakthrough curves, in which the profile of the effluent adsorptive concentration at the outlet of a fixed bed adsorber is measured. It should be noted that these curves can be considered as the last of the essential characterizations of an activated carbon, since they simulate the performance in an industrial application [123]. While it seems reasonable to adopt the same curves to evaluate the performances of BCs as adsorbent for aqueous solutions, most studies work at laboratory scale conditions [124]. This is most likely due to an as yet unripe biochar technology.

Considering pilot/pre-commercial scaled systems, in which higher volumes of water are treated using biochar packed columns, the calculation of adsorption performances is obtained only by transposition of isotherm models from batch tests to pilot scale conditions [121].

Finally, it is interesting to highlight a lack of adsorption performance studies in bench- or pilot-scaled conditions towards organic pollutants, which is the object of our study, whereas, in this regard, a higher attention is devoted to the adsorption of metal ions [125-128]. It is therefore evident that further research and insights are necessary for TRL improvement.

2.2.2.4 Leaching tests

As previously described for ACs (Section 2.2.1 of the text), leaching tests for organic (PAHs) and inorganic compounds (metals) are necessary to evaluate the safety of supports employed for the removal of pollutants in water treatments [52]. Therefore, for BCs intended to be used for water filtration, the same characterizations should be suggested, also in consideration that these adsorbents are produced by thermal treatment, as ACs. Despite this assumption, only few papers evaluate the leaching of some classes of compounds in aqueous medium from biochars studied for water treatment [56, 129]. In more detail, Hong and co-workers [129] extensively describe the release of selected heavy metals from biochar in ultrapure water, together with nutrients and total organic carbon as representative indicator of organic matter, without focusing on any specific class of compounds. In a pioneering vision, Del Bubba and co-workers follow the analytical protocols imposed by UNI EN 12915 [60] for evaluating the leaching characteristics of metals and PAHs while comparing BC vs AC performance.

Apart from the few works previously commented, the actual literature shows a great unbalance of papers regarding the use of leaching tests in BCs used as amendment in agricultural applications [130, 131] over water treatment, highlighting the different maturity stages of BC use in agriculture in respect to water treatment.

2.2.3 Biochar as adsorbent for organic micropollutants

2.2.3.1 Typical target pollutants and performance capabilities

The application of biochar as adsorbent for the removal of organic pollutants from waters and wastewaters has been extensively studied. Indeed, when searching on "Web of Science" database the words "biochar" and "adsorption", about 5800 studies are listed, with about 40% focused on the removal of heavy metals (research refinement using "metal" word) and the

other 40% focused on organic compounds (research refinement using both "organic" and "pollutants" words). However, despite this numerosity, a critical approach investigating the possible correlation between biochar adsorption capacities and both the intrinsic properties of target compounds (i.e. polar character) and/or physicochemical features through statistic tools is missing. Therefore, the following paragraphs will focus on a critical investigation on this topic, limiting the discussion to the literature of the last ten/fifteen-years relating to the removal of organic pollutants by unmodified biochars. As previously mentioned, since activated carbon is the *standard* material for water treatment, ACs will be also considered in parallel.

From the above-mentioned literature, a representative list of the organic compounds most frequently removed by biochars was retrieved and summarized in Table 2.3. Papers were selected only if adsorption capacity data at equilibrium conditions were presented. Each analyte is clustered depending on its ionic form (undissociated, anionic or cationic) at neutral pH value which is typical of raw wastewater. The $logK_{ow}$ together with the pk_a (if available) values are reported. Within each reviewed paper, the comparison of BC performances with those of AC is reported, if present.

Table 2.3. List of the most investigated organic pollutants removed by biochars in the last ten-years literature. Compounds are grouped following their ionizable properties. The values of their $logK_{ow}$ and pK_a (if applicable), as calculated from Chemicalize Software are reported [132].

CATION	Class	logKow	pK_a (ionic group)	Comparison with AC	Ref
Methylene blue	Dye	0.75	/	No	[133-138]
Methyl violet	Dye	0.43	9.17	No	[139]

Malachite green	Dye	0.8	/	No	[140]
Lincomycin	Antibiotic	-0.3	7.97	No	[141]
ANION	**Class**	logKow	pK_a (ionic group)	**Comparison with AC**	**Ref**
Sulphapyridine	Antibiotic	0.35	6.24	Yes	[142, 143]
Sulfamethoxazole	Antibiotic	0.79	6.16	No	[144]
p-coumaric acid	Drug	1.46	3.81	No	[145]
Reactive brilliant blue	Dye	-1.33	-2.69	No	[146]
Congo Red	Dye	2.63	/	No	[135, 147-149]
tris(2-carboxyethyl) phosphine	Flame retardant	1.78	3.22; 4.38	No	[121]
2,4-dichlrophenoxiacetic acid	Herbicide/Pesticide	2.61	2.81	Yes	[150]
t-Cinnamic acid	Precursor	2.13	4.32	No	[145]
NEUTRAL	**Class**	logKow	pK_a (ionic group)	**Comparison with AC**	**Ref**
Amoxicillin	Antibiotic	-2.3	7.22	No	[151]

Tetracycline	Antibiotic	-3.4	7.36	No	[22, 152, 153]
Ciprofloxacin	Antibiotic	-0.8	5.56; 8.77	No	[154]
Sulfadiazine	Antibiotic	0.38	7	No	[22]
Chlortetracycline	Antibiotic	-1.98	2.99	No	[155]
1H-benzotriazole	Corrosion Inhibitor	1.44	9.04	No	[121]
p-nitrotoluene	Dye	2.37	/	No	[156]
Bisphenol-a	Endocrine disruptors	3.32	9.78; 10.39	No	[157]
Atrazine	Herbicide	2.61	/	No/Yes	[121, 158]
Diuron	Herbicide	2.68	13.18	No	[121]
1-naphtol	Herbicide	2.85	9.6	Yes	[159]
Catechol	Herbicide	0.9	9.34; 12.79	No	[160]
Carbaryl	Herbicide	0.9	/	No	[161]
17α-ethinyl estradiol	Estrogen	3.67	10.33	No	[157]
Phenol	Plastic production	1.46	10.02	No	[162]
Phenanthrene	Polycyclic Aromatic Hydrocarbon	3.71	/	No	[157, 163]
Naphthalene	Polycyclic Aromatic Hydrocarbon	2.96	/	No/Yes/No	[156, 159, 163]
Trichloroethylene	Solvent	2.42	/	Yes	[6]

4-tert-Octylphenol TRITON™X-45 (mixture of 4-t-octylphenol polyethoxylated)	Non-ionic Surfactant	5.18	10.23	Yes	[56]
4-(1-Ethyl-1,4-dimethylpentyl)-phenol IGEPAL®CO-520 (mixture of branched 4-nonylphenol polyethoxylated oligomers)	Non-ionic Surfactant	3.49-4.90	15.10[a)]	Yes	[56]
	Surfactant	5.79	10.22	Yes	[56]
	Surfactant	4.26-5.50	/	Yes	[56]

[a)] Referred to the compound 2-[4-(2,4,4-trimethylpentan-2-yl)phenoxy]ethan-1-ol, as retrieved from Chemicalize

Data collected in Table 2.3 allow several considerations hereafter discussed. Most of the organic pollutants tested for removal by biochars are dyes, herbicides or drugs, since they account for the most detected species in wastewaters.

To what concern ionizability properties, reported data clearly show that at pH value typical of wastewater and natural water (pH ~ 7) most of the organic molecules typically investigated are present in neutral form. However, it

should be underlined that, among the neutral compounds considered, many of them are ionizable species with pKa values higher than 7, thus suggesting that the chemistry of their functional groups will be altered at different pH conditions with consequent variation in the adsorption mechanism [164] and in BC removal performances.

The analysis of the reviewed literature shows that most of the studies do not consider ACs in their investigations but limit the discussion to the BCs selected. This approach makes it difficult to assess BC performance and advantages over more traditional adsorbents, i.e. AC. Hence, to understand and to critically discuss BC capabilities, *per se* and in comparison with AC, the range of typical adsorption capacities of BCs and ACs towards the most studied organic pollutants was derived, through a distributional statistical approach. The maximum adsorption capacity at equilibrium conditions (q_e expressed as mg/Kg) derived from data of adsorption isotherm tests (see section 2.2.2.2), was chosen as representative parameter for the adsorption efficiency. The statistical treatment was not limited to the data of Table 2.3 (restricted to the last 10-15 years literature), but extended to less recent literature to achieve a representative population of 50 studies. The collected q_e data for BCs were treated using a boxplot tool (Figure 2.1a) that enabled to evaluate data dispersion and the main statistical indices (i.e. average, median, etc). In a similar manner, a representative data population of q_e for ACs was reported (Figure 2.1b, n= 50 as for BCs). It is important to highlight that due to the scarcity of studies which simultaneously include BCs and ACs, to achieve the same data numerosity (n=50), it was necessary to include also studies related to ACs only.

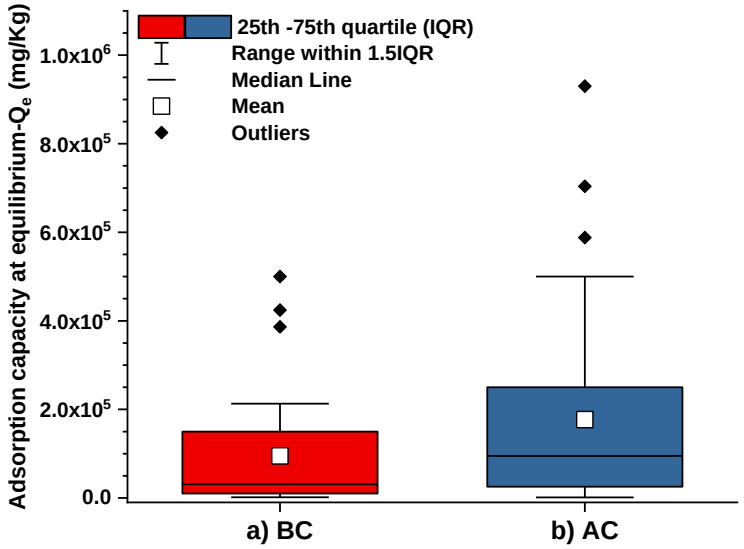

Figure 2.1: Boxplot of adsorption capacities at the equilibrium for BCs (a) and ACs (b). n=50 for both series. inter quartile range (IQR), median, means and ranges were calculated through OrginLab software. Ranges were calculated as 1.5 fold the IQR [165].

Graph results show that the inter quartile range (IQR - green box), between 25th (Q1) and 75th quartile (Q3) obtained for q_e values of ACs is wider than the one obtained for BCs. Indeed, for BCs, Q1 and Q3 values are 10,000 mg/Kg and 150,000 mg/Kg, respectively, with IQR area (Q3-Q1) of 140,000 mg/Kg, while for ACs Q1 and Q3 values are 21,400 mg/Kg and 266,400 mg/Kg, respectively, with IQR area of 245,000 mg/Kg. These data promptly highlight that activated carbons show a wider range of adsorption capacities in respect to BCs of about 50%, and higher values of q_e. A similar gap is also observed when considering the average capacity (95,000 mg/kg and 176,800 mg/Kg for BCs and ACs, respectively).

These observations support the increase of research on properly modified BCs, as discussed in the 2.2 section.

2.2.3.2 Effect of hydrophobic character of analytes on biochar adsorption efficiencies

When considering the intrinsic properties of the compounds under investigation, the hydrophobic/hydrophilic character is probably one of the most important to be accounted for, since it strongly influences the type and the strength of the interaction occurring between biochar surface groups and target pollutants. Therefore, to evidence a possible correlation trend between the adsorption capacity of BCs and the hydrophobic character of the organic compounds removed, a distribution graph was chosen. For this purpose, the distribution of BC q_e (mg/kg) data taken from the literature (n=50) were plotted as a function of the $\log K_{ow}$ values of the target pollutants removed (Figure 2.1A). It should be specified that, among all data previously retrieved (Table 2.3), only molecules having $\log K_{ow}$ ranging from 0.5 (±0.25) and 3.5 (±0.25) were chosen for the statistical treatment, since the outsiders have a reduced frequency, thus making not significative their processing. The $\log K_{ow}$ values of the target compounds here selected are referred to slightly hydrophobic to medium-high hydrophobic analytes.

The same distribution was also represented in Figure 2.2 for the same molecules adsorbed on activated carbons (n=50).

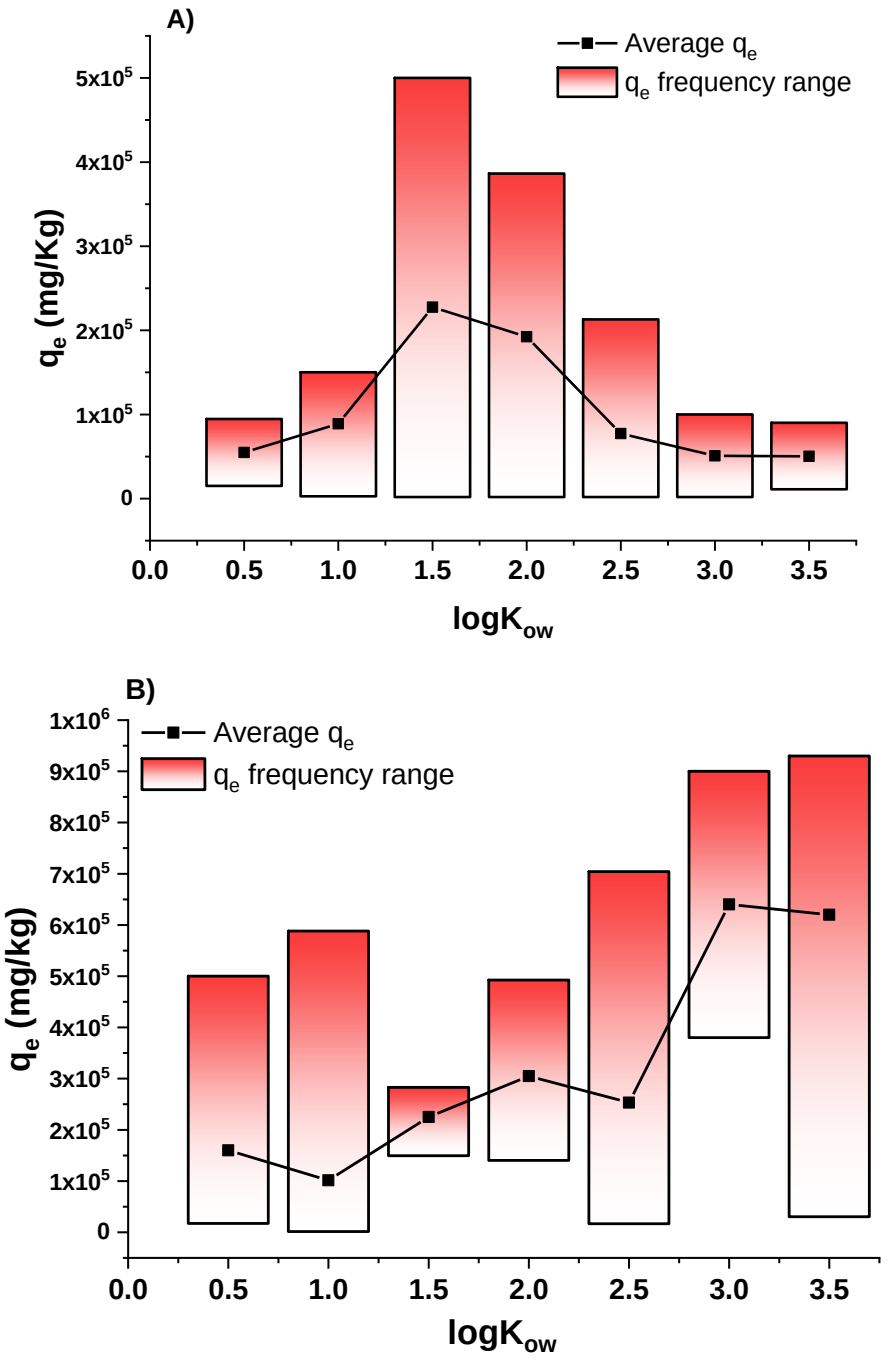

Figure 2.2. Distribution plot of equilibrium adsorption capacities (q_e, mg/kg) as a function of $logK_{ow}$ of organic target pollutants removed by biochars (A)

and activated carbons (B). n=50 for both adsorbents. The clusters considered log K_{ow} range from 0.5 to 3.5.

In more detail, in both graphs (Figure 2.2A and 2.2B), bars represent the min-max q_e frequency range for each 0.5 unit of logK_{ow} cluster (±0.25) in which all the target compounds were divided. The black squares represent the average q_e, and the black lines represent the average q_e trend line.
The data representation of Figure 2.2 leads to interesting observations. When focusing on the average q_e values, a gaussian-similar trend could be observed for BCs (Figure 2.2A). In fact, molecules characterized by logK_{ow} ranging from 1.5 to 2 are more retained from BCs than those characterized by lower and higher hydrophobic character. Conversely, a similar behaviour is not observed when studying the removal of the same compounds using ACs (Figure 2.2B), since adsorption increases with the increase of logK_{ow}, reaching a plateau at logK_{ow} approximatively equal to 3.0 (medium high hydrophobicity).
Such results could be explained considering the different interactions occurring between organic pollutants and biochars or activated carbons, due to the different surface properties of the two adsorbents. Indeed, it is assessed that the surface of ACs is characterized by a higher degree of aromaticity in respect to the surface of BCs, since their production temperature and activation processes are demonstrated to convert aliphatic into aromatic carbons [164, 166]. This feature is reflected to preferred π-π and/or hydrophobic interactions in ACs [167] rather than BCs. Hence, the higher the aromaticity of the molecule and the hydrophobicity of target pollutants, the stronger their interactions, and, therefore, the higher the adsorption capacities of activated carbons.
Differently, due to their typical process production conditions, the BC is characterized by a surface containing both aliphatic ionizable moieties (i.e. -COOH), and, in a less extent, aromatic carbons. In fact, the lower pyrolysis

temperature conditions in BC production reduce the conversion of the aliphatic C to aromatic C so that H/C ratio are typically higher in biochars [168] than in activated carbons [169]. Therefore, a wider range of mechanisms, such as electrostatic, π-π/hydrophobic, hydrogen bond interactions, are involved within the pollutant and the BC surface [164]. Hence, organic pollutants characterized by a medium hydrophobic character, i.e. $\log K_{ow}$ of about 1.5-2 (Figure 2.2B -having both polar and nonpolar functional groups) are expected to interact with biochar surface synergically exploiting all the previously mentioned mechanisms. Conversely, target compounds with lower $\log K_{ow}$ values are expected to interact with BC *via* a reduced number of interactions (electrostatic-if ionizable-or hydrogen bond interactions), thus resulting in lower adsorption on BCs. On the other hand, pollutants with higher $\log K_{ow}$ values are expected to interact with BC via π-π or hydrophobic interactions only which limit the extent of retention.

The distribution plots here reported show that the application of biochar in water tertiary treatments as activated carbon replacement is in particular suggested for medium non-polar compounds (i.e. herbicides), for which the affinity is similar to activated carbons (average q_e about $2.5*10^5$ mg/kg for both sorbents). Hence, the use of highly energy demanding activation processes (typical of ACs) should be avoided.

2.2.4 Considerations on the correlations of physicochemical and performance indices with biochar adsorption efficiencies through chemometric approaches

As described in section 2.2.2 of this text, several physicochemical and performance indices of the biochars strictly influence adsorption performances. Selected authors have tried to correlate one singular properties of biochars at a time (i.e. pyrolysis temperature [6], feedstock [170], etc) to the adsorption efficiencies. Nevertheless, an overall evaluation

which considers as many as possible physicochemical parameters and indices, is still missing. A principal component analysis (PCA), a chemometric approach frequently applied to promptly highlight the correlation status of several variables, would be highly desirable to evaluate possible correlation between the main biochar features described in sections 2.2.1 and 2.2.2 and adsorption capabilities expressed for instance as maximum adsorption capacities derived from Langmuir models (see section 2.2.2.2) or as K_F derived from Freundlich models (see section 2.2.1.2). However, despite the huge number of papers devoted to the removal of organic compounds by biochars, a lack of homogenous data on physicochemical and performance characterization is observed, since most of the studies evaluate only few of the above-mentioned parameters (section 2.2), depending on the author sensibility. Hence, when trying to set-up a PCA matrix by retrieving data from the available literature, too much missing data is present, thus making chemometric treatment impossible [171]. To overcome this obstacle, the only solutions to perform the chemometric PCA treatment could be, therefore, either to treat the data from a single study, in which e.g. several biochars are tested, or reduce the variables to be computed to the few in common among the selected works. However, in both cases, the number of treated samples or variables considered would be so reduced, that significant results from PCA could not be obtained.

2.2.5 Economic evaluation on biochar use over activated carbon

The consideration reported in section 2.2.3.1 showed, for the compounds included in this work, that the adsorption capacities for ACs are superior to BCs. However, removal effectiveness is not the only parameter to consider when evaluating the applicability of adsorbents in wastewater treatment as production costs should also be considered.

Therefore, we have derived an effectiveness/cost index, weighting the adsorption performances with the production costs, evaluated according to a literature survey. Specifically, it has been recently reported that the production costs of ACs range from 1.35 (China) [172] to 2.6 €/Kg (Italy) [56], while for BCs these values range from 0.15 (Italy) [56] to 0.42 €/Kg (U.S.) [173, 174], with average values of 1.98€/Kg and 0.29€/Kg, respectively. Based on the mean values of q_e values discussed above in section 2.2.3.1, (95,000 mg/kg and 176,800 mg/Kg for BCs and ACs, respectively), an effectiveness/cost index has been calculated for both BCs and ACs, dividing the average maximum equilibrium adsorption capacity (q_e, expressed as mg/Kg) by the average cost per Kg of adsorbent. The results ($3.3*10^5$ mg removed for each € of BC and $8.9*10^4$ mg/€ for ACs) show that although BCs have lower adsorption capabilities, their effectiveness/cost index is 3.7 times higher than that of activated carbons, which means that for the same capital investment, a removal of organic pollutants of about 4-fold higher (in terms of mg) is obtained using BCs, compared to ACs.

2.2.6 Conclusions

In the last ten-fifteen years, biochars intended for water remediation became a trend topic, with thousands of published works studying their possible application for the removal of both organic and inorganic contaminants. The data reviewed and treated by boxplot statistics, indicate that BCs exhibit slightly lower adsorption capacities for organic compounds, especially for those of medium-high hydrophobicity, in comparison with the standard adsorption materials (activated carbons). Actually, despite their reduced adsorption capacities, the production cost is much lower, with an effectiveness/cost index, here derived, about 4 times higher for BCs in respect to ACs.

Removal efficiencies of BCs could be correlated with main properties of target compounds, such as the hydrophobic character as expressed by $\log K_{ow}$ values, showing that for medium non-polar compounds the replacement of ACs with BCs in tertiary treatments is highly desirable, since their average adsorption efficiencies are in the same range and, in such way, highly energy expensive activation processes could be avoided.

The correlation of the intrinsic physicochemical and performance parameters with the biochars removal capacity is more challenging. The presented study highlighted an under-investigation of homogenous physicochemical and performance characterization techniques, which in our opinion are mandatory for an overall detailed understanding of the core interactions and correlations between the pollutants and the BC surface. Such a correlation is missing in the literature.

The comprehensive survey on the activated carbon characterization protocols (most of them proposed by regulatory organisms), as reviewed in the first part of the chapter, proves that through these procedures a full understanding of the capability and safety use of ACs in the removal of pollutants from waters can be achieved. It is consequently desirable that, in the lack of regulatory methods specific for biochars, all the above-mentioned protocols should be also homogenously applied for the characterization of BCs intended for water purification, avoiding fragmentary and subjective characterization that depends only on the sensitivity of the authors. A direct comparison between BCs and the ACs is recommended to explore BC capabilities in respect to ACs for the scale up of BCs applications (bench and pilot scales) towards higher TRL levels.

Additionally, through this overview an easy-to-use compendium on the main physicochemical and performance characterization techniques of both BCs and ACs is suggested.

Finally, the currently available literature data for BCs are non-homogeneous which makes it impossible to extract detailed information through the main chemometric tools, such as PCA. Some knowledge as complete as possible on the main physicochemical and performance characteristics of the BC is therefore of fundamental importance to statistically evaluate possible correlations between the removal capacity of the BC and BC physicochemical properties.

2.3 Application of Biochar to water potabilization

The aim of this second section of the research work devoted to biochar was to investigate the physicochemical properties, the regulated leachable substances, and the removal performances of seven biochars (commercially available or synthesized for the purpose), obtained from pyrolysis or gasification of vegetal biomass. Performances of biochars were investigated in comparison with three commercially available vegetal ACs used in an Italian drinking water facility, withdrawn at different age of operation. Data obtained were chemometrically treated through principal component analysis, allowing for selecting the most promising biochars to be further investigated by adsorption tests. In a first stage of this study, adsorption capabilities were tested in ultrapure water, whereas afterwards the sorption capacity was evaluated on a restricted group of biochars in water samples collected at intermediate treatment stages of a potabilization plant. In all cases ACs were also tested as reference comparative materials.

Diiodoacetic acid (DIAA), benzene, and 1,2 dichlorobenzene, were selected as model pollutants commonly monitored in drinking water facilities. Specifically, DIAA is a model emerging disinfection by-product [192] never investigated before for its sorption by biochars. Moreover, 1,2

dichlorobenzene can also originate from disinfection treatments during the potabilization process [193, 194] and its monitoring in tap water is recommended by the World Health Organization guidelines (taste threshold value 1 µg L^{-1}) [195]. Benzene is regulated by the Directive 2020/2184 regarding the quality of water intended for human consumption (1 µg L^{-1}). It should also be noted that benzene and 1,2-dichlorobenzene are volatile organic carbons (VOCs) still detected in some industrial districts [196] and are therefore also important from the wastewater treatment viewpoint.

2.4 Materials and methods

2.4.1 Reagents

For the determination of adsorption indices, the following reagents, supplied by Merck (Kenilworth, NJ, USA), were used: iodine solution (0.1 N), sodium thiosulfate solution (0.1 N), zinc iodide starch solution, hydrochloric acid (37%), potassium hexacyanoferrate (>99%), methylene blue, anhydrous acetic acid (>99.8%). Ammonia solution (28%), dichloromethane and 2-propanol were from VWR International (Radnor, PA, USA). For the evaluation of extractable metals, an ICP multi-element standard solution IX (100 mg L^{-1} of As, Be, Cd, Cr (VI), Ni, Pb, Se, Tl) from Merck was used.

For the determination of extractable polycyclic aromatic hydrocarbons (PAHs), the 16 compounds listed by EPA were purchased from Sigma Aldrich (Darmstadt, Germany). For the analysis of extractable polychlorinated biphenyls (PCBs), the compounds were purchased from LGC Standards (Milan, Italy). They were non dioxin-like PCBs: 3,3'-dichlorobiphenyl (PCB 11), 4,4'-dichlorobiphenyl (PCB 15), 2,4,4'-trichlorobiphenyl (PCB 28), 2,2',5,5'-tetrachlorobiphenyl (PCB 52), 2,2',4,5,5'-pentachlorobiphenyl (PCB 101), 2,2',3,4,4',5-hexachlorobiphenyl (PCB 138), 2,2',4,4',5,5'-hexachlorobiphenyl (PCB 153), 3,3',4,4',5,5'-hexachlorobiphenyl (PCB 169), 2,2',3,4,4',5,5'-heptachlorobiphenyl (PCB 180), 2,3,3',4,4',5,5'-

heptachlorobiphenyl (PCB 189); and dioxin-like PCBs: 3,4,4',5-tetrachlorobiphenyl (PCB 81), 2,3',4,4',5-pentachlorobiphenyl (PCB 118), 2',3,4,4',5-pentachlorobiphenyl (PCB 123), 2,3',4,4',5,5'-hexachlorobiphenyl (PCB 167).

Labelled isotope compounds for PCBs (2 mg L^{-1}) and for PAHs (5 mg L^{-1}), Wellington Laboratories (Ontario, Canada), were used as internal and surrogate standards in order to obtain calibration curves and extraction recoveries, respectively. The ^{13}C surrogate solutions of PAHs contained: [$^{13}C_6$]benzo(a)anthracene [$^{13}C_6$-BaA], [$^{13}C_6$]chrysene [$^{13}C_6$-Chr], [$^{13}C_6$]benzo(b)fluoranthene [$^{13}C_6$-BbFl], [$^{13}C_6$]benzo(k)fluoranthene [$^{13}C_6$-BkFl], [$^{13}C_4$]benzo(a)pyrene [$^{13}C_4$-BaP], [$^{13}C_6$]indeno(1,2,3-cd)pyrene [$^{13}C_4$-Ind], [$^{13}C_6$]dibenzo(a,h)anthracene [$^{13}C_6$-DBA], and [$^{13}C_{12}$]benzo(g,h,i)perylene [$^{13}C_{12}$-BP]. The ^{13}C surrogate solution of PCBs contained: $^{13}C_{12}$-PCB28, $^{13}C_{12}$-PCB52, $^{13}C_{12}$-PCB118, $^{13}C_{12}$-PCB153, and $^{13}C_{12}$-PCB180.

Volatile organic compounds, namely benzene (100 µg L^{-1} in methanol), and 1,2-dichlorobenzene (100 µg L^{-1} in methanol), were purchased from Ultra Scientific Italia (Bologna, Italy). DIAA was supplied by Chemical Research (Rome, Italy). Ultrapure water was obtained by an EMD Millipore Milli-Q Direct Water Purification System (Millipore, Bedford, MA, USA).

2.4.2 Biochar and activated carbon samples

The seven BCs considered in this study were donated for the purpose. The three ACs were supplied by a local potabilization plant at different age of operation: AC1: new activated carbon; AC2: regenerated activated carbon; AC3: regenerated activated carbon in use at the plant. The status of operation, and the characteristics of the feedstock and the thermal process used to produce the ten chars are summarized in Table 2.4.

Before being characterized and used in isotherm studies, all the char samples were repeatedly washed with ultrapure water according to the ASTM D-5919-96 method.

Table 2.4 – Status of operation and production conditions of biochars (BC) and commercial activated carbons (AC); n.a. = not available

Sample	Status	Feedstock	Thermal treatment	Temperature (°C)	Contact time (min)
BC1	Virgin	Wood waste mixture [a]	Pyrolysis	550	10
BC2	Virgin	Wood waste mixture [b]	Pyrolysis	550	10
BC3	Virgin	Wood waste mixture [b]	Pyrolysis	550-600	15
BC4	Virgin	Herbal pomace	Pyrolysis	550-600	15
BC5	Virgin	Wood waste mixture [c]	Gasification	800-900	10
BC6	Virgin	Wood waste mixture [d]	Gasification	800-900	10
BC7	Virgin	Corn cob	Pyrolysis	450	30
AC1	Virgin	Coconut	Pyrolysis+physical activation	800-950	n.a
AC2	Regenerated	Coconut	Pyrolysis+physical activation	800-950	n.a
AC3	In use	Coconut	Pyrolysis+physical activation	800-950	n.a

[a] Composition: 100% Poplar; [b] Unknown composition; [c] Approximate composition: Pine 60%, Beech 25%, Hazel 15%; [d] Approximate composition: Pine 40%, Beech 30%, Hazel 20%, Spruce 10%

2.4.3 Biochar and activated carbon characterization

The chars investigated in this study were physicochemically characterized through the determination of ash content, pH of the point of zero-charge (pH_{pzc}), physisorption analysis, iodine and methylene blue adsorption indices (I_2In and MBIn), as well as for water-extractable substances of environmental concern. The procedures adopted for the aforementioned determinations are briefly described below.

2.4.3.1 Ash content

The ash content was determined according to the ASTM International D 2866-11 [197], which refers to the analysis of ACs.

2.4.3.2 Water-extractable substances

Metals (namely Sb, As, Cd, Cr, Pb, Hg, Ni and Se), PAHs and PCBs were extracted according to the EN 12902 standard [186]. After extraction, metals were determined by an Elan 6100 ICP-MS (Perkin Elmer, Waltham, Massachusetts, USA), whereas PAHs and PCBs were preconcentrated by solid-phase extraction (SPE) and analysed by GC-MS, as elsewhere described [198, 199].

2.4.3.3 pH of the point of zero charge

The pH of the point of zero-charge (pH_{pzc}) was determined using the pH drift method, widely adopted for the evaluation of the surface charge of biochars and ACs [190].

2.4.3.4 Adsorption indices

The determination of I_2In and MBIn was performed according to the definitions indicated by CEFIC for ACs [200].

2.4.3.5 Physisorption analysis

Physisorption analysis of biochars and ACs was performed via nitrogen adsorption and desorption experiments using a Porosity Analyser Thermo Fisher Scientific (Milan, Italy) model SORPTOMATIC 1990 according to the American Society for Testing and Materials specifications [201, 202]. In further detail, the specific surface area (SSA) and micropore surface area (MiSSA) were determined respectively by the Brunauer–Emmett–Teller (BET) method and by t-plot method, whereas mesopore surface area (MeSSA) was measured by the Barrett-Joyner-Halenda (BJH) method applied to desorption data.

2.4.4 Adsorption studies on DIAA and VOCs

Adsorption tests were performed on DIAA and VOCs in ultrapure water (pH = 6.5±0.1) using the micro-isotherm technique for adsorbates at ppb concentrations, as established by ASTM D5919-96 standard [203]. Aliquots of 40 mL and 100 mL, containing fixed amounts of DIAA and VOCs, respectively (DIAA: 5 μg L^{-1} for BCs and 20 μg L^{-1} for ACs; VOCs: 5 μg L^{-1} or 20 μg L^{-1} for BCs and 20 μg L^{-1} for ACs) were put in contact with different amounts of BCs/ACs varying approximately between 0.02 and 0.5 g. The mixture was stirred in an orbital shaker for 24 hours. The solution was then filtered through a mixed cellulose ester membrane (0.45 μm). Control experiments using the same aforementioned concentrations of target analytes were also conducted without the addition of the adsorbent materials, in order to estimate their removal due to mechanisms other than sorption (e.g. volatilization and degradation).

Experimental data were fitted by the Freundlich isotherm model [204]:

$$\log\frac{X}{M}=\log K_F+\frac{1}{n}\log C_e$$

where X/M is the ratio of the amount of analyte adsorbed per mass unit of sorbent (mg g^{-1}), K_F is the constant of the Freundlich isotherm equation ($mg^{1-1/n}$ $L^{1/n}$ g^{-1}) related to adsorption capacity, C_e is the equilibrium concentration (mg L^{-1}), and 1/n is the exponent of non-linearity.

2.4.5 Analytical determination of DIAA and VOCs

Residual DIAA concentrations were determined by ion chromatography coupled with triple-stage quadrupole mass spectrometry as elsewhere described [192]. Residual VOC concentrations were determined by GC-MS after SPE.

2.4.6 Water sample collection and characterization

Water samples were withdrawn from two potabilization plants located in the Piedmont region (North Italy) which treat the same raw water. One sample (labelled as DSB) was taken at the outlet of the dynamic separation basins for the removal of slurry from clarified waters (in which coagulant, hypochlorite and chlorine dioxide solutions are dosed), before entering the activated carbon beds. The other sample (labelled as CB) was taken at the outlet of a clarification basin (in which coagulant only is added), before entering the activated carbon beds. The water samples were characterized for pH and total organic carbon (TOC). TOC was determined using a Shimadzu TOC-V-CSH analyser, by the differential method, i.e. analysing both total carbon (TC) and total inorganic carbon (TIC) through separate measurements and calculating TOC by subtracting TIC from TC.

2.4.7 Data analysis

Least squares regressions and related analyses of variance (ANOVA) were performed with Excel 2016 (Microsoft, Redmond, WA, USA). Principal component analysis (PCA) and cluster analysis (CA) were carried out using the Minitab statistical software package, version 17.1.0 (Minitab Inc., State College, PA, USA). All data plots were performed using Excel 2016.

2.5 Results and discussion

2.5.1 Characterization of chars

2.5.1.1 Ash content

In biochars, ash percentages were found in the quite wide range of 6-49% (Table 2.5), with the lowest value achieved for BC7, which derived from corn cob under pyrolysis treatment at 450°C (Table 2.4). Ash content in materials intended for water filtration is regulated by EN 12915-1 standard, which sets a limit of 15%, since a high ash content in filtering media is expected to reduce adsorption activity [164]. Hence, as regards this parameter, only BC2, BC3, and as previously mentioned BC7, are allowed to be used as sorbent materials in potabilization facilities.

Table 2.5 – Ash (%), pH of the point of zero charge (pH_{pzc}), specific surface area (SSA, BET method, $m^2\ g^{-1}$), surface area of micropores (MiSSA, t-plot method, $m^2\ g^{-1}$), surface area of mesopores (MeSSA, BJH model – desorption cumulative surface area, $m^2\ g^{-1}$), iodine index (I_2In, mg g^{-1}), and methylene blue index (MBIn, mg g^{-1}), determined in biochars (BCs) and activated carbons (ACs). For the parameters tested by replicated analyses (n=3), mean and standard deviations (in bracket) are reported. Available limits set by European regulation EN 12915-1 are also reported; n.a. = not available.

Sample	Ash	pH_{pzc}	SSA	MiSSA	MeSSA	I_2In	MBIn
EN 12915-1	15	n.a.	n.a.	n.a.	n.a.	600	n.a.
BC1	42 (8)	10.5	253 (19)	81 (15)	53 (12)	129 (1)	4 (1)
BC2	12 (2)	8.6	243 (22)	43 (11)	63 (14)	144 (1)	4 (2)
BC3	14.1 (0.5)	8.4	153 (20)	65 (14)	76 (17)	88 (1)	1.4 (0.8)

BC4	29.2 (0.2)	9.1	222 (18)	92 (22)	117 (25)	124 (1)	4 (2)
BC5	49 (4)	12.0	302 (23)	121 (26)	97 (20)	156 (1)	6.0 (0.7)
BC6	25 (2)	11.0	309 (21)	80 (19)	136 (30)	197 (1)	4.1 (0.4)
BC7	6.2 (0.1)	7.0	136 (12)	33 (10)	40 (11)	77 (1)	2.2 (0.4)
AC1	7 (2)	10.9	1053 (88)	634 (118)	384 (81)	1010 (1)	20 (2)
AC2	13 (4)	9.9	714 (65)	300 (72)	359 (78)	540 (1)	15 (1)
AC3	21 (8)	8.1	561 (38)	205 (51)	273 (59)	438 (1)	11 (2)

The data obtained here can be interpreted based on the characteristics of biomass and thermal conversion processes through which the chars were obtained. According to literature, ash concentration of chars is mainly influenced by the type of feedstock, being woody biomass the one providing a lower ash content, compared to other feedstocks, such as non-woody vegetal biomass and animal waste [205]. However, the type of thermal conversion process (i.e. pyrolysis or gasification) and the temperature and contact time conditions adopted in the process may also play a role in determining the ash concentration, which obviously depends on the amount of char obtained. In this regard, it should be remarked that biochar yield is a function of the type of thermal conversion process (i.e. pyrolysis or gasification) and the temperature and contact time conditions adopted in the process, being the highest yields obtained with pyrolysis conducted at low temperature and high contact time (slow pyrolysis) [164]. Hence, it is evident that, if the same feedstock is used, the ash concentration will be higher in

gasification processes than in pyrolysis [206]. Moreover, increasing ash percentages will be obtained with increasing temperature [207] and higher ash concentrations will be found under fast pyrolysis conditions [208]. Based on these considerations, it makes sense that BC2, BC3, and BC7, all deriving from slow pyrolysis processes (Table 2.4), showed ash percentages much lower than BC5 and BC6, which were conversely obtained under gasification conditions using a same patented process and plant. The very high ash concentration found in BC4 (about 29%) compared to BC3, both produced with the patented PYREG® pyrolysis process under the same experimental conditions, could be attributed to the different nature of the feedstocks employed, i.e. non woody vegetal biomass for BC4 and woody waste biomass for BC3 (Table 2.4). Finally, the unexpected high ash content of BC1 probably depends on the peculiar characteristics of the woody waste used as feedstock, which derives from the cutting of a forest planted for the phytoremediation of a soil contaminated by different chemicals, including heavy metals. Virgin activated carbon (AC1) showed a lower ash content (7%), in agreement with the high standard quality requested by the potabilization plant in its specifications. Higher ash percentages were obviously found in regenerated and in-use ACs (i.e. AC2 and AC3).

2.5.1.2 Water-extractable substances

The thermal conversion process that transforms biomasses into chars may lead to the formation of unwanted organic and inorganic hazardous species, depending on the original composition of the feedstocks. Among them, PAHs [209], PCBs [185] and heavy metals [210] can be present in biochars, thus introducing possible limitation in the use of the chars themselves. The EN 12915-1 normative regulates the presence of water extractable pollutants in materials to be applied for water treatments, setting a threshold concentration limit for the sum of six PAH compounds (i.e. fluoranthene,

benzo(b)fluoranthene, benzo(k)fluoranthene, benzo(a)pyrene, benzo(g,h,i)perylene and indeno-(1,2,3-cd)-pyrene) at 0.02 μg L^{-1}. In addition, the EN standard imposes limits to the presence of As (10 μg L^{-1}), Cd (0.5 μg L^{-1}), Cr (5 μg L^{-1}), Hg (0.3 μg L^{-1}) Ni (15 μg L^{-1}), Pb (5 μg L^{-1}), Sb (3 μg L^{-1}) and Se (3 μg L^{-1}). As regards PCBs, no limit is currently established by the EN standard. However, it should be mentioned that PCB concentrations are regulated in biochars to be used for soil conditioning and feed additives [185, 211].

Results obtained for leachable PAHs showed that all the chars fulfil the limits set by EN 12915-1 regulation. In detail, the regulated PAHs were detected in BC1, BC2, BC3, BC4, and BC7 (all deriving from pyrolysis), with the sum of their concentrations ranging from 1.6 ng L^{-1} (BC4) to 13.3 ng L^{-1} (BC7). Conversely, for ACs and the other BCs, the concentrations of PAHs included in the EN standard were below detection limits.

EPA PAHs other than the ones included in the EN standards were also determined (see Table 2.5.1-2.5.2), highlighting that PAHs with 2-3 aromatic rings were generally more abundant than those with higher molecular weight, as also observed elsewhere [212].

Table 2.5.1 – Extractable PAHs from the BCs studied. Concentrations are expressed in ng/L. The sum of concentrations of asterisked PAHs (regulated by the UNI EN 12915-1) is also reported. Regulated limit for these compounds is 20 ng/L.

	BC1	**BC2**	**BC3**	**BC4**	**BC5**	**BC6**	**BC7**
Naphthalene	0.55 (0.01)	< LOD	21.9 (0.97)	4.15 (0.07)	6.64 (20)	7.2 (0.13)	83.14 (3.69)

Acenaphthylene	< LOD	< LOD	0.99 (0.03)	1.18 (0.08)	0.56 (0.07)	0.94 (0.01	6.22 (0.18)
Acenaphthene	0.9 (0.5)	< LOD	3.77 (0.06)	0.94 (0.09)	2.04 (0.09)	2.2 (0.53)	33.34 (3.17)
Fluorene	< LOD	3.56 (0.41)	83.26 (3.42)	8.34 (0.2)	< LOD	< LOD	261.55 (13.33)
Phenantrene	15 (4)	34.47 (0.75)	164.25 (5.56)	8.00 (0.03)	< LOD	< LOD	329.54 (19.31)
Anthracene	1.7 (0.01)	4.36 (0.06)	36.77 (0.94)	0.88 (0.07)	< LOD	< LOD	72.03 (2.84)
Fluoranthene*	3.37 (0.01)	7.21 (0.07)	3.41 (0.20)	1.64 (0.03)	< LOD	< LOD	12.71 (0.3)
Pyrene	3.09 (0.48)	6.36 (0.14)	5.56 (0.03)	0.98 (0.01)	2.05 (0.15)	1.45 (0.07)	26.64 (0.8)
Benzo[a]pyrene	< LOD	< LOD	< LOD	< LOD	< LOD	< LOD	< LOD
Chrysene	0.96 (0.14)	< LOD	1.34 (0.09)	< LOD	< LOD	< LOD	< LOD
Benzo[b]fluoranthene*	1.95 (0.42)	< LOD	< LOD	< LOD	< LOD	< LOD	< LOD
Benzo[k]fluoranthene*	1.53 (0.30)	< LOD	< LOD	< LOD	< LOD	< LOD	0.55 (0.11)
Benzo[g,h,i,]perylene*	< LOD	< LOD	< LOD	< LOD	< LOD	< LOD	< LOD
Indeno[1,2,3-c,d]pyrene*	< LOD	< LOD	< LOD	< LOD	< LOD	< LOD	< LOD
Dibenzo[a,h]anthracene	< LOD	< LOD	< LOD	< LOD	< LOD	< LOD	< LOD
Benzo[g,h,i,]perylene*	< LOD	< LOD	< LOD	< LOD	< LOD	< LOD	< LOD

Σ* UNI EN 12915-1	6.85	7.21	3.41	1.64	< LOD	< LOD	13.26
Σ	29.39	55.96	321.25	26.11	11.29	11.79	825.72
Σ (Benzo[a]pyrene eq. conc.)	0.398	0.095	0.664	0.034	0.011	0.012	1.528

Table 2.5.2 – Extractable PAHs from the ACs studied. Concentrations are expressed in ng/L. The sum of concentrations of asterisked PAHs (regulated by the UNI EN 12915-1) is also reported. Regulated limit for these compounds is 20 ng/L.

	AC1	**AC2**	**AC3**
Naphthalene	2.2 (0.09)	12.5 (0.45)	10.91 (0.24)
Acenaphthylene	< LOD	< LOD	< LOD
Acenaphthene	< LOD	2.73 (0.07)	3.03 (0.15)
Fluorene	1.04 (0.03)	2.34 (0.11)	3.29 (0.21)
Phenantrene	7.04 (0.03)	4.92 (0.21)	7.52 (0.15)
Anthracene	1.99 (0.17)	2.02 (0.28)	2.69 (0.03)
Fluoranthene*	< LOD	< LOD	< LOD
Pyrene	< LOD	0.87 (0.06)	1.11 (0.07)
Benzo[a]pyrene	< LOD	< LOD	< LOD
Chrysene	< LOD	< LOD	< LOD
Benzo[b]fluoranthene*	< LOD	< LOD	< LOD
Benzo[k]fluoranthene*	< LOD	< LOD	< LOD
Benzo[g,h,i,]perylene*	< LOD	< LOD	< LOD
Indeno[1,2,3-c,d]pyrene*	< LOD	< LOD	< LOD
Dibenzo[a,h]anthracene	< LOD	< LOD	< LOD
Benzo[g,h,i,]perylene*	< LOD	< LOD	< LOD
Σ* UNI EN 12915-1	< LOD	< LOD	< LOD
Σ	12.27	25.38	28.55
Σ (Benzo[a]pyrene eq. conc.)	0.030	0.044	0.053

BC7, which was produced under pyrolysis at the lowest temperature (450°C), was the material providing by far the highest total leachable PAH concentration (826 ng L^{-1}), while biochars obtained under gasification conditions showed the lowest PAHs release (11-12 ng L^{-1}). These BCs were also the ones providing respectively the highest and the lowest benzo(a)pyrene equivalent concentrations ($BaPy_{eq}$), based on toxic equivalence factors (TEFs) available in literature [213]. PAHs occurrence in BCs can be explained based on re-polymerization phenomena of the radical hydrocarbon fragments formed during the thermal process, which are favoured by the absence of oxygen. Moreover, the presence of PAHs depends also on the conversion temperature adopted, which plays a main role in PAH formation up to about 500°C, but also in their degradation beyond this value [212, 214]. An influence of the biomass composition in the presence of leachable PAHs can also be evidenced from the comparison of BC3 (321 ng L^{-1}) and BC4 (26 ng L^{-1}), which were obtained under exactly the same pyrolysis conditions, but with completely different feedstocks.

The concentrations of extractable PCBs found in the BCs and ACs leachate are reported in Table 2.61 and 2.6.2.

Table 2.6.1 – Extractable PCBs from the BCs studied. Concentrations are expressed in ng/L.

	BC1	**BC2**	**BC3**	**BC4**	**BC5**	**BC6**	**BC7**
PCB15	0.5 (0.1)	0.56 (0.05)	1.29 (0.02)	2.8 (0.1)	21.7 (0.1)	29 (1)	20 (2)
PCB101	6.3 (0.2)	< LOD	< LOD	< LOD	< LOD	< LOD	< LOD
PCB81	8 (2)	< LOD	< LOD	< LOD	< LOD	< LOD	< LOD
PCB118	7 (2)	< LOD	< LOD	< LOD	< LOD	< LOD	< LOD
PCB123	12 (3)	< LOD	< LOD	< LOD	< LOD	< LOD	< LOD
PCB153	16 (4)	< LOD	< LOD	< LOD	< LOD	< LOD	< LOD
PCB167	21 (5)	< LOD	< LOD	< LOD	< LOD	< LOD	< LOD
PCB180	25 (7)	< LOD	< LOD	< LOD	< LOD	< LOD	< LOD

Σ	95.8	0.56	1.29	2.8	21.7	29	20

Table 2.6.2 – Extractable PCBs from the ACs studied. Concentrations are expressed in ng/L.

	AC1	**AC2**	**AC3**
PCB15	< LOD	4 (2)	1.1 (0.2)
PCB101	< LOD	< LOD	< LOD
PCB81	< LOD	< LOD	< LOD
PCB118	< LOD	< LOD	< LOD
PCB123	< LOD	< LOD	< LOD
PCB153	< LOD	< LOD	< LOD
PCB167	< LOD	< LOD	< LOD
PCB180	< LOD	< LOD	< LOD
Σ	< LOD	4	1.1

BC1 was the only char exhibiting the presence of all the PCBs investigated in its leachate, with total concentration of about 96 ng L^{-1}. Conversely, all the other BCs showed PCB15 as the only leachable chlorinated biphenyl, the concentration of which was in the low ng L^{-1} range (0.56-2.8 ng L^{-1}) in BC2, BC3, and BC4 and about one order of magnitude higher (21.7-29 ng L^{-1}) in BC5 and BC6. PCBs occurrence in the BC leachate could be ascribed to the thermal transformation of chloride, originally contained in feedstocks [215] and in this regard, it should be recalled that BC1 has been prepared with wood waste deriving from a multi-contaminated soil. To the best of our knowledge, this is the first study investigating PCBs in BC leachates, thus preventing any comparison with literature data.

The concentrations of metals determined in BC and AC leachates are illustrated in Table 2.7.1 and 2.7.2, respectively, where the limits set by UNI EN 12915-1 are also reported.

Table 2.7.1 – Extractable metals from the BCs studied. Concentrations are expressed in µg/L. The limits established by the UNI EN 12915-1 are also reported.

	BC1	**BC2**	**BC3**	**BC4**	**BC5**	**BC6**	**BC7**	**UNI EN limits**
Cd	< LOD	< LOD	< LOD	< LOD	< LOD	< LOD	< LOD	0.5
As	< LOD	< LOD	< LOD	< LOD	< LOD	< LOD	< LOD	10
Cr	**17.3 (0.1)**	< LOD	< LOD	2.8 (0.1)	3.1 (0.1)	3.45 (0.07)	< LOD	5
Ni	< LOD	< LOD	< LOD	< LOD	< LOD	< LOD	< LOD	15
Pb	< LOD	< LOD	< LOD	< LOD	< LOD	< LOD	< LOD	5
Sb	< LOD	< LOD	0.73 (0.05)	< LOD	1.07 (0.01)	2.68 (0.05)	< LOD	3
Se	< LOD	< LOD	< LOD	< LOD	1.01 (0.02)	0.55 (0.08)	< LOD	3
Hg	< LOD	< LOD	< LOD	< LOD	< LOD	< LOD	< LOD	0.3

Table 2.7.2 – Extractable metals from the ACs studied. Concentrations are expressed in µg/L. The limits established by the UNI EN 12915-1 are also reported.

	AC1	**AC2**	**AC3**	**UNI EN limits**
Cd	< LOD	< LOD	< LOD	0.5
As	< LOD	< LOD	< LOD	10
Cr	< LOD	< LOD	< LOD	5
Ni	< LOD	< LOD	< LOD	15
Pb	< LOD	< LOD	< LOD	5
Sb	< LOD	< LOD	< LOD	3

Se	< LOD	< LOD	**5.0 (0.2)**	3
Hg	< LOD	< LOD	< LOD	0.3

BCs generally complied with the release limits set by the aforementioned regulation, with the only exception of BC1, which exceeded the limit for Cr, with an observed concentration (17.3 µg L^{-1}) three times higher than this limit, in agreement with the considerations previously reported. As regards ACs, only AC3 exceeded limit for Se (5 µg L^{-1} versus 3 µg L^{-1}, see Table 2.7.2), suggesting that a possible saturation of adsorption sites occurred during service.

2.5.1.3 pH of the point of zero charge

The values of pH_{pzc} were characterized by a high variability (7.0-12.0), in agreement with the wide range of the production conditions, including the type of feedstock that, as already reported in literature, significantly influence this property [216]. For BCs, a significant linear correlation with positive slope was found by plotting ash concentrations as a function of pH_{pzc} values (R^2 = 0.780, P<0.05). This correlation can be ascribed to the ash composition typically reported in literature [216], which mainly consists in metals present in the hydroxide form, thus promoting the increase of the pH in solution. ACs did not follow this trend, as the higher the amount of ash, the lower the pH_{pzc} observed. This finding is in agreement with the increasing amount of chemicals other than organic carbon adsorbed by ACs during operation, which however do not influence the alkalinity of material surfaces.

The measurement of the pH_{pzc} values allowed us to make some considerations about the net surface charge of the chars, which mainly depends on the surface functional groups of the material and is extremely useful to explain the adsorption behaviours of BCs towards ionized or ionisable compounds. Most BCs (with the only exception of BC7) exhibited

pH_{pzc} higher than pH values of drinking water collected before entering AC filters of the aforementioned potabilization plants, which ranged between 7.6 and 7.7. Hence, BC1-BC6 are expected to exhibit positively charged surfaces when they were applied to the treatment of these waters, whereas BC7 is supposed to be negatively charged [217].

2.5.1.4 Adsorption indices of chars

The adsorption efficiency of the BCs was evaluated in comparison with ACs through the determination of I_2In and MBIn (see previous Table 2.5).

I_2In is commonly considered as related to the presence in the structure of micropores (average diameter less than 2 nm) and should be therefore informative for the removal efficiency of small-size organic water pollutants [190]. Conversely, MBIn should be associated to the abundance of mesopores (average diameter in the range 2-50 nm) and thus considered as a useful indicator of adsorption capacity towards medium-large sized organic pollutants [190]. For BCs, the I_2In was found in the range 77-197 mg I_2 g^{-1}, with BCs obtained from gasification (i.e. BC5 and BC6) showing the highest values (156-197 mg I_2 g^{-1}), while the lowest ones (77-88 mg I_2 g^{-1}) were exhibited by materials produced under pyrolytic conditions (i.e. BC3 and BC7). The range determined for I_2In in BCs was about five times lower than that determined in virgin and regenerated ACs (i.e. AC1 and AC2), ranging between 540 and 1010 mg I_2 g^{-1}. As expected, the I_2In of AC3 (i.e. AC2 after some use in the potabilization plant) was lower than that of AC2 (438 mg I_2 g^{-1}), in agreement with the progressive pore saturation phenomena occurring during operation.

The MBIn showed a trend within the BCs and ACs clusters, and among them, similar to that described for I_2In (e.g. higher values for ACs than BCs and for BC5 and BC6 compared to the other BCs). The two indices showed a very

good linear correlation (R^2 = 0.945, P<<0.05), in agreement with findings observed elsewhere for different types of ACs and BCs [190], even though a lower determination coefficient was observed by excluding ACs from the correlation (R^2= 0.534, P=0.062). The much lower correlation was mainly ascribable to the opposite trend observed for some pairs of materials, such as BC5 and BC6, the latter exhibiting lower MBIn but higher I_2In than the former. These findings can be explained by the general differences in micro, meso, and macroporosity distributions of BCs due to the different experimental conditions adopted for their production.

2.5.1.5 Physisorption analysis

Table 2.5 illustrated the results obtained for the porosimetry analyses (i.e. BET SSA, t-plot MiSSA and BJH desorption cumulative MeSSA) of the investigated BCs and ACs.

As expected, ACs exhibited much higher values of the SSA (561-1053 $m^2\ g^{-1}$) than BCs (136-309 $m^2\ g^{-1}$), being the latter group characterized by a data trend similar to those observed for adsorption indices. To elaborate, BC5 and BC6, in addition to showing greater values of the adsorption indices, also exhibited the highest SSA, whereas BC7 had the lowest values of the aforementioned parameters. These findings can be explained by the well-recognized role of temperature in increasing the surface area [18, 218], since BC5/BC6 and BC7 were obtained by the highest and lowest conversion temperature, respectively (Table 2.4). Indeed, very good linear correlations (R^2 = 0.981-0.984, P<<0.05) were observed between SSA and adsorption indices even excluding ACs from the regression (R^2 = 0.781-0.904, data not shown).

In general, BCs showed a higher percentage of macroporosity than ACs. However, it should be noted that BC3 and BC4, produced with the same

patented PYREG® pyrolysis system, had a very small microporosity, comparable to that observed in ACs. The relative percentages of microporosity and mesoporosity were comparable in all materials, with the exception of AC1, which was strongly characterized by microporosity. Moreover, high correlations were found between MiSSA and I_2In (R^2 = 0.972, P<<0.05), as well as between the MeSSA and MBIn (R^2 = 0.922, P<<0.05). However, similarly to findings observed for the correlation between adsorption indices, also these relationships were mainly driven by the presence of ACs, since their exclusion strongly lowered the determination coefficients, making null the significance of the correlation (data not shown).

Differently from adsorption indices, SSA is often reported as fundamental parameter for the characterization of sorption properties of BCs. In order to understand the overall significance of SSA data obtained here, it is therefore interesting to compare them with the values reported in literature for the numerous biochars obtained from vegetal feedstocks. However, the kind of conversion process, its temperature and time, as well as the type of biomass used, strongly affects the SSA of BCs. Accordingly, this comparison was restricted to biochars obtained from woody vegetal feedstocks, which represent the main type of biomass used for the production of BCs here investigated, obtaining SSA values in the range 2-637 m^2 g^{-1} [219-222]. Therefore, the SSA values between 136 and 309 m^2 g^{-1} measured in this study are fully in the range reported in the literature.

2.5.2 Principal component analysis of the char characterization parameters

To summarize the wide group of information discussed above, deriving from the determination of the several characterization parameters in the ten char samples, a multivariate elaboration of the autoscaled original data was performed by means of PCA. In more detail, PCA elaboration included the following eleven parameters: conversion temperature (T), the seven

parameters reported in Table 2.5 (i.e. ash, pH_{pzc}, SSA, MiSSA, MeSSA, I_2In, and MBIn), total PAHs (expressed as BaPy TEF concentrations), total PCBs, and total metals. Three principal components (PCs), characterized by eigenvalues > 1 and accounting for percentages of explained variances (E.V.) of 54.9%, 26.4%, and 11.0%, were obtained (total E.V. = 92.3%). Figure 2.3 illustrates the plots of scores (Fig. 2.3A-B) and loadings (Fig. 2.3C-D) of PC1 versus PC2 and PC1 versus PC3, which represent E.V. of 81.3% and 65.9%, respectively.

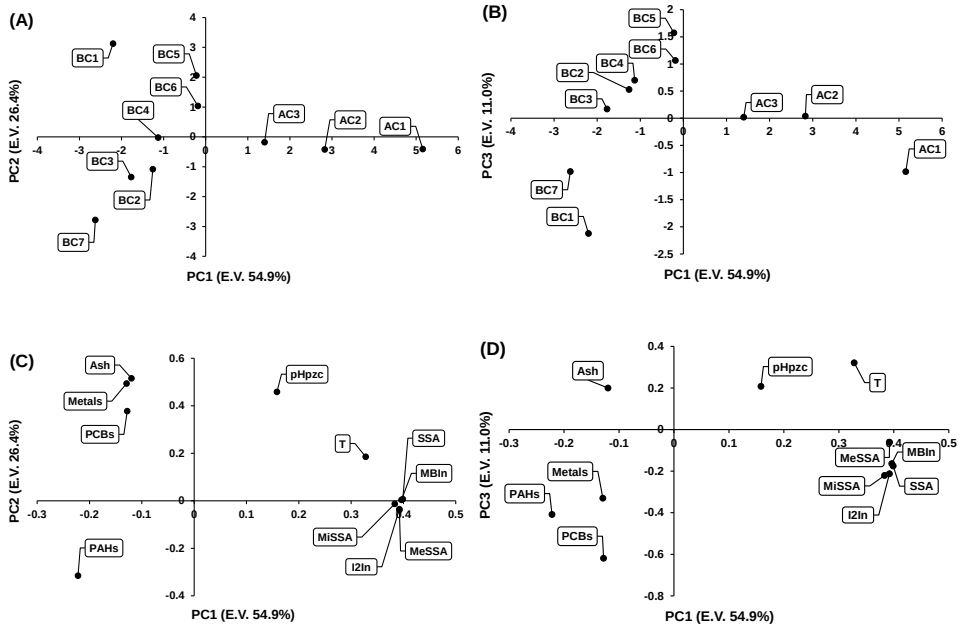

Figure 2.3 – Score (A-B) and loading (C-D) plots of PC1 versus PC2 and PC1 versus PC3, representing a percentage of explained variance (E.V.) of 81.3% and 65.9%, respectively. PCA values were calculated using the autoscaled values determined for the eleven original variables in the ten char samples. Note that the terms PAHs, PCBs, and Metals refer to their total leachable concentrations.

The contributions of each variable to the three significant PCs were not always well differentiated, even though most original variables showed remarkably different absolute values of loadings among the three components. In more detail, SSA, MiSSA, MeSSA, I_2In, and MBIn contributed mainly in PC1, pH_{pzc} and above all ash were mainly represented on PC2, whilst total PCBs exhibited by far the highest loading on PC3. Conversely, T was represented in PC1 and PC3 to the same extent, whereas total PAHs and metals contributed almost equally to PC2 and PC3. Among the ten investigated chars, ACs clustered in both score plots, mainly due to their peculiar characteristics in terms of adsorption indices and physisorption data. BC5 and BC6, which derived from the same gasification process, also clustered in both score plots mostly because of the particularly high values of ash and very low leachable concentrations of total PAHs. Actually, BC6 was the closest char to the AC cluster, suggesting interesting adsorption properties. This consideration points out that PCA is a valuable tool to select the best sorbents for adsorption measurements, when one or more reference materials are included in the unsupervised multivariate analysis as comparators. BC2, BC3, and BC4 identified a further cluster in both score plots. Conversely, BC1 and BC7 behaved as outliers, being they quite distant from the other BCs and the farthest from ACs, due to their peculiar values of the coordinates on PC2 and PC3. In fact, their scores, were mainly governed by the concentration values of ash (the highest in BC1 and the lowest in BC7), total PAHs (intermediate value for BC1 and the highest one for BC7), and total metals (the highest in BC1 and the lowest in BC7), which strongly contributed to these PCs.

In order to have a quantitative confirmation of the findings of PCA, CA was carried out, by using the complete linkage method and the Euclidean distances on the autoscaled values of the aforementioned eleven variables (Figure 2.4).

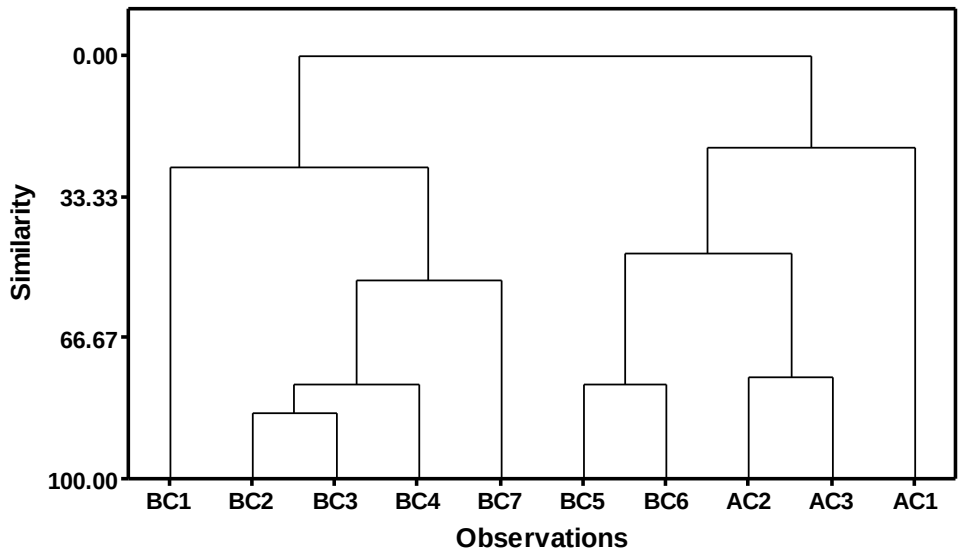

Figure 2.4 – Dendrogram of similarity of the ten investigated char samples, calculated through the complete linkage method on the basis of Euclidean distances of the autoscaled values of the eleven original variables.

The dendrogram confirmed the results of PCA, especially for BC2, BC3, and BC4, for BC5 and BC6, and for AC1 and AC2, which were grouped in three clusters at similarity percentages higher than 75%. It is also worth noting that BC5 and BC6 clustered with AC2 and AC3 with a similarity of about 50%. CA also highlighted the high distance between the virgin activated carbon (AC1) and the regenerated ones (AC1 and AC2), which exhibited a very low degree of similarity (about 20%).

Based on the results of the multivariate characterization of BCs and ACs and their summarising picture obtained by PCA and CA, BC6 and BC7 were selected for the successive adsorption studies, as the closest and the farthest materials to the ACs cluster, respectively. Within this latter group, the virgin

(AC1) and the regenerated (AC2) activated carbon were chosen as comparators.

2.5.3 Adsorption studies on DIAA and VOCs

Adsorption isotherm experiments were performed on BC6, BC7, AC1, and AC2, using the anion DIAA and the neutral VOCs benzene and 1,2-dichlorobenzene in order to (i) hypothesize possible retention mechanisms of BCs [164] and (ii) estimate sorption capacity of chars towards these pollutants, which are of environmental concern, *per se*.

2.5.3.1 DIAA

As regards DIAA, at 5 µg/L, both ACs exhibited a quantitative removal for all the char concentrations tested, since target analyte was not detected in water solutions after 24 h of contact. Conversely, removal in the ranges of 18.8-70.8 % and 5.1-28.4% were observed for BC6 and BC7, respectively (Table 2.6).

Table 2.6 – Sorbent masses of chars (M, g) used in adsorption experiments of diiodoacetic acetic (DIAA), DIAA equilibrium concentrations (Ce, mg L^{-1}), DIAA removal (R, %), ratio of the amount of DIAA adsorbed per mass unit of sorbent (X/M, mg g^{-1}), and values of the Freundlich constant (K_F, $mg^{1-1/n}$ $L^{1/n}$ g^{-1}). Initial concentrations of DIAA tested for each char are reported in bracket.

M	Ce	R	X/M	K_F
BC6 (5 µg L^{-1})				
0.490	0.00146	70.8	0.00029	
0.324	0.00226	54.8	0.00034	
0.243	0.00272	45.6	0.00038	0.00484
0.163	0.00335	33.0	0.00040	
0.113	0.00377	24.6	0.00044	
0.084	0.00406	18.8	0.00045	

BC7 (5 μg L^{-1})				
0.459	0.00358	28.4	0.00012	0.00141
0.304	0.00402	19.6	0.00013	
0.218	0.00426	14.8	0.00014	
0.133	0.00454	9.2	0.00014	
0.103	0.00465	7.0	0.00014	
0.072	0.00475	5.1	0.00014	
AC1 (20 μg L^{-1})				
0.486	0.000032	99.8	0.00164	3.18
0.323	0.000051	99.7	0.00247	
0.244	0.000102	99.5	0.00326	
0.163	0.000147	99.3	0.00487	
0.122	0.000278	98.6	0.00647	
0.033	0.001510	92.5	0.02241	
0.017	0.001970	90.2	0.04242	
AC2 (20 μg L^{-1})				
0.244	0.000028	99.9	0.00327	0.922
0.163	0.000048	99.8	0.00489	
0.122	0.000103	99.5	0.00652	
0.083	0.000208	99.0	0.00954	
0.033	0.001630	91.9	0.02227	
0.016	0.002100	89.5	0.04475	

The different adsorption performances exhibited by BC6 and BC7 should be ascribed not only to the different surface area, but also to the surface charge, as derived by pH_{pzc} measures. In fact, pH_{pzc} tests indicated a significantly higher positive surface charge for BC6 (pH_{pzc}=11.0) than BC7 (pH_{pzc}=7.0) at the working pH value (pH=6.5), which is responsible for electrostatic interactions between biochar and DIAA [164].

As no detectable DIAA concentrations were found for ACs at 5 μg L^{-1}, adsorption isotherm experiments were repeated using an initial concentration of 20 μg L^{-1}. With this concentration, the removal percentage of the two ACs remained quite similar, ranging approximately from about 89 % to 100 % in both cases (Table 2.6). As illustrated by Figure 2.5, adsorption data were fitted by the linearized Freundlich equation, observing in all cases determination coefficients ≥ 0.925 and statistically significant models based on ANOVA (*P*-values << 0.05).

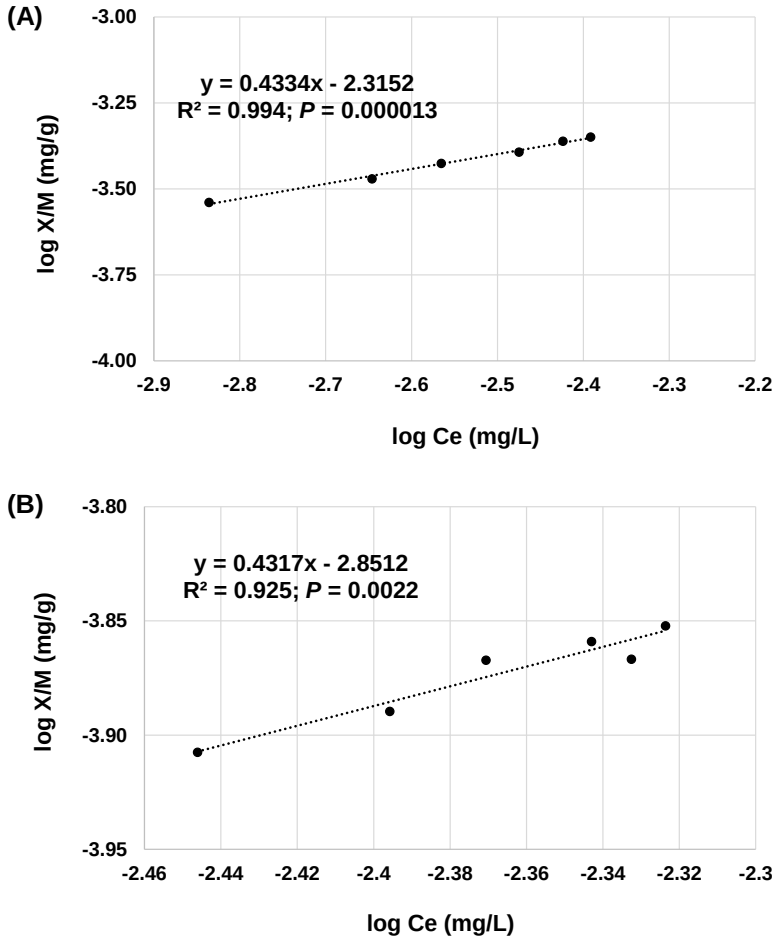

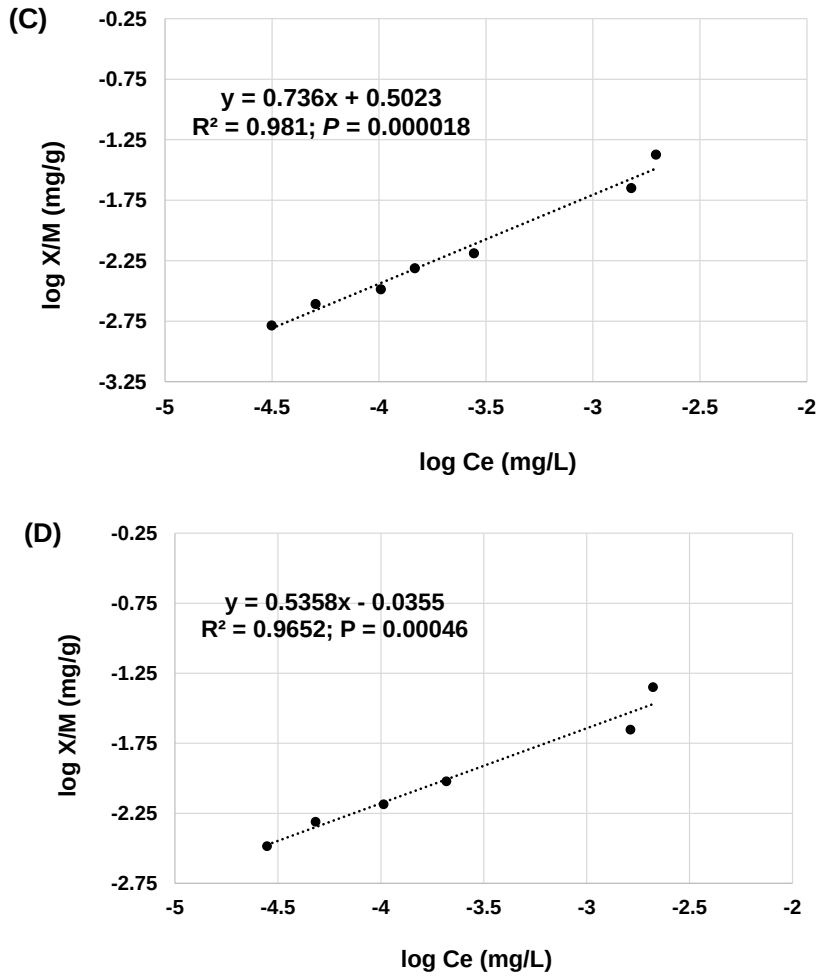

Figure 2.5 – Plots of linearized Freundlich isotherms obtained for BC6 (A), BC7 (B), AC1 (C), and AC2 (D).

Values of K_F (Table 2.6) for BCs were about three orders of magnitude lower than those for ACs. Hence, BCs provided a poor adsorption ability compared to those determined for materials routinely used in water treatment plants. In more detail, based on the K_F values, BC6 exhibited sorption ability about 3 times higher than BC7. A similar efficiency ratio was observed for AC1 vs.

AC2, in accordance with the fact that the former is a virgin material, while the latter is a regenerated char. Slope (1/n) values of the regression lines (Fig. 2.5) were in all cases < 1 (from 0.432 for BC7 to 0.736 for AC1), following the order BC7≈BC6<<AC2<AC1. The values determined for slopes suggest an L-type isotherm behaviour [223] for the adsorption of DIAA on the investigated chars, notwithstanding the pseudo-linear aspect of the experimental equilibrium concentration data (i.e. X/M vs. Ce), which is probably related to the quite high concentrations of material and their narrow range tested here (i.e. about one order of magnitude). This means that when DIAA concentration increases, the relative adsorption decreases due to the saturation of adsorption sites available to DIAA, resulting in relatively less intense adsorption, with increasing the amount of chemical adsorbed onto the material, as commonly observed for the sorption of organic compounds on chars.

2.5.3.2 VOCs

Adsorption isotherm experiments on VOCs showed a not negligible variability of data, probably due to the high vapour pressure and low water solubility of these analytes (Henry constants of $5.5 \cdot 10^{-4}$ and $2.3 \cdot 10^{-3}$ atm·m^3 mol^{-1}, for benzene and 1,2-dichlorobenzene, respectively). In this regard, it should be noted that control experiments evidenced losses of both the investigated VOCs (about 15-25%). Accordingly, adsorption isotherms were not calculated for VOCs. However, it is possible to state that both BCs showed good adsorption properties, since, at both 20 and 5 µg/L the removal percentage was almost quantitative for ACs and BC6, and approximately equal to 60-70% and 70-80%, for BC7 towards benzene and 1,2-dichlorobenzene, respectively.

2.5.4 Removal tests in water samples collected in drinking water plants

The removal capabilities of BC6 and BC7 were additionally tested in two water samples (i.e. DSB and CB) collected from the drinking water plant treatment train (before entering the final refinement stage with activated carbon beds) and compared with those of commercial AC1. These tests were performed by putting in contact for 24 h 0.4 g of chars with 100 mL of DSB and CB spiked with 20 μg L^{-1} of DIAA or VOCs. In such a way, the possible competitive effects exhibited by the matrix can be assessed and results obtained from adsorption experiments in ultrapure water eventually confirmed. To better explain possible competitions mechanisms, Total Organic Carbon (TOC) was initially measured in the two samples, obtaining TOC values of 4.3 mg L^{-1} and 2.4 mg L^{-1} for CB and DSB, respectively. The lower TOC value observed for DSB should be ascribed to the disinfection stage operated in this treatment train. The results obtained in these removal tests are summarized in Table 2.7.

Table 2.7 – Mean values (n=3) and standard deviation (in bracket) of the removal performances of 0.4 g of BC6, BC7, and AC1 towards 20 μg/L of DIAA, benzene, and 1,2-dichlororbenzene (contact time 24 h) in two real water samples (DSB and CB) from a potabilization plant, in comparison with ultrapure water (UP). Tests were performed in triplicate. "Q" means quantitative removal, i.e. concentration of the contaminant at the end of the experiment below the detection limit.

	DIAA			**Benzene**			**1,2-Dichlorobenzene**		
	UP	**DSB**	**CB**	**UP**	**DSB**	**CB**	**UP**	**DSB**	**CB**
BC6	47 (1)	41 (3)	37 (2)	Q	Q	Q	Q	Q	Q

BC7	14 (2)	12 (3)	15 (3)	74 (10)	60 (12)	51 (9)	76 (9)	78 (11)	74 (10)
AC1	99 (1)	99 (4)	99 (3)	Q	Q	Q	Q	Q	Q

As a general consideration, the use of water samples collected within the treatment train of the potabilization plants did not alter the performance of the BCs, even though the lower performances of biochars compared to the activated carbon were confirmed. Results obtained in real water samples fully support the design of column experiments to assess accurately the removal capacity and exhausting time of BCs, with particular reference to BC6.

2.6 Conclusions

Within the actions pursued in a circular economy approach fostered by European Union for waste management, the reuse of waste is promoted for the reduction of resources consumption. Biochar is one successful example of valorisation of wastes.

In this section of the thesis, seven BCs obtained from gasification or pyrolysis processes of waste vegetal biomass, were characterized in depth for numerous parameters, in comparison with a virgin commercial AC, a freshly regenerated AC, and a regenerated AC in use at a potabilization facility. The characterization included the evaluation of "environmental concern" parameters (e.g. PAHs and metals release), for which mandatory limits are provided at European level for materials intended as sorbents for drinking water filtration, but seldom evaluated elsewhere. Most BCs met these limits, whilst the "sorption performance parameters" regulated in the European standard (i.e. I_2In and ash in the UNI EN 12915-1) were in almost all cases

outside the acceptance thresholds, suggesting lower efficiencies compared to ACs.

Multivariate analyses (i.e. PCA and CA) allowed for easily identifying the materials with the closest (BC5 and BC6) or the farthest (BC1 and BC7) characteristics to those of ACs, and their use should be promoted in the field of exploration of data deriving from material characterization.

Adsorption tests towards DIAA and VOCs carried out in ultrapure water highlighted the much lower sorption ability of BC7 compared to BC6, in agreement with findings of multivariate analyses. Interestingly, removal tests in waters withdrawn from potabilization plants did not evidence any significant decrease of the sorption ability of BCs towards the investigated contaminants compared to tests in ultrapure water, thus supporting the implementation of column experiments for establishing the maximum loading capacity of the materials in experimental conditions more similar to the real scale.

Even though the sorption performances of BCs are much lower than those of ACs, it should be noted that BCs did not undergo any physical or chemical activation process, which can surely improve their removal capacity. Moreover, the management of waste biomass to produce biochar as adsorbent for water treatment may be regarded as a "win–win" solution for pursuing circular economy principles and protecting the environment.

2.7 References

1. Colantoni, A., et al., *Characterization of biochars produced from pyrolysis of pelletized agricultural residues.* Renewable and Sustainable Energy Reviews, 2016. **64**: p. 187-194.
2. Wang, Y., et al., *Comparisons of Biochar Properties from Wood Material and Crop Residues at Different Temperatures and Residence Times.* Energy & Fuels, 2013. **27**(10): p. 5890-5899.
3. Cao, X. and W. Harris, *Properties of dairy-manure-derived biochar pertinent to its potential use in remediation.* Bioresource Technology, 2010. **101**(14): p. 5222-5228.
4. Méndez, A., et al., *The effect of sewage sludge biochar on peat-based growing media.* Biological Agriculture & Horticulture, 2017. **33**(1): p. 40-51.
5. DeSisto, W.J., et al., *Fast pyrolysis of pine sawdust in a fluidized-bed reactor.* Energy & Fuels, 2010. **24**(4): p. 2642-2651.
6. Ahmad, M., et al., *Effects of pyrolysis temperature on soybean stover-and peanut shell-derived biochar properties and TCE adsorption in water.* Bioresource technology, 2012. **118**: p. 536-544.
7. Brewer, C.E., et al., *Characterization of biochar from fast pyrolysis and gasification systems.* Environmental Progress & Sustainable Energy, 2009. **28**(3): p. 386-396.
8. Rillig, M.C., et al., *Material derived from hydrothermal carbonization: effects on plant growth and arbuscular mycorrhiza.* Applied Soil Ecology, 2010. **45**(3): p. 238-242.
9. Antal, M.J., K. Mochidzuki, and L.S. Paredes, *Flash carbonization of biomass.* Industrial & engineering chemistry research, 2003. **42**(16): p. 3690-3699.
10. Meyer, S., B. Glaser, and P. Quicker, *Technical, economical, and climate-related aspects of biochar production technologies: A literature review.* Environmental Science and Technology, 2011. **45**(22): p. 9473-9483.
11. Mohan, D., et al., *Organic and inorganic contaminants removal from water with biochar, a renewable, low cost and sustainable adsorbent–a critical review.* Bioresource technology, 2014. **160**: p. 191-202.
12. Woolf, D., et al., *Sustainable biochar to mitigate global climate change.* Nature communications, 2010. **1**(1): p. 1-9.
13. Hu, Q., et al., *Biochar industry to circular economy.* Science of The Total Environment, 2021. **757**: p. 143820.
14. Khawkomol, S., et al., *Potential of Biochar Derived from Agricultural Residues for Sustainable Management.* Sustainability, 2021. **13**(15): p. 8147.
15. Pan, S.-Y., et al., *The Role of Biochar in Regulating the Carbon, Phosphorus, and Nitrogen Cycles Exemplified by Soil Systems.* Sustainability, 2021. **13**(10): p. 5612.
16. Atkinson, C.J., J.D. Fitzgerald, and N.A. Hipps, *Potential mechanisms for achieving agricultural benefits from biochar application to temperate soils: a review.* Plant and Soil, 2010. **337**(1): p. 1-18.
17. Thompson, K.A., et al., *Environmental comparison of biochar and activated carbon for tertiary wastewater treatment.* Environmental science & technology, 2016. **50**(20): p. 11253-11262.
18. Ahmad, M., et al., *Biochar as a sorbent for contaminant management in soil and water: A review.* Chemosphere, 2014. **99**: p. 19-33.
19. Abbas, Z., et al., *A critical review of mechanisms involved in the adsorption of organic and inorganic contaminants through biochar.* Arabian Journal of Geosciences, 2018. **11**(16): p. 1-23.
20. Dai, Y., et al., *The adsorption, regeneration and engineering applications of biochar for removal organic pollutants: a review.* Chemosphere, 2019. **223**: p. 12-27.
21. Gong, H., et al., *Preparation of biochar with high absorbability and its nutrient adsorption–desorption behaviour.* Science of The Total Environment, 2019. **694**: p. 133728.

22. Li, C., et al., *Adsorption of two antibiotics on biochar prepared in air-containing atmosphere: influence of biochar porosity and molecular size of antibiotics.* Journal of Molecular Liquids, 2019. **274**: p. 353-361.
23. Ni, B.-J., et al., *Competitive adsorption of heavy metals in aqueous solution onto biochar derived from anaerobically digested sludge.* Chemosphere, 2019. **219**: p. 351-357.
24. Cheng, N., et al., *Adsorption of emerging contaminants from water and wastewater by modified biochar: A review.* Environmental Pollution, 2021: p. 116448.
25. Hasan, M.S., et al., *Enhanced heavy metal removal from synthetic stormwater using nanoscale zerovalent iron–modified biochar.* Water, Air, & Soil Pollution, 2020. **231**(5): p. 1-15.
26. Yaashikaa, P., et al., *A critical review on the biochar production techniques, characterization, stability and applications for circular bioeconomy.* Biotechnology Reports, 2020: p. e00570.
27. Yargicoglu, E.N., et al., *Physical and chemical characterization of waste wood derived biochars.* Waste management, 2015. **36**: p. 256-268.
28. Chen, T., et al., *Sorption of tetracycline on H3PO4 modified biochar derived from rice straw and swine manure.* Bioresource Technology, 2018. **267**: p. 431-437.
29. Qian, W.C., et al., *Removal of methylene blue from aqueous solution by modified bamboo hydrochar.* Ecotoxicology and Environmental Safety, 2018. **157**: p. 300-306.
30. Li, Y., et al., *Hydrochars from bamboo sawdust through acid assisted and two-stage hydrothermal carbonization for removal of two organics from aqueous solution.* Bioresource Technology, 2018. **261**: p. 257-264.
31. Ahmed, M.B., et al., *Single and competitive sorption properties and mechanism of functionalized biochar for removing sulfonamide antibiotics from water.* Chemical Engineering Journal, 2017. **311**: p. 348-358.
32. Wei, Z., et al., *Selecting activated carbon for water and wastewater treatability studies.* Environmental Progress, 2007. **26**(3): p. 289-298.
33. European Council of Chemical Manufacturers' Federations (CEFIC), *Test Methods for Activated Carbon, European Council of Chemical Manufacturers' Federation (CEFIC), Belgium*. 1986.
34. D2854-09, A., *Standard Test Method for Apparent Density of Activated Carbon.* ASTM International, West Conshohocken, PA, 2014, www.astm.org, 2014.
35. ASTM D2862-16, *Standard Test Method for Particle Size Distribution of Granular Activated Carbon.* ASTM International, West Conshohocken, PA, 2016, www.astm.org, 2016.
36. ASTM D3802-16, *Standard Test Method for Ball-Pan Hardness of Activated Carbon.* ASTM International, West Conshohocken, PA, 2016, www.astm.org, 2016.
37. AWWA B604, *Standard for Granular Activated Carbon.* American Water Works Association, Denver, CO, www.awwa.org, 2012.
38. ASTM D3860-98, *Standard Practice for Determination of Adsorptive Capacity of Activated Carbon by Aqueous Phase Isotherm Technique.* ASTM International, West Conshohocken, PA, 2014, www.astm.org, 2014.
39. ASTM D 5919-96, *Standard Practice for Determination of Adsorptive Capacity of Activated Carbon by a Micro-Isotherm Technique for Adsorbates at ppb Concentrations.* ASTM International, West Conshohocken, PA, www.astm.org, 2017.
40. EN 12915-1, *Products used for the treatment of water intended for human consumption - Granular activated carbon - Part 1: Virgin granular activated carbon.* European Committee for Standardization, Brussels, www.cen.eu, 2009.
41. AWWA B600-16, *Powdered Activated Carbon.* American Water Works Association, Denver, CO, www.awwa.org, 2016.

42. ASTM D4607-14, *Standard Test Method for Determination of Iodine Number of Activated Carbon.* ASTM International, West Conshohocken, PA, www.astm.org, 2014.
43. EPA 625171002A, *U.S. Environmental Protection Agency, Process design manual for carbon adsorption, www.epa.gov.* 1973.
44. ASTM D3838-05, *Standard Test Method for pH of Activated Carbon.* ASTM International, West Conshohocken, PA, www.astm.org, 2017.
45. ASTM D6851-02, *Standard Test Method for Determination of Contact pH with Activated Carbon.* ASTM International, West Conshohocken, PA, www.astm.org, 2011.
46. Aygün, A., S. Yenisoy-Karakaş, and I. Duman, *Production of granular activated carbon from fruit stones and nutshells and evaluation of their physical, chemical and adsorption properties.* Microporous and mesoporous materials, 2003. **66**(2-3): p. 189-195.
47. Ahmedna, M., et al., *Potential of agricultural by-product-based activated carbons for use in raw sugar decolourisation.* Journal of the Science of Food and Agriculture, 1997. **75**(1): p. 117-124.
48. Caturla, F., M. Molina-Sabio, and F. Rodriguez-Reinoso, *Preparation of activated carbon by chemical activation with ZnCl2.* Carbon, 1991. **29**(7): p. 999-1007.
49. Rodriguez-Reinoso, F. and M. Molina-Sabio, *Activated carbons from lignocellulosic materials by chemical and/or physical activation: an overview.* Carbon, 1992. **30**(7): p. 1111-1118.
50. Malusis, M.A., E.J. Barben, and J.C. Evans, *Hydraulic conductivity and compressibility of soil-bentonite backfill amended with activated carbon.* Journal of geotechnical and geoenvironmental engineering, 2009. **135**(5): p. 664-672.
51. Achaw, O.-W., *A study of the porosity of activated carbons using the scanning electron microscope*, in *Scanning Electron Microscopy*. 2012, InTech.
52. UNI EN 12902, *Products used for treatment of water intended for human consumption. Inorganic supporting and filtering materials.* 2004.
53. Nunes, C.A. and M.C. Guerreiro, *Estimation of surface area and pore volume of activated carbons by methylene blue and iodine numbers.* Química Nova, 2011. **34**(3): p. 472-476.
54. ASTM D 1783-70, *Phenolic Compounds in Water.*
55. Water Research Commission, *WRC Report No. K5/1124.* 2003.
56. Del Bubba, M., et al., *Physicochemical properties and sorption capacities of sawdust-based biochars and commercial activated carbons towards ethoxylated alkylphenols and their phenolic metabolites in effluent wastewater from a textile district.* Science of The Total Environment, 2020. **708**: p. 135217.
57. Wu, Y., et al., *Controlling pore size of activated carbon through self-activation process for removing contaminants of different molecular sizes.* Journal of Colloid and Interface Science, 2018. **518**: p. 41-47.
58. Wu, M., Q. Guo, and G. Fu, *Preparation and characteristics of medicinal activated carbon powders by CO2 activation of peanut shells.* Powder technology, 2013. **247**: p. 188-196.
59. Ronowicz, J., et al., *Development and optimization of the activated charcoal suspension composition based on a mixture design approach.* Acta Pharmaceutica, 2015. **65**(1): p. 83-90.
60. UNI EN 12915-1, *Products used for the treatment of water intended for human consumption - Granular activated carbon - Part 1: Virgin granular activated carbon.* 2009.

61. Freddo, A., C. Cai, and B.J. Reid, *Environmental contextualisation of potential toxic elements and polycyclic aromatic hydrocarbons in biochar.* Environmental Pollution, 2012. **171**: p. 18-24.
62. Rafiq, M., et al., *Influence of Pyrolysis Temperature on Physico-Chemical Properties of Corn Stover (Zea mays L.) Biochar and Feasibility for Carbon Capture and Energy Balance*. Vol. 11. 2016. e0156894.
63. To, M.H., et al., *Mechanistic study of atenolol, acebutolol and carbamazepine adsorption on waste biomass derived activated carbon.* Journal of Molecular Liquids, 2017. **241**: p. 386-398.
64. Contescu, A., et al., *Surface acidity of carbons characterized by their continuous pK distribution and Boehm titration.* Carbon, 1997. **35**(1): p. 83-94.
65. Youssef, A., T. El-Nabarawy, and S. Samra, *Sorption properties of chemically-activated carbons: 1. Sorption of cadmium (II) ions.* Colloids and Surfaces A: Physicochemical and Engineering Aspects, 2004. **235**(1-3): p. 153-163.
66. Munera-Echeverri, J.L., et al., *Cation exchange capacity of biochar: An urgent method modification.* Science of The Total Environment, 2018. **642**: p. 190-197.
67. Yang, J. and K. Qiu, *Preparation of activated carbons from walnut shells via vacuum chemical activation and their application for methylene blue removal.* Chemical Engineering Journal, 2010. **165**(1): p. 209-217.
68. Van Krevelen, D., *Graphical-statistical method for the study of structure and reaction processes of coal.* Fuel, 1950. **29**: p. 269-284.
69. Benstoem, F., et al., *Elimination of micropollutants by activated carbon produced from fibers taken from wastewater screenings using hydrothermal carbonization.* Journal of Environmental Management, 2018. **211**: p. 278-286.
70. Tan, X., et al., *Application of biochar for the removal of pollutants from aqueous solutions.* Chemosphere, 2015. **125**: p. 70-85.
71. Fan, S., et al., *Removal of methylene blue from aqueous solution by sewage sludge-derived biochar: Adsorption kinetics, equilibrium, thermodynamics and mechanism.* Journal of Environmental Chemical Engineering, 2017. **5**(1): p. 601-611.
72. Li, R., et al., *Enhanced adsorption of ciprofloxacin by KOH modified biochar derived from potato stems and leaves.* Water Science and Technology, 2018. **77**(4): p. 1127-1136.
73. Zhang, J., et al., *Insight into the effects of biochar as adsorbent and microwave receptor from one-step microwave pyrolysis of sewage sludge.* Environmental Science and Pollution Research, 2018. **25**(19): p. 18424-18433.
74. Gu, H., et al., *Life cycle assessment of activated carbon from woody biomass.* Wood and Fiber Science, 2018. **50**(3): p. 229-243.
75. Gu, J., et al., *Characteristics of camellia shell pyrolysis products and optimization of preparation parameters of activated carbon.* Nongye Gongcheng Xuebao/Transactions of the Chinese Society of Agricultural Engineering, 2015. **31**(21): p. 233-239.
76. Strubinger, A., et al., *Assessment of the energy recovery of Aloe Vera solid residues by pyrolysis and hydrothermal conversion.* Chemical Engineering Transactions, 2017. **57**: p. 19-24.
77. Yin, Z., et al., *Activated magnetic biochar by one-step synthesis: Enhanced adsorption and coadsorption for 17β-estradiol and copper.* Science of the Total Environment, 2018. **639**: p. 1530-1542.
78. Igalavithana, A.D., et al., *Advances and future directions of biochar characterization methods and applications.* Critical Reviews in Environmental Science and Technology, 2017. **47**(23): p. 2275-2330.

79. Maiti, S., S. Purakayastha, and B. Ghosh, *PRODUCTION OF LOW-COST CARBON ADSORBENTS FROM AGRICULTURAL WASTES AND THEIR IMPACT ON DYE ADSORPTION.* Chemical Engineering Communications, 2007. **195**(4): p. 386-403.
80. Long, L., et al., *Synthesis, characterization and mechanism analysis of modified crayfish shell biochar possessed ZnO nanoparticles to remove trichloroacetic acid.* Journal of Cleaner Production, 2017. **166**: p. 1244-1252.
81. Lin, Y., et al., *Chemical and structural analysis of enhanced biochars: Thermally treated mixtures of biochar, chicken litter, clay and minerals.* Chemosphere, 2013. **91**(1): p. 35-40.
82. Yang, F., et al., *Effective sorption of atrazine by biochar colloids and residues derived from different pyrolysis temperatures.* Environmental Science and Pollution Research, 2018. **25**(19): p. 18528-18539.
83. Komnitsas, K.A. and D. Zaharaki, *Morphology of Modified Biochar and Its Potential for Phenol Removal from Aqueous Solutions.* Frontiers in Environmental Science, 2016. **4**(26).
84. Tan, Z., et al., *Cadmium removal potential by rice straw-derived magnetic biochar.* Clean Technologies and Environmental Policy, 2017. **19**(3): p. 761-774.
85. Sun, J., et al., *Effects of pyrolysis temperature and residence time on physicochemical properties of different biochar types.* Acta Agriculturae Scandinavica, Section B—Soil & Plant Science, 2017. **67**(1): p. 12-22.
86. Lawal, A.A., et al., *Effect of oil palm biomass cellulosic content on nanopore structure and adsorption capacity of biochar.* Bioresource Technology, 2021. **332**: p. 125070.
87. Carrier, M., et al., *Production of char from vacuum pyrolysis of South-African sugar cane bagasse and its characterization as activated carbon and biochar.* Journal of Analytical and Applied Pyrolysis, 2012. **96**: p. 24-32.
88. Hilber, I., et al., *Quantitative Determination of PAHs in Biochar: A Prerequisite To Ensure Its Quality and Safe Application.* Journal of Agricultural and Food Chemistry, 2012. **60**(12): p. 3042-3050.
89. Yao, Y., et al., *Adsorption of sulfamethoxazole on biochar and its impact on reclaimed water irrigation.* Journal of Hazardous Materials, 2012. **209-210**: p. 408-413.
90. Shaaban, A., et al., *Characterization of biochar derived from rubber wood sawdust through slow pyrolysis on surface porosities and functional groups.* Procedia Engineering, 2013. **68**: p. 365-371.
91. Essandoh, M., et al., *Sorptive removal of salicylic acid and ibuprofen from aqueous solutions using pine wood fast pyrolysis biochar.* Chemical Engineering Journal, 2015. **265**: p. 219-227.
92. KS, A.S., et al., *Kinetic and Isotherm Studies Biochar on Ammonium Solution.* 2020.
93. Suliman, W., et al., *Influence of feedstock source and pyrolysis temperature on biochar bulk and surface properties.* Biomass and Bioenergy, 2016. **84**: p. 37-48.
94. Lu, H., et al., *Characterization of sewage sludge-derived biochars from different feedstocks and pyrolysis temperatures.* Journal of Analytical and Applied Pyrolysis, 2013. **102**: p. 137-143.
95. Oliveira, F.R., et al., *Environmental application of biochar: Current status and perspectives.* Bioresource Technology, 2017. **246**: p. 110-122.
96. Vithanage, M., et al., *Kinetics, thermodynamics and mechanistic studies of carbofuran removal using biochars from tea waste and rice husks.* Chemosphere, 2016. **150**: p. 781-789.
97. Zhang, B., Y. Wu, and L. Cha, *Removal of methyl orange dye using activated biochar derived from pomelo peel wastes: performance, isotherm, and kinetic studies.* Journal of Dispersion Science and Technology, 2020. **41**(1): p. 125-136.

98. Zhang, Y.P., et al., *Adsorption of metal ions with biochars derived from biomass wastes in a fixed column: adsorption isotherm and process simulation.* Journal of Industrial and Engineering Chemistry, 2019. **76**: p. 240-244.
99. Shin, J., et al., *Effects of physicochemical properties of biochar derived from spent coffee grounds and commercial activated carbon on adsorption behavior and mechanisms of strontium ions (Sr 2+).* Environmental Science and Pollution Research, 2020: p. 1-10.
100. Choudhary, V., et al., *Batch and Continuous Fixed-Bed Lead Removal Using Himalayan Pine Needle Biochar: Isotherm and Kinetic Studies.* ACS omega, 2020. **5**(27): p. 16366-16378.
101. Bruzzoniti, M.C., et al., *Novel insights in Al-MCM-41 precursor as adsorbent for regulated haloacetic acids and nitrate from water.* Environmental Science and Pollution Research, 2012. **19**(9): p. 4176-4183.
102. Bruzzoniti, M.C., et al., *Regenerable, innovative porous silicon-based polymer-derived ceramics for removal of methylene blue and rhodamine B from textile and environmental waters.* Environmental Science and Pollution Research, 2018: p. 1-11.
103. Zand, A.D. and M.R. Abyaneh, *Adsorption of Lead, manganese, and copper onto biochar in landfill leachate: implication of non-linear regression analysis.* Sustainable Environment Research, 2020. **30**(1): p. 1-16.
104. Zhao, S., N. Ta, and X. Wang, *Absorption of Cu (II) and Zn (II) from Aqueous Solutions onto Biochars Derived from Apple Tree Branches.* Energies, 2020. **13**(13): p. 3498.
105. Choudhary, B. and D. Paul, *Isotherms, kinetics and thermodynamics of hexavalent chromium removal using biochar.* Journal of Environmental Chemical Engineering, 2018. **6**(2): p. 2335-2343.
106. Aygün, A., S. Yenisoy-Karakaş, and I. Duman, *Production of granular activated carbon from fruit stones and nutshells and evaluation of their physical, chemical and adsorption properties.* Microporous and Mesoporous Materials, 2003. **66**(2): p. 189-195.
107. Yao, H., et al., *Adsorption of fluoroquinolone antibiotics by wastewater sludge biochar: role of the sludge source.* Water, Air, & Soil Pollution, 2013. **224**(1): p. 1370.
108. Cheng, G., et al., *Adsorption of methylene blue by residue biochar from copyrolysis of dewatered sewage sludge and pine sawdust.* Desalination and Water Treatment, 2013. **51**(37-39): p. 7081-7087.
109. Park, J.-H., et al., *Lead sorption characteristics of various chicken bone part-derived chars.* Environmental geochemistry and health, 2019. **41**(4): p. 1675-1685.
110. Wu, L., et al., *Phosphorus retention using iron (II/III) modified biochar in saline-alkaline soils: Adsorption, column and field tests.* Environmental Pollution, 2020. **261**: p. 114223.
111. Shao, F., et al., *Antibiotic removal by activated biochar: performance, isotherm, and kinetic studies.* Journal of Dispersion Science and Technology, 2020: p. 1-12.
112. Solanki, A. and T.H. Boyer, *Physical-chemical interactions between pharmaceuticals and biochar in synthetic and real urine.* Chemosphere, 2019. **218**: p. 818-826.
113. Lam, Y.Y., S.S. Lau, and J.W. Wong, *Removal of Cd (II) from aqueous solutions using plant-derived biochar: Kinetics, isotherm and characterization.* Bioresource Technology Reports, 2019. **8**: p. 100323.
114. Hamzenejad Taghlidabad, R., et al., *Characterization of cadmium adsorption on two cost-effective biochars for water treatment.* Arabian Journal of Geosciences, 2020. **13**: p. 1-10.
115. Jung, K.-W., et al., *Adsorption of phosphate from aqueous solution using electrochemically modified biochar calcium-alginate beads: batch and fixed-bed column performance.* Bioresource technology, 2017. **244**: p. 23-32.

116. Ayawei, N., A.N. Ebelegi, and D. Wankasi, *Modelling and Interpretation of Adsorption Isotherms.* Journal of Chemistry, 2017. **2017**: p. 11.
117. Ahmad, M., et al., *Trichloroethylene adsorption by pine needle biochars produced at various pyrolysis temperatures.* Bioresource Technology, 2013. **143**: p. 615-622.
118. Kajjumba, G.W., et al., *Modelling of adsorption kinetic processes—errors, theory and application.* Advanced sorption process applications, 2018: p. 187-206.
119. Qiu, H., et al., *Critical review in adsorption kinetic models.* Journal of Zhejiang University-Science A, 2009. **10**(5): p. 716-724.
120. Jung, C., et al., *Adsorption of selected endocrine disrupting compounds and pharmaceuticals on activated biochars.* Journal of Hazardous Materials, 2013. **263**: p. 702-710.
121. Ashoori, N., et al., *Evaluation of pilot-scale biochar-amended woodchip bioreactors to remove nitrate, metals, and trace organic contaminants from urban stormwater runoff.* Water research, 2019. **154**: p. 1-11.
122. Ulrich, B.A., et al., *Biochar and activated carbon for enhanced trace organic contaminant retention in stormwater infiltration systems.* Environmental science & technology, 2015. **49**(10): p. 6222-6230.
123. Marsh, H. and F. Rodríguez-Reinoso, *CHAPTER 4 - Characterization of Activated Carbon*, in *Activated Carbon*, H. Marsh and F. Rodríguez-Reinoso, Editors. 2006, Elsevier Science Ltd: Oxford. p. 143-242.
124. Kearns, J., E. Dickenson, and D. Knappe, *Enabling organic micropollutant removal from water by full-scale biochar and activated carbon adsorbers using predictions from bench-scale column data.* Environmental Engineering Science, 2020. **37**(7): p. 459-471.
125. Park, J.-H., et al., *Competitive adsorption and selectivity sequence of heavy metals by chicken bone-derived biochar: batch and column experiment.* Journal of Environmental Science and Health, Part A, 2015. **50**(11): p. 1194-1204.
126. Mahdi, Z., J.Y. Qiming, and A. El Hanandeh, *Removal of lead (II) from aqueous solution using date seed-derived biochar: batch and column studies.* Applied Water Science, 2018. **8**(6): p. 1-13.
127. Mahdi, Z., Q.J. Yu, and A. El Hanandeh, *Investigation of the kinetics and mechanisms of nickel and copper ions adsorption from aqueous solutions by date seed derived biochar.* Journal of environmental chemical engineering, 2018. **6**(1): p. 1171-1181.
128. Boni, M.R., A. Chiavola, and S. Marzeddu, *Application of biochar to the remediation of Pb-contaminated solutions.* Sustainability, 2018. **10**(12): p. 4440.
129. Hong, N., et al., *Assessing the effect of surface hydrophobicity/hydrophilicity on pollutant leaching potential of biochar in water treatment.* Journal of Industrial and Engineering Chemistry, 2020. **89**: p. 222-232.
130. Yuan, H., et al., *Sewage sludge biochar: Nutrient composition and its effect on the leaching of soil nutrients.* Geoderma, 2016. **267**: p. 17-23.
131. Chen, X., et al., *Leaching of polycyclic aromatic hydrocarbons (PAHs) from sewage sludge-derived biochar.* Chemical Engineering Journal, 2019. **373**: p. 840-845.
132. ChemAxon, *Chemicalize*. 2021.
133. Inyang, M., et al., *Synthesis, characterization, and dye sorption ability of carbon nanotube–biochar nanocomposites.* Chemical Engineering Journal, 2014. **236**: p. 39-46.
134. Mahmoud, D.K., et al., *Batch adsorption of basic dye using acid treated kenaf fibre char: equilibrium, kinetic and thermodynamic studies.* Chemical Engineering Journal, 2012. **181**: p. 449-457.
135. Park, J.-H., et al., *Adsorption/desorption behavior of cationic and anionic dyes by biochars prepared at normal and high pyrolysis temperatures.* Colloids and Surfaces A: Physicochemical and Engineering Aspects, 2019. **572**: p. 274-282.

136. Jian, X., et al., *Comparison of characterization and adsorption of biochars produced from hydrothermal carbonization and pyrolysis.* Environmental Technology & Innovation, 2018. **10**: p. 27-35.
137. Parra-Marfíl, A., et al., *Synthesis and characterization of hydrochar from industrial Capsicum annuum seeds and its application for the adsorptive removal of methylene blue from water.* Environmental research, 2020. **184**: p. 109334.
138. Nguyen, D.H., et al., *Effect of nitric acid oxidation on the surface of hydrochars to sorb methylene blue: An adsorption mechanism comparison.* Adsorption Science & Technology, 2019. **37**(7-8): p. 607-622.
139. Xu, R.-k., et al., *Adsorption of methyl violet from aqueous solutions by the biochars derived from crop residues.* Bioresource technology, 2011. **102**(22): p. 10293-10298.
140. Hameed, B. and A. Rahman, *Removal of phenol from aqueous solutions by adsorption onto activated carbon prepared from biomass material.* Journal of hazardous materials, 2008. **160**(2-3): p. 576-581.
141. Liu, C.-H., et al., *Sorption of lincomycin by manure-derived biochars from water.* Journal of environmental quality, 2016. **45**(2): p. 519.
142. Inyang, M., et al., *Sorption and cosorption of lead and sulfapyridine on carbon nanotube-modified biochars.* Environmental Science and Pollution Research, 2015. **22**(3): p. 1868-1876.
143. Liu, P., et al., *Modification of bio-char derived from fast pyrolysis of biomass and its application in removal of tetracycline from aqueous solution.* Bioresource technology, 2012. **121**: p. 235-240.
144. Xie, M., et al., *Adsorption of sulfonamides to demineralized pine wood biochars prepared under different thermochemical conditions.* Environmental Pollution, 2014. **186**: p. 187-194.
145. Ni, J., J.J. Pignatello, and B. Xing, *Adsorption of aromatic carboxylate ions to black carbon (biochar) is accompanied by proton exchange with water.* Environmental science & technology, 2011. **45**(21): p. 9240-9248.
146. Qiu, Y., et al., *Effectiveness and mechanisms of dye adsorption on a straw-based biochar.* Bioresource technology, 2009. **100**(21): p. 5348-5351.
147. Lin, Y.-C., et al., *Highly efficient adsorption of dyes by biochar derived from pigments-extracted macroalgae pyrolyzed at different temperature.* Bioresource technology, 2018. **259**: p. 104-110.
148. Li, Y., et al., *Microwave assisted hydrothermal preparation of rice straw hydrochars for adsorption of organics and heavy metals.* Bioresource technology, 2019. **273**: p. 136-143.
149. Li, Y., et al., *Production and optimization of bamboo hydrochars for adsorption of Congo red and 2-naphthol.* Bioresource technology, 2016. **207**: p. 379-386.
150. Kearns, J.P., et al., *2, 4-D adsorption to biochars: Effect of preparation conditions on equilibrium adsorption capacity and comparison with commercial activated carbon literature data.* Water research, 2014. **62**: p. 20-28.
151. Peng, B., et al., *Adsorption of antibiotics on graphene and biochar in aqueous solutions induced by π-π interactions.* Scientific reports, 2016. **6**(1): p. 1-10.
152. Jang, H.M. and E. Kan, *A novel hay-derived biochar for removal of tetracyclines in water.* Bioresource technology, 2019. **274**: p. 162-172.
153. Dai, Y., J. Li, and D. Shan, *Adsorption of tetracycline in aqueous solution by biochar derived from waste Auricularia auricula dregs.* Chemosphere, 2020. **238**: p. 124432.
154. Shang, J., et al., *Low-cost biochar derived from herbal residue: characterization and application for ciprofloxacin adsorption.* International journal of environmental science and technology, 2016. **13**(10): p. 2449-2458.
155. Zhang, L., et al., *Adsorption of chlortetracycline onto biochar derived from corn cob and sugarcane bagasse.* Water Science and Technology, 2018. **78**(6): p. 1336-1347.

156. Chen, B., Z. Chen, and S. Lv, *A novel magnetic biochar efficiently sorbs organic pollutants and phosphate.* Bioresource technology, 2011. **102**(2): p. 716-723.
157. Sun, K., et al., *Sorption of bisphenol A, 17α-ethinyl estradiol and phenanthrene on thermally and hydrothermally produced biochars.* Bioresource Technology, 2011. **102**(10): p. 5757-5763.
158. Cao, X., et al., *Dairy-manure derived biochar effectively sorbs lead and atrazine.* Environmental science & technology, 2009. **43**(9): p. 3285-3291.
159. Chen, B. and Z. Chen, *Sorption of naphthalene and 1-naphthol by biochars of orange peels with different pyrolytic temperatures.* Chemosphere, 2009. **76**(1): p. 127-133.
160. Kasozi, G.N., et al., *Catechol and humic acid sorption onto a range of laboratory-produced black carbons (biochars).* Environmental science & technology, 2010. **44**(16): p. 6189-6195.
161. Zhang, P., et al., *Adsorption and catalytic hydrolysis of carbaryl and atrazine on pig manure-derived biochars: impact of structural properties of biochars.* Journal of hazardous materials, 2013. **244**: p. 217-224.
162. Karakoyun, N., et al., *Hydrogel–Biochar composites for effective organic contaminant removal from aqueous media.* Desalination, 2011. **280**(1-3): p. 319-325.
163. Reddy, K.R., T. Xie, and S. Dastgheibi, *Evaluation of biochar as a potential filter media for the removal of mixed contaminants from urban storm water runoff.* Journal of Environmental Engineering, 2014. **140**(12): p. 04014043.
164. Inyang, M. and E. Dickenson, *The potential role of biochar in the removal of organic and microbial contaminants from potable and reuse water: a review.* Chemosphere, 2015. **134**: p. 232-240.
165. Upton, G. and I. Cook, *Understanding statistics*. 1996: Oxford University Press.
166. Park, J., et al., *Activated carbon from biochar: Influence of its physicochemical properties on the sorption characteristics of phenanthrene.* Bioresource technology, 2013. **149**: p. 383-389.
167. Ania, C., et al., *Importance of the hydrophobic character of activated carbons on the removal of naphthalene from the aqueous phase.* Adsorption Science & Technology, 2007. **25**(3-4): p. 155-167.
168. Ding, Z., et al. *Sorption of polycyclic aromatic hydrocarbons by biochars of wheat straw with different pyrolysis temperatures*. in *IOP Conference Series: Earth and Environmental Science*. 2019. IOP Publishing.
169. Ravichandran, P., et al., *Optimizing the route for production of activated carbon from Casuarina equisetifolia fruit waste.* Royal Society open science, 2018. **5**(7): p. 171578.
170. Gai, X., et al., *Effects of feedstock and pyrolysis temperature on biochar adsorption of ammonium and nitrate.* PloS one, 2014. **9**(12): p. e113888.
171. Grung, B. and R. Manne, *Missing values in principal component analysis.* Chemometrics and Intelligent Laboratory Systems, 1998. **42**(1-2): p. 125-139.
172. VV. AA., *Global and China Activated Carbon Industry Report, 2018-2023*. 2018.
173. Gopinath, A., et al., *Conversion of sewage sludge into biochar: A potential resource in water and wastewater treatment.* Environmental Research, 2021. **194**: p. 110656.
174. Karim, A.A., et al., *Enrichment of primary macronutrients in biochar for sustainable agriculture: A review.* Critical Reviews in Environmental Science and Technology, 2020: p. 1-42.
175. European Commission, *Water Framework Directive, ENV 09-018, https://ec.europa.eu/environment/pubs/pdf/factsheets/water-framework-directive.pdf.* 2010.
176. Ali, I. and V. Gupta, *Advances in water treatment by adsorption technology.* Nature protocols, 2006. **1**(6): p. 2661.

177. Perrich, J.R., *Activated carbon adsorption for wastewater treatment*. 2018: CRC press.
178. Kyzas, G.Z. and K.A. Matis, *Nanoadsorbents for pollutants removal: A review.* Journal of Molecular Liquids, 2015. **203**: p. 159-168.
179. Rivoira, L., et al., *Functionalized iron oxide/SBA-15 sorbent: investigation of adsorption performance towards glyphosate herbicide.* Environ Sci Pollut Res Int, 2016. **23**(21): p. 21682-21691.
180. Bruzzoniti, M.C., et al., *Polymer-derived ceramic aerogels as sorbent materials for the removal of organic dyes from aqueous solutions.* Journal of the American Ceramic Society, 2018. **101**(2): p. 821-830.
181. Jana, P., et al., *Processing of polymer-derived silicon carbide foams and their adsorption capacity for non-steroidal anti-inflammatory drugs.* Ceramics International, 2016. **42**(16): p. 18937-18943.
182. McHenry, M.P., *Carbon-based stock feed additives: a research methodology that explores ecologically delivered C biosequestration, alongside live weights, feed use efficiency, soil nutrient retention, and perennial fodder plantations.* Journal of the Science of Food and Agriculture, 2010. **90**(2): p. 183-187.
183. Singh, B., B.P. Singh, and A.L. Cowie, *Characterisation and evaluation of biochars for their application as a soil amendment.* Soil Research, 2010. **48**(7): p. 516-525.
184. Palansooriya, K.N., et al., *Occurrence of contaminants in drinking water sources and the potential of biochar for water quality improvement: A review.* Critical Reviews in Environmental Science and Technology, 2020. **50**(6): p. 549-611.
185. European Biochar Foundation (EBC), *EBC (2012) European Biochar Certificate - Guidelines for a Sustainable Production of Biochar. Arbaz, Switzerland. http://www.europeanbiochar.org/en/download. Version 8.2E of 19th April 2019, DOI: 10.13140/RG.2.1.4658.7043.*
186. Comite Europeen de Normalisation (CEN), *EN 12902:2004 Products used for treatment of water intended for human consumption - Inorganic supporting and filtering materials - Methods of test.* 2004.
187. Comite Europeen de Normalisation (CEN), *EN 12915-1:2009 Products used for the treatment of water intended for human consumption. Granular activated carbon. Virgin granular activated carbon.* 2009.
188. Wang, X., et al., *Recent advances in biochar application for water and wastewater treatment: a review.* PeerJ, 2020. **8**: p. e9164-e9164.
189. Gwenzi, W., et al., *Biochar-based water treatment systems as a potential low-cost and sustainable technology for clean water provision.* Journal of Environmental Management, 2017. **197**: p. 732-749.
190. Del Bubba, M., et al., *Physicochemical properties and sorption capacities of sawdust-based biochars and commercial activated carbons towards ethoxylated alkylphenols and their phenolic metabolites in effluent wastewater from a textile district.* Science of the Total Environment, 2020.
191. Castiglioni, M., et al., *Characterization techniques as supporting tools for the interpretation of biochar adsorption efficiency in water treatment: a critical review.* Molecules, 2021. **26, 5063**: p. 1-22.
192. Bruzzoniti, M.C., et al., *Towards the revision of the drinking water directive 98/83/EC. Development of a direct injection ion chromatographic-tandem mass spectrometric method for the monitoring of fifteen common and emerging disinfection by-products along the drinking water supply chain.* Journal of Chromatography A, 2019. **1605, 360350**.
193. Hou, Y., W. Chu, and M. Ma, *Carbonaceous and nitrogenous disinfection by-product formation in the surface and ground water treatment plants using Yellow River as water source.* Journal of Environmental Sciences, 2012. **24**(7): p. 1204-1209.

194. Lahaniatis, E.S., et al., *Formation of chlorinated hydrocarbons by water chlorination.* Chemosphere, 1994. **28**(2): p. 229-235.
195. World Health Organization, *Guidelines for drinking-water quality, available at https://apps.who.int/iris/bitstream/handle/10665/254637/9789241549950-eng.pdf?sequence=1&isAllowed=y.* 2017.
196. Martínez, E., et al., *Multicomponent analysis of volatile organic compounds in water by automated purge and trap coupled to gas chromatography–mass spectrometry.* Journal of Chromatography A, 2002. **959**(1): p. 181-190.
197. American Standard Test Method (ASTM), *D2866-11 Standard Test Method for Total Ash Content of Activated Carbon.* 2018.
198. Rivoira, L., et al., *Impact of effluents from wastewater treatments reused for irrigation: Strawberry as case study.* Environmental Engineering and Management Journal, 2019. **18**(10): p. 2133-2143.
199. Bruzzoniti, M.C., et al., *Extraction of Polycyclic Aromatic Hydrocarbons and Polychlorinated Biphenyls from Urban and Olive Mill Wastewaters Intended for Reuse in Agricultural Irrigation.* J AOAC Int, 2019.
200. Conseil Européen des Fédérations de l'Industrie Chimique (CEFIC), *Test Methods for Activated Carbon, available at https://acpa.cefic.org/images/Test_method_for_Activated_Carbon_86.pdf.* 1986.
201. American Society for Testing and Materials, *Standard Test Method for Carbon Black—Total and External Surface Area by Nitrogen Adsorption (ASTM-D6556-10). ASTM International, West Conshohocken, PA.* 2012.
202. American Society for Testing and Materials, *Standard Practice for Calculation of Pore Size Distributions of Catalysts and Catalyst Carriers from Nitrogen Desorption Isotherms (ASTM-D4641-17). ASTM International, West Conshohocken, PA.* 2017.
203. American Standard Test Method (ASTM), *D 5919-96 Standard Practice for Determination of Adsorptive Capacity of Activated Carbon by a Micro-Isotherm Technique for Adsorbates at ppb Concentrations.* 1996.
204. Foo, K.Y. and B.H. Hameed, *Insights into the modeling of adsorption isotherm systems.* Chemical engineering journal, 2010. **156**(1): p. 2-10.
205. Tomczyk, A., Z. Sokołowska, and P. Boguta, *Biochar physicochemical properties: pyrolysis temperature and feedstock kind effects.* Reviews in Environmental Science and Bio/Technology, 2020. **19**(1): p. 191-215.
206. Fryda, L. and R. Visser, *Biochar for Soil Improvement: Evaluation of Biochar from Gasification and Slow Pyrolysis.* Agriculture, 2015. **5**(4): p. 1076-1115.
207. Rafiq, M.K., et al., *Influence of pyrolysis temperature on physico-chemical properties of corn stover (Zea mays L.) biochar and feasibility for carbon capture and energy balance.* PloS one, 2016. **11**(6): p. e0156894.
208. Brewer, C.E., et al., *Characterization of biochar from fast pyrolysis and gasification systems.* Environmental Progress & Sustainable Energy, 2009. **28**(3): p. 386-396.
209. Wang, C., Y. Wang, and H. Herath, *Polycyclic aromatic hydrocarbons (PAHs) in biochar–Their formation, occurrence and analysis: A review.* Organic Geochemistry, 2017. **114**: p. 1-11.
210. Lievens, C., et al., *Fast pyrolysis of heavy metal contaminated willow: Influence of the plant part.* Fuel, 2009. **88**(8): p. 1417-1425.
211. International Biochar Initiative, *Standardized Product Definition and Product Testing Guidelines for Biochar That Is Used in Soil available at https://www.biochar-international.org/wp-content/uploads/2018/04/IBI_Biochar_Standards_V2.1_Final.pdf.* 2015.
212. Lyu, H., et al., *Effect of pyrolysis temperature on potential toxicity of biochar if applied to the environment.* Environmental pollution, 2016. **218**: p. 1-7.

213. Berardi, C., et al., *Removal efficiency and mass balance of polycyclic aromatic hydrocarbons, phthalates, ethoxylated alkylphenols and alkylphenols in a mixed textile-domestic wastewater treatment plant.* Science of The Total Environment, 2019. **674**: p. 36-48.
214. Parker, D.S., et al., *Hydrogen abstraction/acetylene addition revealed.* Angewandte Chemie International Edition, 2014. **53**(30): p. 7740-7744.
215. Reed, K.W.a.D., *IBI White Paper, Implications and Risks of Potential Dioxin Presence in Biochar, available at https://biochar-international.org/ibi-publications/.*
216. Ippolito, J.A., et al., *Feedstock choice, pyrolysis temperature and type influence biochar characteristics: a comprehensive meta-data analysis review.* Biochar, 2020. **2**(4): p. 421-438.
217. Li, H., et al., *Mechanisms of metal sorption by biochars: Biochar characteristics and modifications.* Chemosphere, 2017. **178**: p. 466-478.
218. Liu, Z., F.-S. Zhang, and J. Wu, *Characterization and application of chars produced from pinewood pyrolysis and hydrothermal treatment.* Fuel, 2010. **89**(2): p. 510-514.
219. Chen, W., et al., *Characteristics of wood-derived biochars produced at different temperatures before and after deashing: Their different potential advantages in environmental applications.* Science of The Total Environment, 2019. **651**: p. 2762-2771.
220. Chen, D., et al., *Pyrolysis polygeneration of pine nut shell: Quality of pyrolysis products and study on the preparation of activated carbon from biochar.* Bioresource Technology, 2016. **216**: p. 629-636.
221. Grojzdek, M., et al., *Pyrolysis of different wood species: influence of process conditions on biochar properties and gas-phase composition.* Biomass Conversion and Biorefinery, 2021: p. 1-11.
222. Hansen, V., et al., *The effect of straw and wood gasification biochar on carbon sequestration, selected soil fertility indicators and functional groups in soil: an incubation study.* Geoderma, 2016. **269**: p. 99-107.
223. European Centre for Ecotoxicology and Toxicology of Chemicals (ECETOC), *Environmental exposure assessment of ionisable organic compounds, Technical Report No. 123. Brussels.* 2013.

3. Amino-modified SBA-15 for the Removal of Sugars from Food and Beverage wastewaters

M. Castiglioni, L. Rivoira, M. Gallo, I. Ingrando, M. Del Bubba, B. Onida, M. C. Bruzzoniti, (2021)
"Removal of sugars from food and beverage wastewaters by amino-modified SBA-15",
Journal of Cleaner Production, 324, 129236

3.1 Introduction

Sugars are present in food matrices both as additives or as natural components. Their presence poses some concerns in the field of environmental chemistry [1, 2]. In fact, sugars from food and beverage industrial wastewaters (e.g. sugar, carbonated soft-drink industries) can impact on the water quality with Biochemical Oxygen Demand (BOD_5) as high as 5,000-8,000 mg/L [3]. These BOD_5 values are far higher than the limits imposed by regulations for discharging into natural waters and in sewage systems, thus exceeding the capabilities of the local sewage treatment plant. Therefore, wastewaters from such industrial processes needs in-site treatment before being discharged in municipal sewerage systems. For encouraging the control of trade wastewaters by industrial consumers, some local quality water management offices, such as that of New South Wales, impose discharge fees calculated on the basis of BOD_5 concentration in the liquid trade waste discharged [4, 5], thus preventing the increase of BOD_5 by an a-priori strategy.

The treatment methods of wastewater effluents from sugar [6], artificial sweeteners [7], confectionary [8] and soft-drink [3] industries are reviewed or discussed by several authors. The most used treatment approach to remove BOD_5 relies on biological processes. For example, in the wastewater treatment of soft-drink industries, the anaerobic stage can reduce BOD_5 from a few thousand to a few hundred mg/L, but additional aerobic treatment is still required for the effluent to meet the regulations [9]. Chemical and physical treatment processes (e.g., coagulation and sedimentation/flotation)

are also used to reduce the organic content before the wastewater enters the biological treatment. Various technological solutions (e.g. bio-reactors of nano-ceramic gel with deposited biofilm [10]) are proposed in the market as stand-alone solutions for the pre-treatment of sugar wastewater.

On the other side, the reuse of wastewater for non-potable purposes is encouraged by many EU policies and has the advantage of being an economically viable solution. The treated effluent of food and beverages industries can be used as such or after dilution with other freshwater for irrigation purposes [2, 11] and for reutilization in industrial aqueducts [6], provided that the presence of sugars is limited, as sugars provides nutrients to support bacterial growth responsible of microbial fouling on surfaces [12]. Adsorption techniques based on different kinds of substrates like bentonite and lignite [13], bagasse fly ash [14] and silica [12] were identified as alternative economic approaches for pre-treatments of food and beverages wastewaters and they deserve further insights.

Ordered mesoporous silicas and organosilicas have been largely investigated as adsorbents [15-17], due to their high specific surface area and uniform porosity, together with the possibility of tailoring their surface chemical properties through synthesis conditions and post-synthesis modification.

Mesoporous silica functionalized with amino groups was previously investigated for adsorption and removal of anionic pollutants in drinking and wastewater [18, 19].

The aim of this part of PhD thesis is to show the capabilities of ordered mesoporous silica of SBA-15 family functionalized with primary and secondary amino groups (3-aminopropyl)-triethoxysilane and N-3-trimethoxypropylaniline, respectively) to be used for the removal of sugars. Glucose, fructose and sucrose, the disaccharide derivative of glucose and fructose, were chosen since they are commonly present in the food and beverage industry processes and since they are naturally contained in fruit.

The SBA-15 was functionalized in laboratory and its physico-chemical properties were characterized. The adsorption behaviour towards glucose, fructose and sucrose at higher concentrations than those really found in soft-drink wastewaters was studied as a function of pH and sorbent amount.
As a proof of concept, the suitability of the use of amino modified SBA-15 as adsorbent for the reduction of the BOD_5 in industrial wastewaters was finally tested, simulating the typical composition of wastewater from a soft drink production process.

3.2 Material and methods

The reagents and the experimental procedures followed are hereafter described.

3.2.1 Reagents

Ordered mesoporous silica of the SBA-15 (ACS Material Advanced Chemical, Pasadena, CA, USA) was used. For functionalization of SBA-15, (3-aminopropyl) triethoxysilane (APTES, 99 %), N-[3-(Trimethoxysilyl)propyl]aniline, toluene (99.8 %) from Sigma Aldrich (Steinheim, DE) were used. D(+) glucose was from Merck (Darmstadt, DE), D(-), whereas fructose and sucrose were from J.T. Baker (Phillipsburg, NJ, USA).
Hydrochloric acid (35 % w/w, d = 1.187 g/ml) and NaOH (>98 %) were from Carlo Erba (Milano, IT). All reagents used were of analytical grade. For standard solution and eluent preparation, high-purity water (18.2 M Ω·cm resistivity at 25°C) produced by an Elix-Milli Q Academic system (Millipore, Vimodrone, MI, Italy) was used.

3.2.2 Preparation of sorbents

SBA-15 (1 g) previously washed with deionized water (50 mL), was stirred with toluene (200 mL) for 30 minutes, at room temperature. The functionalizing reagent (2 mL of APTES or N-[3-(trimethoxysilyl)propyl]aniline) was added dropwise. The flask with the solution was heated to 110 ° C, after connection to a water-refrigerated system. The solution, kept under stirring for 24 hours at room temperature, was filtered and dried, according to previous work [18, 19].

For the sake of clarity, the sample functionalized with APTES is labelled as S-APTES and the sample functionalized with N-[3-(trimethoxysilyl)propyl]aniline as S-Aniline.

3.2.3 Physico-chemical characterization

For the measurement of nitrogen adsorption-desorption isotherms, a Quantachrome AUTOSORB-1 (Boynton Beach, FL, USA) was used. Before measurement, S-APTES and S-Aniline samples were outgassed (393 K, 6 h). The BET specific surface areas (SSA_{BET}) were calculated in the relative pressure range 0.04-0.1; pore size distribution was determined through the NLDFT (Non-Localized Density Functional Theory) method, using the equilibrium model for cylindrical pores.

TG analyses were obtained between 298 K and 1,073 K in air (flow rate: 100 mL/min, heating rate: 10 K/min) by a SETARAM 92 (Caluire, France) instrument.

Infrared spectroscopy characterization was carried out on powders pressed in self-supporting wafers. Spectra were recorded at room temperature with a Bruker Tensor 27 (Bruker, Billerica, MA, USA) spectrometer operating at 2 cm^{-1} resolution, after outgassing the sample at room temperature (residual pressure of 0.1 Pa).

3.2.4 Analysis of sugars

Sugar content was determined by ion-chromatography (ICS-3000 gradient pump, Thermo Fisher Scientific, Waltham, MA, USA), coupled to pulsed amperometric detection (AD40 Electrochemical Detector, Thermo Fisher Scientific), equipped with Ag/AgCl reference and a gold working electrode. The detection potential was 0.1 V (400 ms: 200 ms as delay time and 200 ms as determination time). The potential was then instantaneously set at -2 V (10 ms) and at 0.6 V (10 ms) to restore the gold oxide on the working electrode surface. The potential was finally set at -0.1V (60 ms).

The column used was a CarboPacPA10, 250x4 mm (100 μeq/column), Thermo Fisher Scientific. Sample loop was 10 μL. After optimization (data available upon request), the eluent concentration was 55 mM KOH.

Before injection, solutions were diluted in order to achieve a final concentration within 500 μg/L and 1 mg/L, so as to avoid column overload. Data were collected and managed by the Chromeleon v.6.80 software (Thermo Fisher Scientific).

3.2.4.1 Detection limits

Limits of detections (LOD) were expressed as $s_m=s_m+3s_b$, with s_m=average signal of blank, s_b= standard deviation of blank on 10 measurements and were 69, 56 and 11 μg/L for glucose, fructose and sucrose, respectively.

3.2.5 Simulated wastewater samples

As a proof of concept, the use of the amino-modified SBA-15 was tested in the treatment of wastewaters derived from the soft-drink industry. In detail, a simulated wastewater sample (SD-WW) was prepared according to the maximum levels of contamination reported for this type of effluent [20]. Hence, the simulated soft-drink wastewater contained 70 mg/L K^+, 20 mg/L Fe^{3+}, 2,500 mg/L Na^+, 300 mg/L NH_4^+, 5 mg/L Zn^{2+}, 2.5 mg/L Ni^{2+}, 8 mg/L

Co^{2+}, 20 mg/L SO_4^{2-}, 40 mg/L PO_4^{3-}. In this matrix, the BOD_5 of 5,000 mg/L was obtained in two different ways: (i) by adding 4,500 ppm of sucrose (SD-WW-suc) and (ii) by adding a proper volume of a cola-like drink (SD-WW-cola) which original contained 10.9 g sugars. The final pH of the two samples was of 4.1 and 3.0, respectively.

3.2.6 Adsorption tests

Adsorption tests on simulated wastewaters were carried out in triplicate with a $6 \cdot 10^{-5}$ g:L adsorbent:solution ratio, at room temperature under stirring 1,100 xg for 1 h.

Preliminary tests on sugars solution were also performed to investigate the role of parameters such as pH and solid:liquid ratio, by the one-variable at a time method.

3.2.6.1 Effect of pH

Tests were performed in triplicate on 0.25 g of sorbent (S-APTES/S-Aniline) put in contact with 4 mL solution containing a mixture of 350,000 mg/L glucose, 350,000 mg/L fructose and 170,000 mg/L sucrose, stirred at 1,100 xg between 10 and 60 min. These concentrations can be considered representative of the sugar content in some kinds of fruit, i.e. strawberries [21] and precautionary, about 70-folds higher, in respect to an average BOD_5 of wastewaters of sugary drink production [22, 23]. Experiments were performed at pH 2.1, 5.0 and 8.5; for each pH value, experiments were performed in triplicate.

3.2.6.2 Solid:liquid ratio (effect of sorbent amount)

Tests were performed in triplicate using different adsorbent amounts with the same sugar solution volume. In detail, amounts of adsorbent were 0.1 g and 0.25 g for the two tests. These amounts of adsorbent were put in contact

with 4 mL of solution (pH 2.1) containing 350,000 mg/L glucose and fructose and 170,000 mg/L sucrose and kept under stirring between 10 and 60 min. The solid:liquid (S:L) ratios in the two tests were 1:16 and 1:40 for 0.1 g and 0.25 g of adsorbent, respectively. These values can be expressed as mg:L ratios, which are 0.025 mg/L and 0.06 mg/L.

3.3 Results and discussion

The results obtained by the physico-chemical characterization are hereafter discussed.

3.3.1 Physico-chemical features

S-APTES and S-Aniline were characterized by nitrogen adsorption-desorption isotherms (Figure 3.1). For both samples, isotherms are type IV according to IUPAC classification, which are typical of mesoporous materials. Hysteresis loops are type H1, revealing well-defined cylindrical-like pores. Figure 3.2 reports the pore size distributions, which appear narrow and unimodal for both materials, confirming their uniform porosity.

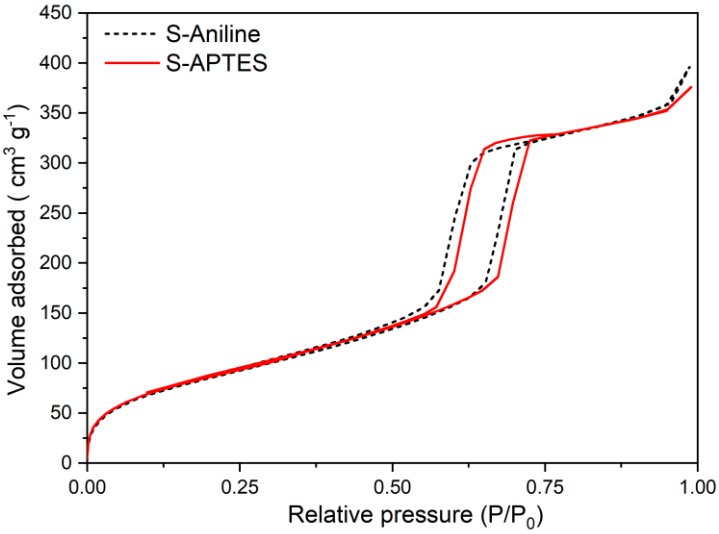

Figure 3.1. Nitrogen adsorption-desorption isotherms at 77 K of S-Aniline and S-APTES

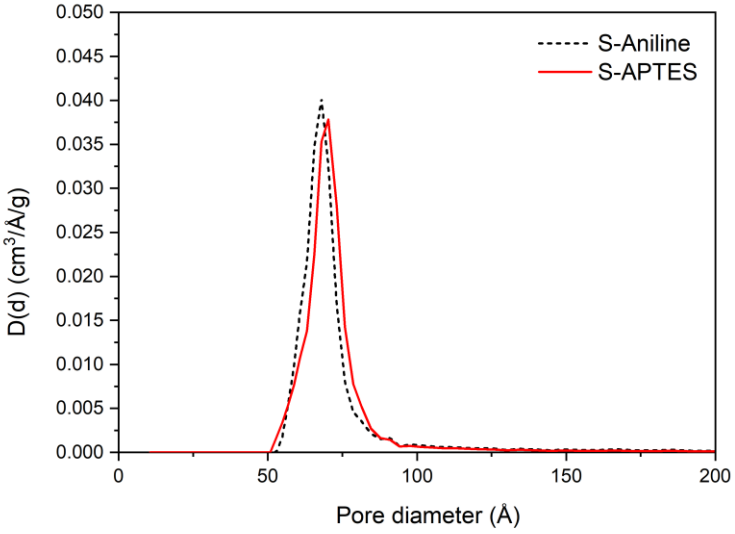

Figure 3.2. Pore size distributions (NLDFT) of S-Aniline and S-APTES.

In respect to the pristine SBA-15 (SSA_{BET}=490 m^2/g, pore volume 0.92 cm^3/g, pore diameter 81 Å [18, 19], the textural properties of functionalized sorbents are in agreement with the grafting of the amino groups on the SBA-15 internal surface. Indeed, for S-APTES, SSA_{BET} is reduced to 325 m^2/g, pore volume is equal to 0.53 cm^3/g and pore diameter results 70 Å and for S-Aniline, the corresponding values are 299 m^2/g, 0.54 cm^3/g, and 68 Å, respectively.
The presence of functional groups in S-APTES and S-Aniline was confirmed by FTIR spectra (Fig. 3.3).

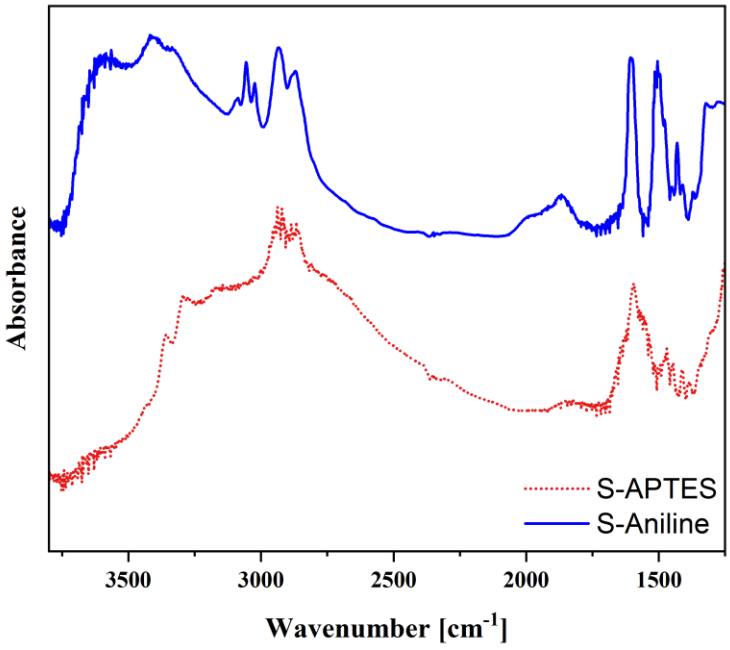

Figure 3.3. FT-IR Spectra of S-APTES (red dotted curve) and S-Aniline (blue curve).

By TG analysis, the amount of amino groups in S-APTES and S-Aniline was estimated. Figure 3.4 shows the percentage mass loss measured between 298 K and 1073 K in air flow.

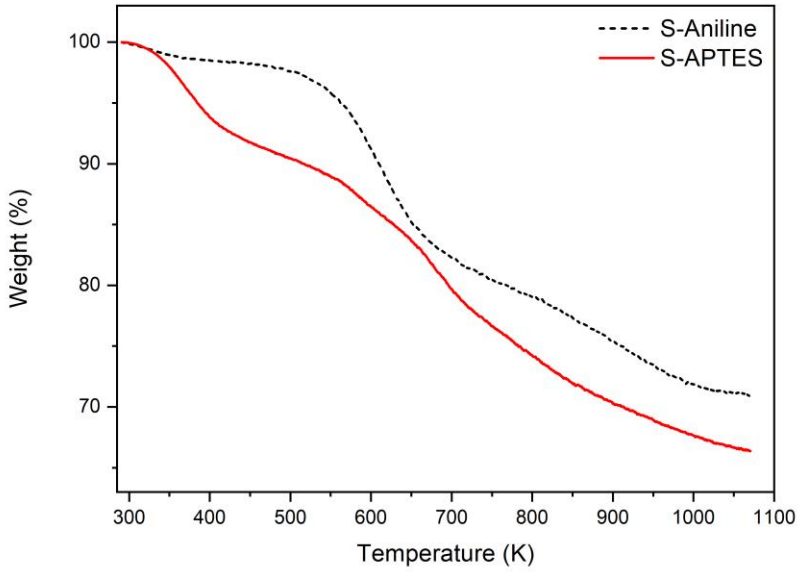

Figure 3.4. Thermogravimetric analysis of S-Aniline and S-APTES

The first mass loss is observed between 298 K and 473 K which is ascribed to molecular water desorption. This loss is lower for S-Aniline (almost negligible) than for S-APTES (about 10 % w/w) revealing a lower hydrophilicity of S-Aniline than S-APTES in agreement with the more hydrophobic functional moiety.

The weight loss above 473 K was ascribed to the combustion of grafted amines and it is 26.9 % for S-Aniline and 25.6 % for S-APTES. Based on the molecular weight assumed for the removed species, these values of mass loss allowed to estimate the content of surface amines which resulted to be 2.23 mmol/g for S-Aniline and 4.41 mmol/g for S-APTES (corresponding to $7.5 \cdot 10^{-21}$ mmol/nm^2 and to $13.6 \cdot 10^{-21}$ mmol/nm^2, respectively).

3.3.2 Adsorption experiments

The adsorption performance of S-APTES and S-Aniline were studied investigating the effect of the solution pH and the effect of solid:liquid ratio. Adsorption tests were also conducted in simulated soft-drink wastewaters. Results are hereafter described and discussed.

3.3.2.1 Effect of pH

The removal of sugars by the functionalized adsorbents was studied as a function of pH (2.1, 5.0 and 8.5) in view of a possible tuning of the removal conditions. It is worth mentioning that sugars are in the undissociated form at all the pH values investigated (pK_a=12.2 for glucose, 12.0 for fructose and 12.6 for sucrose).

As shown in Fig. 3.5, both S-APTES and S-Aniline are effective in the removal of sugars from water solution. This is ascribed to the interaction of sugar molecules with the amino groups grafted at the surface of SBA-15. Indeed, negligible adsorption of glucose from water solution was reported for bare SBA-15 by Majumdar et al. [24] and by Zhao and Shantz [25].

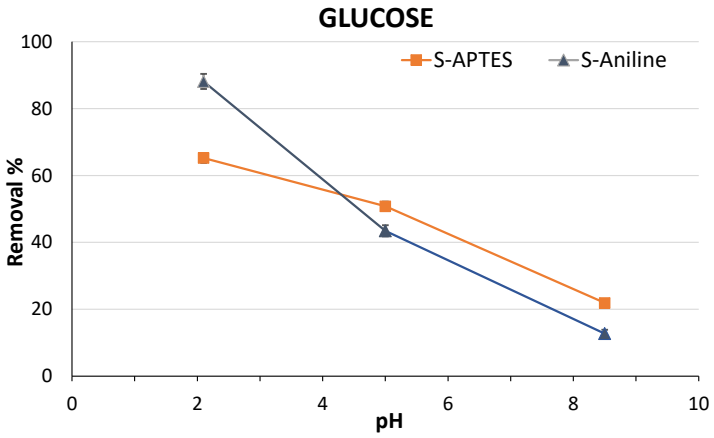

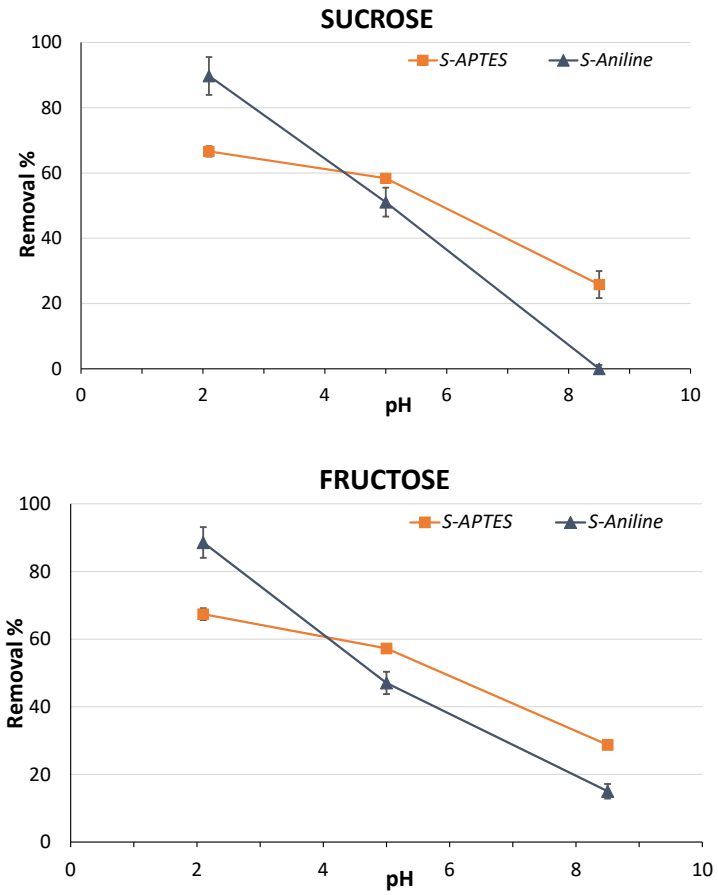

Figure 3.5. Effect of pH on sugar removal by S-APTES and S-Aniline. Error bars (n=3) are also reported. For experimental conditions, see text.

For S-APTES and S-Aniline removal capabilities decrease with the increase of pH: this may be explained considering the role of H-bonding between protonated amines (proton donor) and sugar molecules (proton acceptor) in the interaction between sugar molecules and adsorption sites [26]. In fact, with the variation of the pH of the solution, a change of the protonated amine concentrations occurs. Increasing the pH, the population of protonated amines decreases, thus decreasing the population of H-bonding donor sites. It is worth noting that the decreasing of the removal capabilities upon

increasing pH is larger for S-Aniline than for S-APTES. This may be due to the weaker basicity of propylaniline (pK_b 8.96) than propylamine (pK_b 3.5) so that the decrease of protonated amine population upon increasing pH is expected to be relatively larger in S-Aniline than S-APTES.

Since the highest removal yields were achieved at pH 2.1, further investigations were carried out at this pH value.

3.3.2.2 Solid:liquid ratio (effect of sorbent amount)

The choice of the most suitable S:L ratio is important for the correct dosage of adsorbent that minimize the mass of reagent required to achieve the desired performance, maximizing the cost-effectiveness of the approach. As shown by the data reported in Table 3.1, the use of higher S:L ratio 1:16 in respect to 1:40 improves removal performances. As a consequence, S:L=1:16 was used for the further removal tests. It is important to highlight that this S:L value, corresponding to $6 \cdot 10^{-5}$ g:L adsorbent:solution is seven orders of magnitude lower than the dosage reported for amorphous silica functionalized with APTES used to remove similar nominal amount of sucrose only (i.e. around 400 g/L ratio) [12].

Table 3.1. Removal performance of S-APTES and S-Aniline at different S:L ratios. Sugar concentrations: 350,000 mg/L glucose-fructose, 170,000 mg/L sucrose). Standard deviation (n=3) is also indicated.

Sorbent	***Sugar***	***Removal %***	
		S:L	
		1:40	**1:16**
S-APTES	Glucose	13.4 ± 3.0	65.2 ± 1.5
	Fructose	10.3 ± 1.1	67.4 ± 1.7
	Sucrose	14.4 ± 1.6	66.6 ± 1.6
S-Aniline	Glucose	11.7 ± 0.0	88.1 ± 2.3
	Fructose	12.8 ± 0.7	88.6 ± 4.6
	Sucrose	14.7 ± 1.0	89.7 ± 5.8

3.3.3 Sugar removal in simulated wastewaters

The functionalized S-APTES and S-Aniline were tested for real case applications on a simulated soft-drink wastewater (SD-WW) in which BOD_5 was obtained by adding sucrose (SD-WW-suc) or a cola-like beverage (SD-WW-cola).

As an example, the chromatograms obtained for simulated wastewaters derived from the soft-drink industry (SD-WW-cola) before and after the treatment with S-APTES and S-Aniline is reported in Figure 3.6.

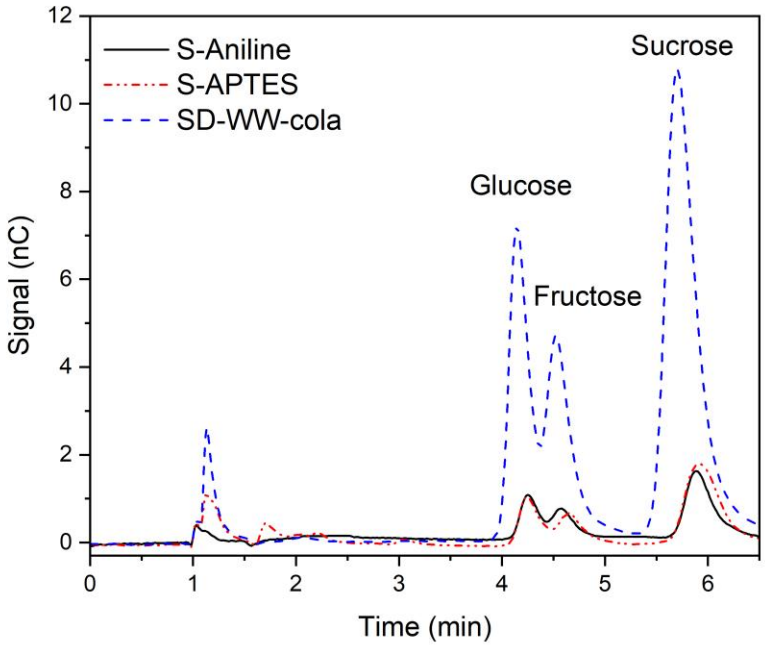

Figure 3.6. Chromatograms of simulated wastewaters derived from the soft-drink industry (SD-WW-cola) before (blue line) and after the treatment with S-APTES (red line) and S-Aniline (black line).

Figure 3.7A shows the abatement of BOD_5 (expressed as sucrose) in the simulated wastewater sample. In the case of SD-WW-suc, the abatement of BOD_5 is about 63 % (relative standard deviations, RSD, below 2 %) for both S-APTES and S-Aniline. For SD-WW-cola, the analysis allowed us to detect glucose, fructose and sucrose already present in the pristine cola-like drink. For this sample, the sugar removal capabilities for the two adsorbents were above (70 %, RSD< 7 %).

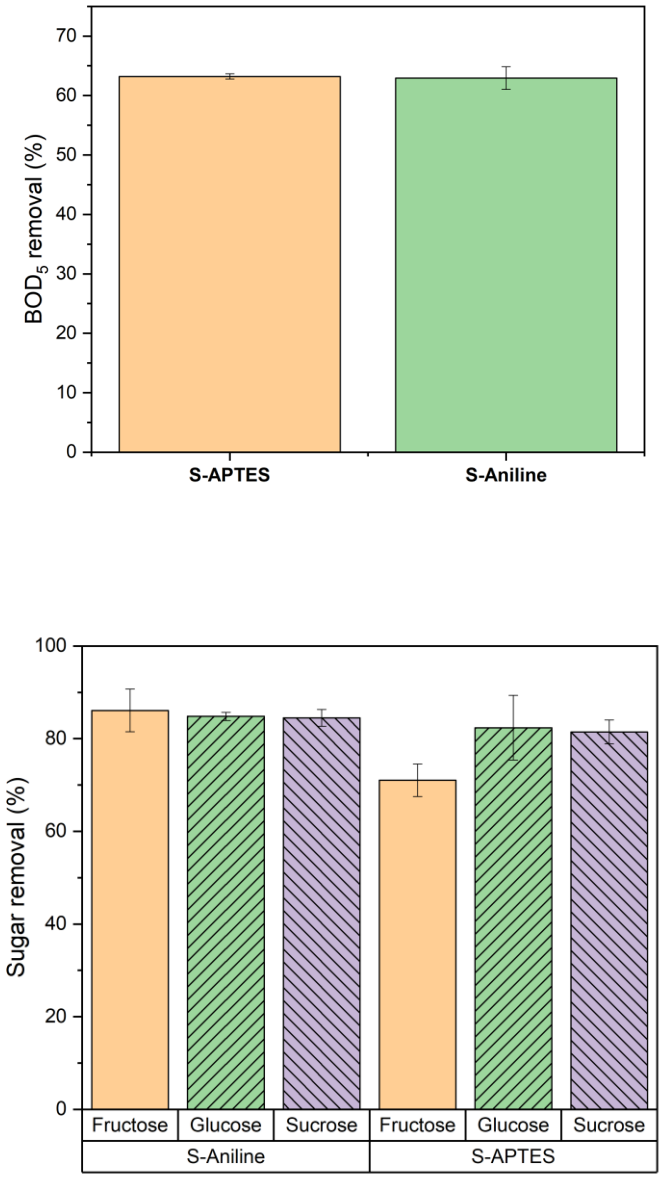

Figure 3.7. Removal of sugars from simulated wastewaters in which BOD_5 of 5,000 mg/L was obtained by adding sucrose (SD-WW-suc, A) or a cola-like beverage (SD-WW-cola, B). Error bars (n=3) are also reported.

The differences observed for the two simulated wastewater samples is ascribed to the different pH values of the samples (pH 4.1 for SD-WW-suc; 3.0 for SD-WW-cola), as detailed in section 3.3.2.1. The S-Aniline adsorbent exhibits higher removal than S-APTES for the three sugars in the SD-WW-cola test (Fig. 3.7B). This result is in agreement with previous results on adsorption of polycyclic aromatic hydrocarbons [21] and data in Fig. 3.4, showing higher removal for S-Aniline at low pH values (below pH 4). This effect cannot be ascribed to features such as SSA and concentration of adsorption sites which are both lower for S-Aniline (299 m^2/g and 2.23 mmol/g, respectively) than S-APTES (325 m^2/g and 4.41 mmol/g). The higher sugar removal observed for S-Aniline compared to that of S-APTES can be tentatively ascribed to its lower hydrophilicity, as revealed by molecular water loss in TGA analysis. This would cause a weaker competition of water molecules in the adsorption, so favouring the removal of organic solutes from water solution, similarly to what proposed for adsorption on activated carbons [27].

The organic load removal performance exhibited by S-Aniline and S-APTES are highly encouraging in respect to many processes reviewed by the literature.

Regarding other adsorption systems, the materials here proposed need lower adsorbent dosage (0.025 mg/L) and contact times (10 to 60 min) in respect to metakaolin or carbon (800 mg/L, for 180-240 min) to achieve comparable removal yields [28]. Amino modified amorphous silica used by Majewski et al. [12] proves to be capable to remove low organic load (BOD_5< 2 mg/L) with very high adsorbent dosage such as 100 g/L.

The BOD_5 removal by the proposed adsorbents demonstrates promising capabilities even towards the physico-chemical treatment (equalization and coagulation/flocculation) that usually precedes the biological treatment, which ensure BOD_5 removal of about 43% [9]. Worth to be mentioned that

BOD_5 removal by S-Aniline and S-APTES could also compete with high rate aerobic processes, which are characterized by BOD_5 removal of about 64 % [9].

The use of lower dosages of adsorbent reduces the management/disposal procedures of the exhausted material. This feature is expected to introduce costs saving and advantages especially over physico-chemical treatment where high concentrations of coagulant (500 mg/L [29]) or mixed coagulant/flocculant (100 mg/L / 25 mg/L) [30] are used to abate the organic load.

3.4 Conclusions

The ordered mesoporous SBA-15 modified with (3-aminopropyl)-triethoxysilane (S-APTES) and N-[3-(trimethoxysilyl)propyl]aniline (S-Aniline) allows to obtain adsorbents suitable for the removal of high concentrations of glucose, fructose, sucrose. This feature has been exploited to test them through this PhD thesis in the treatment of wastewater sample simulating the one derived from food process industry which are rich in the above-mentioned sugars and are characterized by high values of BOD_5.

The performance of S-APTES and S-Aniline adsorbents is pH dependent and is mainly ascribed to the formation of hydrogen bond which provide strong interactions with sugars. The better removal performance observed for S-Aniline is ascribed to the lower hydrophilicity of the functional group, which lead to weaker competition by water molecules. The efficient removal of BOD_5 by the modified SBA-15 adsorbents is achieved at an adsorbent dosage:solution ratio of $6 \cdot 10^{-5}$ g:L which is a far lower value than the ones usually reported in the literature with advantages even for disposal procedures at the end of the life cycle of the materials.

3.5 References

1. Ozgun, H., et al., *Confectionery industry: a case study on treatability-based effluent characterization and treatment system performance.* Water Science and Technology, 2012. **66**(1): p. 15-20.
2. Poddar, P.K. and O. Sahu, *Quality and management of wastewater in sugar industry.* Applied Water Science, 2017. **7**(1): p. 461-468.
3. Boguniewicz-Zabłocka, J., A.G. Capodaglio, and D. Vogel. *Analysis of wastewater treatment efficiency in a soft drinks industry*. in *E3S Web of Conferences*. 2017. EDP Sciences.
4. Sydney Water, *Industrial Consumers - Trade wastewater fees and charges for 2017-18.* 2017. p. 3.
5. Pagan, B. and P. Prasad, *The Queensland food eco-efficiency project: reducing risk and improving competitiveness.* Journal of Cleaner Production, 2007. **15**(8): p. 764-771.
6. Kushwaha, J.P., *A review on sugar industry wastewater: sources, treatment technologies, and reuse.* Desalination and Water Treatment, 2015. **53**(2): p. 309-318.
7. Pang, L., A.G.L. Borthwick, and E. Chatzisymeon, *Determination, occurrence, and treatment of saccharin in water: A review.* Journal of Cleaner Production, 2020. **270**: p. 122337.
8. Zajda, M. and U. Aleksander-Kwaterczak, *Wastewater Treatment Methods for Effluents from the Confectionery Industry–an Overview.* Journal of Ecological Engineering, 2019. **20**(9).
9. Seng, S.-S., Y.-T. Hung, and J. Paul Chen, *Soft Drink Waste Treatment*, in *Waste Treatment in the Food Processing Industry*. 2005, CRC Press. p. 255-269.
10. Biogill. *Food & Beverages Case Study*. 2015; Available from: http://www.biogill.com/uploads/74946/ufiles/Multinational_Confectionery_Company_Case_Study_October_2015.pdf.
11. Wang, Y. and L. Serventi, *Sustainability of dairy and soy processing: A review on wastewater recycling.* Journal of Cleaner Production, 2019. **237**: p. 117821.
12. Majewski, P., J. Luong, and K. Stretton, *The application of surface engineered silica for the treatment of sugar containing wastewater.* Water Science and Technology, 2012. **65**(1): p. 46-52.
13. Sunitha, M. and M.A. Rafeeq, *Sugar Industry Wastewater Treatment Using Adsorption‖.* Jr. of Industrial Pollution Control, 2009. **25**(2).
14. Lakdawala, M.M. and B.N. Oza, *Removal of BOD contributing components from sugar industry waste water using bagasse fly ash-waste material of sugar industry.* Der Chemica Sinica, 2011. **2**: p. 244-251.
15. Wu, Z. and D. Zhao, *Ordered mesoporous materials as adsorbents.* Chemical Communications, 2011. **47**(12): p. 3332-3338.
16. Li, C.M., et al., *Functionalized Porous Silica-Based Nano/Micro Particles for Environmental Remediation of Hazard Ions.* Nanomaterials, 2019. **9**(2): p. 247.
17. Bruzzoniti, M.C., et al., *Retention properties of mesoporous silica-based materials.* Analytica Chimica Acta, 2000. **422**(2): p. 231-238.

18. Fiorilli, S., et al., *Iron oxide inside SBA-15 modified with amino groups as reusable adsorbent for highly efficient removal of glyphosate from water.* Applied Surface Science, 2017. **411**: p. 457-465.
19. Rivoira, L., et al., *Functionalized iron oxide/SBA-15 sorbent: investigation of adsorption performance towards glyphosate herbicide.* Environmental Science and Pollution Research, 2016. **23**(21): p. 21682-21691.
20. Wang, L.K., et al., *Waste Treatment in the Food Processing Industry*. 2005: CRC Press.
21. Castiglioni, M., et al., *Amino groups modified SBA-15 for dispersive-solid phase extraction in the analysis of micropollutants by QuEchERS approach.* Journal of Chromatography A, 2021. **1645**: p. 462107.
22. Castillo, A., et al., *Selection of industrial (food, drink and milk sector) wastewater treatment technologies: A multi-criteria assessment.* Journal of Cleaner Production, 2017. **143**: p. 180-190.
23. Junior, D.A., et al., *Integration of Improved Methods for the Treatment of Wastewater from a Soft Drink Industry.* 2021.
24. Majumdar, P., A.Y. Khan, and R. Bandyopadhyaya, *Diffusion, adsorption and reaction of glucose in glucose oxidase enzyme immobilized mesoporous silica (SBA-15) particles: Experiments and modeling.* Biochemical Engineering Journal, 2016. **105**: p. 489-496.
25. Zhao, Y.-H. and D.F. Shantz, *Phenylboronic acid functionalized SBA-15 for sugar capture.* Langmuir, 2011. **27**(23): p. 14554-14562.
26. Ling, C., et al., *High adsorption of sulfamethoxazole by an amine-modified polystyrene–divinylbenzene resin and its mechanistic insight.* Environmental science & technology, 2016. **50**(18): p. 10015-10023.
27. Moreno-Castilla, C., *Adsorption of organic molecules from aqueous solutions on carbon materials.* Carbon, 2004. **42**(1): p. 83-94.
28. Parande, A.K., et al., *Performance evaluation of low cost adsorbents in reduction of COD in sugar industrial effluent.* Journal of hazardous materials, 2009. **168**(2-3): p. 800-805.
29. Amuda, O., I. Amoo, and O. Ajayi, *Performance optimization of coagulant/flocculant in the treatment of wastewater from a beverage industry.* Journal of hazardous materials, 2006. **129**(1-3): p. 69-72.
30. Amuda, O. and I. Amoo, *Coagulation/flocculation process and sludge conditioning in beverage industrial wastewater treatment.* Journal of Hazardous Materials, 2007. **141**(3): p. 778-783.

4. Geopolymers for inorganic and organic pollutant removal

Preliminary Results Project PRIN 2017 (017PMR932)
M. Castiglioni, L. Rivoira, K. Goulart de Oliveira, G. Franchin, P. Colombo, M.C. Bruzzoniti "Geopolymer based ion-exchange media for the removal of metals from water matrices", 8° Workshop Nazionale Gruppo interdivisionale di Green Chemistry – Chimica Sostenibile, 29 September 2020

M. Castiglioni, L. Rivoira, I. Ingrando, S. Calanni, K. Goulart, R. Botti, G. Franchin, P. Colombo, M.C. Bruzzoniti, "Affinity of geopolymer based ion-exchange media for glyphosate in water matrices", XXVII Congresso nazionale della Società Chimica Italiana, Milano 14-23 September 2021

M. Castiglioni, L. Rivoira, I. Ingrando, S. Calanni, K. Goulart, R. Botti, G. Franchin, P. Colombo, M.C. Bruzzoniti, "Geopolymer based supports for the removal of organic and inorganic pollutants from water matrices*", Merck Young Chemists' Symposium 2021, Rimini, 22-24 November 2021*

4.1 Introduction

In recent years, geopolymers (GPs), aluminosilicate-based materials, have caught attention in several areas. Their first use was reported for civil engineering applications (as a replacement of concrete) due to their excellent chemical, mechanical and thermal resistances [1]. In addition, excellent abilities in the purification of waters contaminated by organic and inorganic pollutants were observed, exploiting several approaches such as adsorption [2], photodegradation [3], encapsulation [4] and immobilization [5]. Hence, an increase in the number of studies focusing on geopolymer-type materials was recently registered. In particular, GPs have been used as new adsorbents for the treatment of water contaminated by hazardous pollutants.

Rapid population growth together with industrialization has affected water quality. Dissolved toxic heavy metal ions or organic pollutants generated by different industries can be poorly treated and discharged into water bodies. The industrial processes, including mineral processing, paint formulation, and electroplating, increase the level of heavy metal ions concentration in water remarkably [6]. The intake of these heavy metals through drinking water is hazardous since in the medium-long time period it can cause different types of diseases and damages to the skin, renal, pulmonary, digestive systems, etc. [7]. At the same time, the intensive use of active formulations like herbicides leads all the countries of the world to face different problems, such

as the rapid evolution of herbicide-resistant weeds [8, 9], the environmental impact of these compounds, [10], and the impact on human health, with particular attention to worker exposure [11, 12]. In particular, glyphosate is probably the herbicide most used in the world. Glyphosate has been the subject of controversial discussions due to its impact on the environment and human health. Therefore, the need to purify polluted water resources is highly demanding.

In this regard, the aim of this part of the thesis was the evaluation of adsorption properties of selected geopolymers towards organic and inorganic contaminants in water matrices. In particular, selected heavy metals and glyphosate were chosen as probe compounds. Several classes of geopolymers were considered, prepared as spheres, powders and 3-dimensional (3D) printed GPs. In addition, the specific modification of the supports was evaluated, with the aim to maximize the specific interaction between the GP and the pollutant to be removed. The use of a natural mineral, the stratlingite, was also tested and compared.

4.2 Experimental Methods

4.2.1 Geopolymers

Geopolymers of different composition were prepared by the research group of professor P. Colombo (University of Padua) under the activities of the PRIN 2017 project (I.D. 017PMR932). Table 4.1 summarizes GP characteristics.

Table 4.1. - *Geopolymer samples tested for the removal of metals*

Name	Sample	Washing procedure	Type	Surface Charge
GP1	Na+K (PEG 400)	3 times, 10 min, 20 mL	spheres	Neg.
GP2	Na+K (PEG 600)	3 times, 10 min, 20 mL	spheres	Neg.

GP3	K (PEG 400)	3 times, 10 min, 20 mL	spheres	Neg.
GP4	K (PEG 600)	3 times, 10 min, 20 mL	spheres	Neg.
GP5	GP olive oil	3 times, 10 min, 20 mL	Monolithic form	Neg.
GP6.1	3D Na-GP+CA 363	5 times, 10 min, 50 mL	powder	Pos.
GP6.2	3D Na-GP+CA 363 [PEG1000]	5 times, 10 min, 50 mL	3D structure	Pos.
GP6.3	3D Na-GP+CA 363 [Bentonite]	5 times, 10 min, 50 mL	3D structure	Pos.
GP7	3D Na-GP+ZSM-5 [PEG1000]	5 times, 10 min, 50 mL	3D structure	Pos.
GP8.1	Powder Na-GP+CA 242	5 times, 10 min, 50 mL	powder	Pos.
GP8.2	3D Na-GP+CA 242 [PEG1000]	5 times, 10 min, 50 mL	3D structure	Pos.
GP8.3	3D Na-GP+CA 242 [bentonite]	5 times, 10 min, 50 mL	3D structure	Pos.
GP9.1	Powder 3D Na-GP+hydrotalcite	5 times, 10 min, 50 mL	powder	Pos.
GP9.2	3D Na-GP+hydrotalcite [PEG1000]	5 times, 10 min, 50 mL	3D structure	Pos.
GP9.3	3D Na-GP+hydrotalcite [bentonite]	5 times, 10 min, 50 mL	3D structure	Pos.
	Stratlingite	5 times, 10 min, 50 mL	spheres	Pos.

GP1 and GP2, produced using NaOH and KOH activating solutions, can exchange Na^+ and K^+ with other cations, while GP3 and GP4 are able to exchange only K^+. PolyEthylene Glycol (PEG) was used to provide a spherical shape to geopolymers. PEG 400 and PEG 600 give a different porosity to the material (i.e PEG 600 confers higher pore diameters to the final material).

GP5 was synthesized following the same procedure of previous GPs, but replacing, in the gelation step, PEG with an aliquot of olive oil and, therefore, triglycerides. Such compounds, once inside the GP structure, produce fatty acids and glycerol that can be finally washed away once the material is hardened, thus promoting a high-porosity structure. As a result of not using PEG, such geopolymer was not in a spherical form, but rather in a monolithic form. For the above-mentioned cation exchange properties, GPs 1-5 were tested for metal ions removal.

To promote the retention of glyphosate, characterized by a negative charge at neutral pH values typical of waters, GP composition was specifically tuned and modified to obtain anion-exchange sites. In details, GP6-9, contain an Na-based alkoxide and were filled with specific reagents in order to selectively retain glyphosate. In addition, they were printed using a 3D printer device, to obtain solid lattices (like cubic filters) being able to increase the contact between the pollutant and the active sites, without the typical pressure drop of powders. In more detail: GP6 and GP8 were modified encapsulating commercially available active carbons (CA363 and CA242), GP7 with a zeolite (ZSM-5) and GP9 with hydrotalcite, both having anion exchange properties [13, 14]. PEG1000 or bentonite were used as printing agents.

In addition to GPs previously described, some stratlingite spheres were also tested in the removal of glyphosate. Stratlingite is a calcium silico-aluminate hydrate ($2CaO*Al_2O_3*SiO_2*8H_2O$), having a positively charged layer.

4.2.2 Reagents

NaOH (>98%) and HNO_3 (65%) were from Carlo Erba (Milano, Italy). Glyphosate, NaCl (for ionic strength control) and H_2SO_4 (95-97%, d=1.84 g/ml) were from Sigma-Aldrich. High-purity water (18.2 MΩ*cm resistivity at 25 °C), produced by an Elix-Milli Q Academic system (Millipore, Vimodrone, MI, Italy) was used for standard and eluent preparation.

4.2.2 Instrumental and calibration

4.2.2.1 Heavy metals

As, Pb, Ni, Cd, Se, Cr were determined thorough ICP-MS analysis (Perkin Elmer Elan 6100). A 1000 mg/L As, Pb, Ni, Cd, Se, Cr stock solution (Merck, Readington, New Jersey) was used to calibrate ICP-MS, over 8 levels (0.3-0.5-1-2.5-5-7.5-10 µg/L). Prior to analysis, samples were 1:1000 diluted. Limits of detection (LOD) and quantitation (LOQ) are reported in Table 4.2.

Table 4.2. *- LOD and LOQ for the metals analyzed.*

Metals	LOD (µg/L)	LOQ (µg/L)
Cd	0,08	0,24
Be	0,23	0,69
Fe	0,78	2,37
Cu	0,13	0,41
As	0,14	0,42
Cr	0,10	0,30
Ni	0,10	0,30
Pb	0,13	0,40
Sb	0,07	0,34
Se	0,11	0,34
Sn	0,07	0,21

4.2.2.2 Glyphosate

Glyphosate concentration was determined through suppressed ion chromatography. A Dionex 4000i chromatograph (25µL-injection loop) with a conductivity detector and IonPac AG16 (50 x 4 mm) and IonPac AS16 (250 x 4 mm) columns was used. The mobile phase was a NaOH solution (1.0 mL/min). Detection was performed by chemical suppressed conductivity and

a 4 mm ASRS-300 membrane suppressor. Chromatographic data were collected by PeakNet 2.8 software.

A calibration curve was built using standard solutions of glyphosate at 6 different concentration levels: 0.1-0.5-1-2-5-10 mg/L. LOD was 0.18 mg/L and LOQ 0.55 mg/L.

The peak area obtained for glyphosate ($A_{filtrate}$) was compared with the one obtained by injecting a standard solution of 8 mg/L ($A_{standard}$). The percentage of metals/glyphosate adsorbed was calculated according to the following equation:

$$\%GLY\_ads = (1-A\_filtrate/A\_standard)*100$$

4.2.3 Adsorption tests

Before application, all GPs were washed in ultrapure water following the procedure reported in Table 4.1. GPs adsorption was tested in batch conditions both for metals and glyphosate.

To test metal removal, aliquots of 0.2 g of each material were put in contact with 20 mL of an aqueous solution containing 8 mg/L solution of As, Pb, Ni, Cd, Se, Cr (final pH 3.8). Solutions were shaken for 24h and filtered with 0.45µm nylon membrane. Analysis of residual concentrations were performed thorough ICP-MS analysis. Tests were performed in triplicate. To what concern glyphosate, the same procedure was applied except for a 0.5g aliquot. Moreover, filtration of extracts was performed with mixed cellulose esters. The 8 mg/L glyphosate solution was shown to have a 5.6 pH.

4.3 Results and discussion

4.3.1 Metal removal

Adsorption results obtained after the removal tests of metal ions are shown in Table 4.3 and Figure 4.1.

***Table 4.3**. - Adsorption percentages of tested geopolymers towards selected heavy metals (n=3).*

		% Adsorption					
Sample ID	**Sample type**	**Cd**	**CrO_4^{2-}**	**Ni**	**Pb**	**As**	**Se**
GP1	Na+K (PEG 400)	44.3±4.9	65±7.5	66.3±1.1	93.2±16.7	n.a	n.a
GP2	Na+K (PEG 600)	39.3±6.4	52.8±0.6	54.9±1.1	n.a	76.5±6.9	59.6±8.4
GP3	K (PEG 400)	43.6±8.9	47±4.9	57.4±8.8	60±1.9	78.8±3.6	62.8±3.4
GP4	K (PEG 600)	26.9±1.7	29.3±0.7	45.3±0.7	67.6±3.9	74.6±5.9	50.2±7.3
GP5	GP olive oil	51.7±2.3	n.a	71.5±13.2	96.7±11.5	n.a	n.a

na: data not available due instrumental mismatch

Among the GPs tested, GP1 showed the highest adsorption rate, while GP4 the lowest. Within GPs, the adsorption percentages changes significantly.

Even if the specific surface area of the GPs (Table 4.4) is a crucial parameter to drive and enhance metal-GP interactions (See GP5), other parameters such as the chemical characteristics of metals and of their ionic forms should be considered to better understand the whole removal process.

Table 4.4. - *SSA, pore volume and pore diameter for GPs sample tested*

Sample ID	SSA (m^2/g)	Pore Volume (cm^3/g)	Pore Diameter (A)
GP1	5.01	0.035	3.49
GP2	6.07	0.046	3.12
GP3	3.84	0.018	3.92
GP4	3.48	0.014	3.93
GP5	98.05	na	na

na: data not available

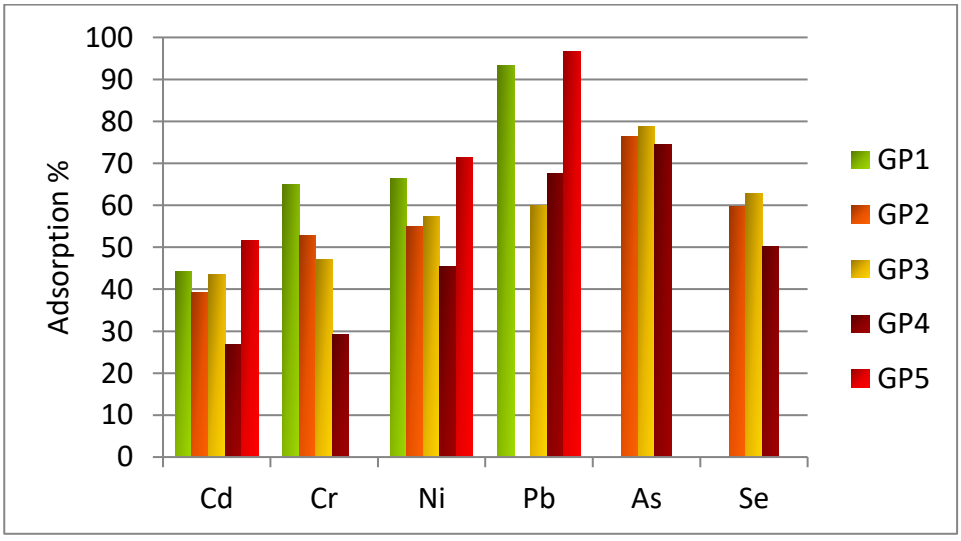

Figure 4.1. - *Adsorption percentages of metals on GPs*

In aqueous solution Pb^{2+}, Ni^{2+} and Cd^{2+} are present as cations (whereas As (III), Cr(VI), Se (IV) can be present as neutral or anionic compounds.
To what concern cations, the adsorption percentages averagely follows the order: $Pb^{2+} > Ni^{2+} > Cd^{2+}$, with Pb^{2+} showing the highest adsorption yield. This result is in good agreement with a previous work [15] on the use of metakaolin-based geopolymer for heavy metal adsorption, in which, among other cations, Pb^{2+} and Cd^{2+} were studied at the same solid/liquid ratio and at the same pH conditions here studied. The higher affinity of Pb^{2+} for the GPs could be explained with the low hydration radius of Pb^{2+} which in turns determines a higher charge density , thus increasing interactions with the negative charged of Al sites, located on GP surface [15].

To what concern metals that are in neutral/anionic form, the observed adsorption percentage follows the scale: As > Se > Cr, with the exception of GP5 that did not show interactions with such metals. The highest interaction between arsenic and GPs can be explained with the acid-basic dissociation equilibria. Indeed, since pKa value for arsenic acid is 9.22, at the experimental conditions tested (pH 3.8) As is present as neutral species. In this form, arsenic acid can form hydrogen bonds with surface oxygens of GPs. Conversely, dichromic/chromic acid (pK_1a=-0.98) and selenous acid (pK_1a=2.62) which are in a fully and partially dissociated form (negatively charged), respectively, undergo a partial repulsion between their negative charge and the cation exchange sites on GPs surface. It could be assumed that the slightly higher retention of Se, in respect to Cr, could be ascribed to the small neutral fraction of selenous acid retained by hydrogen bonds.

Surprisingly, when comparing Cr adsorption yields to Cd it is possible to see how Cr exhibited higher interactions towards GPs.

Focusing on GP5, made by olive oil, as previously recalled, only Pb^{2+}, Ni^{2+} and Cd^{2+} are retained (Figure 4.2), with adsorption yields even higher than GP1-

4. The enhanced retention is tentatively ascribed to additional interactions between metals and residual fatty acids (negatively charged) still present after the synthesis of the GP besides to its higher SSA.

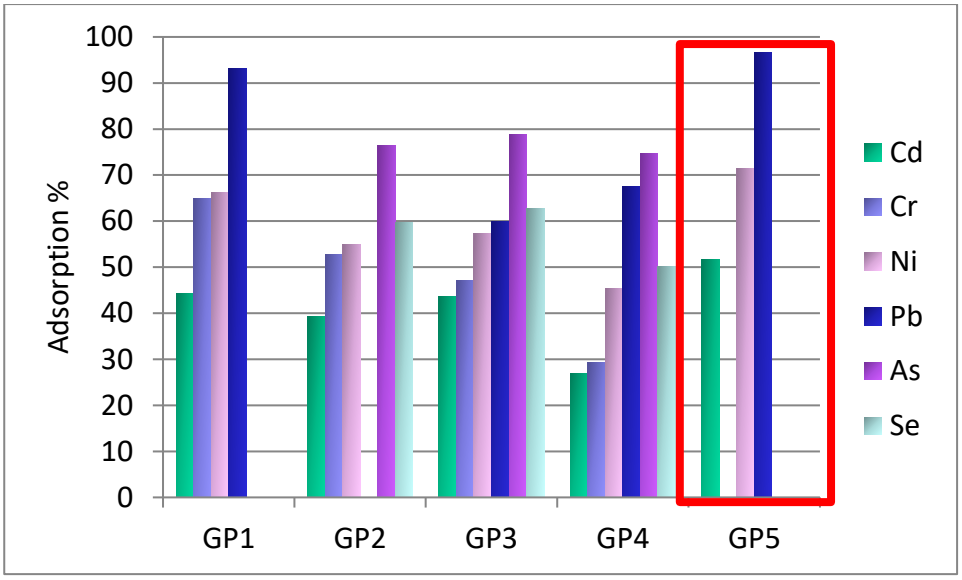

Figure 4.2 *- Adsorption yields for GPs tested*

4.3.2 Glyphosate adsorption

The adsorption results obtained for glyphosate when using geopolymers and stratlingite are summarized in Table 4.3. In the same table, the adsorption of glyphosate observed with each filler is also shown.

Table 4.5. *- Glyphosate adsorption yields of fillers and filler-geopolymer systems.*

Filler	Ads. (%)	Filler-geopolymer systems	Ads. (%)
CA363	96.9±0.2	**powder 3D Na-GP+CA 363 (GP6.1)**	23.2
		3D Na-GP+CA 363 [PEG1000] (GP6.2)	41.5±2.8
		3D Na-GP+CA 363 [Bentonite] (GP6.3)	27.3±0.7
ZSM-5	2.6±0.5	**3D Na-GP+ZSM-5 [PEG1000] (GP7)**	44.4±0.5
CA242	96.3±1.6	**powder Na-GP+CA 242 (GP8.1)**	28.7
		3D Na-GP+CA 242 [PEG1000] (GP8.2)	19.2±0.5
		3D Na-GP+CA 242 [bentonite] (GP8.3)	0
Hydrotalcite	79.7±1.7	**powder 3D Na-GP+hydrotalcite [PEG1000] (GP9.1)**	0.0
		3D Na-GP+hydrotalcite [PEG1000] (GP9.2)	14.9±1.1
		3D Na-GP+hydrotalcite [bentonite] (GP9.3)	0
Stratlingite spheres			62.8±0.4

Data show that good adsorption yields were obtained for both 3D Na-GP+ZSM-5 [PEG1000] (44%) and 3D Na-GP+CA 363 [PEG1000] (42%). In contrast, the other geopolymers showed poor efficiencies since adsorption rates below 27% were observed. It is interesting to highlight that, despite the low contribution of ZSM-5 (below 5%) to glyphosate removal, the ZSM-5-GP system showed the highest adsorption efficiency. Differently, CA363 exploited its removal efficiency also without the GPs structure.

The effect of synthesis parameters could be hence tentatively summarized as follows: i) GPs shape: 3D structures were shown to have higher adsorption rates than powder materials; ii) printing templating agents: bentonite was shown to negatively affect the retention of glyphosate, differently from PEG1000 which presence in the printed materials enhances retention in comparison to powders which of course do not contain PEG1000. The enhanced retention could be explained since PEG1000 is fully removed after GPs pre-application washing, leaving pores available for interaction with glyphosate, differently from bentonite which is not removed by the washing procedure and hence can partially obstruct the adsorbent reticulate.

Finally, moving to stratlingite, this material showed the highest retention rate among all the tested materials (more than 60%).

4.4 Conclusions

Geopolymers were tested and successfully applied as adsorbent materials for the removal of pollutants from water, both organic (glyphosate) and inorganic (heavy metals). Results showed that interactions geopolymer-metal depends on the exchangeable ion and could be further mainly ascribed to the properties of metal ion (i.e. size of the hydrated ionic radius, and pka of related oxospecies). In contrast, to what concern glyphosate-geopolymers, the removal efficiency is strongly dependent on both the GP shape and the

final composition (i.e. type of filler and templating agent) d inside the structure. In both cases, their potential use for water treatments is encouraged by the adsorption results obtained throughout this thesis and by their well-known limited backpressure in respect to traditional powder systems. These results pose the basis for further investigations on adsorption capacities through the set-up of adsorption isotherm tests.

4.5 References

1. Duxson, P., et al., *Geopolymer technology: the current state of the art.* Journal of materials science, 2007. **42**(9): p. 2917-2933.
2. Yu, Z., et al., *Improved simultaneous adsorption of Cu (II) and Cr (VI) of organic modified metakaolin-based geopolymer.* Arabian Journal of Chemistry, 2020. **13**(3): p. 4811-4823.
3. Falah, M., et al., *New composites of nanoparticle Cu (I) oxide and titania in a novel inorganic polymer (geopolymer) matrix for destruction of dyes and hazardous organic pollutants.* Journal of hazardous materials, 2016. **318**: p. 772-782.
4. Ke, X., et al., *Alkali aluminosilicate geopolymers as binders to encapsulate strontium-selective titanate ion-exchangers.* Dalton Transactions, 2019. **48**(32): p. 12116-12126.
5. Ji, Z. and Y. Pei, *Immobilization efficiency and mechanism of metal cations (Cd2+, Pb2+ and Zn2+) and anions (AsO43-and Cr2O72-) in wastes-based geopolymer.* Journal of hazardous materials, 2020. **384**: p. 121290.
6. Nguyen, T.C., et al., *Adsorptive removal of five heavy metals from water using blast furnace slag and fly ash.* Environmental science and pollution research, 2018. **25**(21): p. 20430-20438.
7. Slasli, A., et al., *Water adsorption by activated carbons in relation to their microporous structure.* Carbon, 2003. **41**(3): p. 479-486.
8. Egan, J.F., et al., *2, 4-dichlorophenoxyacetic acid (2, 4-D)–resistant crops and the potential for evolution of 2, 4-D–resistant weeds.* Proceedings of the National Academy of Sciences, 2011. **108**(11): p. E37-E37.
9. Powles, S.B. and J.M. Matthews, *Multiple herbicide resistance in annual ryegrass (Lolium rigidum): a driving force for the adoption of integrated weed management*, in *Resistance'91: Achievements and Developments in Combating Pesticide Resistance*. 1992, Springer. p. 75-87.
10. Rose, M.T., et al., *Impact of herbicides on soil biology and function.* Advances in agronomy, 2016. **136**: p. 133-220.
11. Korres, N.E., *Herbicide effects on humans: exposure, short and long-term effects and occupational hygiene.* Weed control: sustainability, hazards, and risks in cropping systems worldwide. CRC Press, Taylor Francis Group, Boca Raton, FL, 2018. **14**.
12. Da Silva Pinto, B.G., et al., *Occupational exposure to pesticides: Genetic danger to farmworkers and manufacturing workers–A meta-analytical review.* Science of The Total Environment, 2020: p. 141382.

13. Ghiaci, M., et al., *Adsorption of chromate by surfactant-modified zeolites and MCM-41 molecular sieve.* Separation and Purification Technology, 2004. **40**(3): p. 285-295.
14. Miyata, S., *Anion-exchange properties of hydrotalcite-like compounds.* Clays and Clay minerals, 1983. **31**(4): p. 305-311.
15. Cheng, T., et al., *The heavy metal adsorption characteristics on metakaolin-based geopolymer.* Applied Clay Science, 2012. **56**: p. 90-96.

5. Conclusions

In this doctoral thesis, different green sorbents have been studied with the aim of integrating them within the technologies applied for the removal of organic emerging contaminant and heavy metals from waters.

Part of the scientific research presented was dedicated to biochar that represents one successful example of valorization and reuse of wastes for water treatment. To elaborate, the correlation of the intrinsic physicochemical and performance parameters of biochars with the removal capacity was investigated through the careful review of published data and through the laboratory test of seven biochars in the removal of model disinfection byproducts (i.e. diiodoacetic acid) and volatile organic compounds (i.e. benzene, 1,2-dichlorobenzene). Both data retrieved from the literature and laboratory experiments are in accordance with the fact that BCs exhibit slightly lower adsorption capacities for organic compounds than activated carbons, which is considered the reference material in water depuration. Nevertheless, the production cost of BCs is much lower than the one required for activated carbon. Finally, the management of waste biomass to produce biochar to be further used as adsorbent for water treatment may be regarded as a "win–win" solution for pursuing circular economy principles and protecting the environment.

Another part of the research was dedicated to ordered silica based mesoporous adsorbents belonging to the SBA-15 family. In more detail, it was shown how mesoporous SBA-15 functionalized with (3-aminopropyl)-triethoxysilane (S-APTES) and N-[3-(trimethoxysilyl)propyl]aniline (S-Aniline) proved suitable for the removal of high concentrations (up to 350,000 mg/L) of glucose, fructose, sucrose from food industry wastewaters, characterized by high values of BOD_5, with removal rates higher than 70%. These removal capabilities were achieved optimizing the main parameters affecting

adsorption conditions (i.e. pH dependency, dosage:solution ratio), finding operational conditions fully compatible with real sample applications.
Additional part of the research was focused on geopolymers, that for their optimal mechanic and chemical properties, were presented as adsorbent materials for the removal of glyphosate and selected heavy metals of environmental concern. Geopolymers spheres with ion-exchange properties were shown promising materials for the removal of heavy metals (up to about 80%), independently from the metal charge. In addition, an innovative application of properly designed 3D printed geopolymers was proposed in the removal of herbicides. These adsorbents were shown to have a great potential in the removal of contaminants from water, even because they can avoid the backpressures typical of powdered sorbents.

In conclusion, this thesis leads the basis for the use of several kinds of green or low-cost materials (i.e. biochars, ordered mesoporous silica and geopolymers) in the removal of toxic substances which affect the quality of water compartments. Among the different properties of the investigated materials, functional moieties and surface chemistry were shown to be the most important parameters to be optimized to selectively retain the target compounds.
Concerning the economic aspects, a preliminary survey indicates that costs associated with the production of biochars and geopolymers are significantly lower than those required for the production of functionalized ordered silica mesoporous materials. Nevertheless, a case-to-case evaluation is recommended depending on target pollutants to be removed.
The use of these materials for water treatment, which at the moment was limited to the laboratory scale, could be expanded to a larger scale study (pilot or full-scale, with higher TRL) which includes the evaluation of both the technical and the economic aspects.

6. Appendix

The study of the materials presented in this PhD allowed me to investigate further applications, not directly connected with the removal of pollutants from waters, that represent technical solution to the analysis of complex environmental samples or strategies to prevent the spread of environmental pollution. In more detail, in this appendix, following investigations are reported:

1. innovative transversal characterization of previously presented amino modified SBA-15 materials, to be employed in the pre-treatment of food samples within the control of food contamination by organic micropollutants. In fact, the surface moieties active in the removal of sugars in wastewaters (see Chapter 3) could be exploited to produce dispersive solid phase extraction (d-SPE) sorbents to be used in QuEChERS extraction for the removal of interfering compounds of the food matrix (included sugars).
2. prevention of environmental contamination and human exposure through suitable substrates capable of prolonged release of active substances (i.e. herbicides), directly incorporated in Al-montmorillonite based sorbents, through the Al-Gly complexation. This procedure, innovatively investigated for glyphosate allows for a direct application in soils since it promotes a prolonged release of the herbicide, while limiting the operator's exposure in a great extent, due to the fact that inhalation is not involved during the spread of the herbicide. With this approach, agrochemical leaching, volatilization, dispersion in adjacent compartments and degradation are also reduced.

Hereafter, both research results are reported in details.

6.1 Amino groups modified SBA-15 for dispersive-solid phase extraction in the analysis of micropollutants by QuEChERS approach.

M. Castiglioni, B. Onida, L. Rivoira, M. Del Bubba, S. Ronchetti, M.C. Bruzzoniti, (2021)
"Amino groups modified SBA-15 for dispersive-solid phase extraction in the analysis of micropollutants by QuEchERS approach"
Journal of Chromatography A, 1645, 462107

6.1.1 Introduction

Fruits and their transformation products (e.g. beverages and jams) may be altered by organic micropollutants due to many contamination sources, such as soil and irrigation water [1, 2], as well as packaging materials [3] and pesticide application [4].

Current regulation regarding the presence of organic micropollutants in fruits and vegetables includes polycyclic aromatic hydrocarbons (PAHs), polychlorinated dibenzo(p)dioxins (PCCDs), polychlorinated dibenzo(p)furans (PCDFs), and polychlorinated biphenyls (PCBs) with dioxin-like properties, referred to as dioxine-like PCBs (DL-PCBs) [5].

Most of the above-mentioned compounds in fruits and derived products are analysed by using the QuEChERS approach followed by gas chromatographic-mass spectrometric analysis (GC-MS) [2, 6]. QuEChERS extraction is based on the partition of target analytes between water and acetonitrile.

Sugars present as natural components or as additives are well-known interferents in the QuEChERS approach since they are co-extracted in acetonitrile and must be removed prior to the analysis of the extracted samples by chromatographic methods.

This task is usually accomplished using solid-phase extraction (SPE) cleanup, even through on-line approaches [7], or by a dispersive solid phase extraction (*d*-SPE) clean-up step, with a primary secondary amine (PSA) sorbent [8, 9]. Several manufacturers make commercially available proprietary PSA sorbents which are based on silica chemically modified with ethylenediamine-N-propyl

group, as bulk packing, or within ready-to-use kits for QuEChERS analysis. PSA is usually claimed to be a sorbent more retentive than aminopropyl phases due to presence of the secondary amine [10], even if dedicated studies on the adsorption mechanisms are not yet available.

Ordered mesoporous silicas and organosilicas have been largely investigated as adsorbents [11-14] due to their high specific surface area and uniform porosity, together with the possibility of tailoring their surface chemical properties through synthesis conditions and post-synthesis modification. In particular, in the context of analytical chemistry, ordered mesoporous organosilicas have been tested as adsorbents for food samples cleanup [15]. Mesoporous silica functionalized with amino groups was previously investigated for adsorption and removal of anionic pollutants in wastewater [16, 17].

The aim of this research is to synthesize and study the performance of organically modified ordered mesoporous silicas to be innovatively included as *d*-SPE sorbents in a QuEChERS protocol for the removal of co-extracted sugars for the analysis of contamination of strawberries by 13 PAHs and 14 PCBs, including dioxine-like congeners. PCBs and PAHs are often found in fruit [18, 19] and are therefore a major concern for health protection.

Ordered mesoporous silica of SBA-15 family was functionalized with the primary amine (3-aminopropyl)-triethoxysilane (APTES) and, in another case, with the secondary amine N-[3-(Trimethoxysilyl)propyl]aniline, in order to mimic the commercial PSA. After the determination of the main physico-chemical characteristics, the adsorption of glucose, fructose and sucrose (sugars naturally contained in fruit) was studied. The performances of the two organically modified SBA-15 silica as QuEChERS d-SPE sorbents were investigated determining the signal to noise ratio and the extraction recoveries for target compounds, in comparison with those obtained by commercial PSA.

To the best of our knowledge no reports are currently available on the use of ordered mesoporous organosilicas in the QuEChERS technique.

6.1.2 Materials and Methods

6.1.2.1 Reagents

All reagents used were of analytical grade. Ordered mesoporous silica of the SBA-15 type was purchased from ACS Material Advanced Chemical Supplier (Pasadena, CA, USA). (3-aminopropyl) triethoxysilane (APTES, 99%), N-[3-(Trimethoxysilyl)propyl]aniline, toluene (99.8%), acetonitrile (>99.9%) were purchased from Sigma Aldrich (Steinheim, DE). Primary Secondary Amine (PSA, Figure 6.1A) was purchased from Agilent Technologies (Santa Clara, CA, USA). D(+) glucose was purchased from Merck (Darmstadt, DE), D(-) fructose and sucrose were purchased from J.T. Baker (Phillipsburg, NJ, USA).

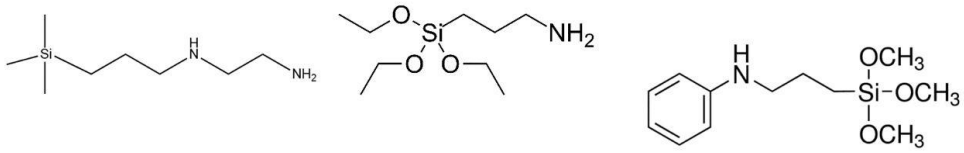

A B C

Fig. 6.1. Schematic representation of PSA (A) and structure of the precursors APTES (B) and N-[3-(trimethoxysilyl)propyl]aniline (C).

The PAHs studied were the 13 PAH compounds listed by EPA 525.1 procedure and were purchased from Sigma Aldrich-Merck (Darmstadt, Germany): acenaphtylene (AcPY), fluorene (Flu), phenathrene (Phe), anthracene (Ant), pyrene (Pyr), benzo[a]anthracene (BaA), chrysene (Chr), benzo[b]fluoranthene (BbFl), benzo[k]fluoranthene (BkFl), benzo[a]pyrene (BaP), indeno[1,2,3-cd]pyrene (Ind), dibenzo[a,h]anthracene (DBA),

benzo[ghi]perylene (BP). PCBs were purchased from LGC Standards (Milan, Italy). They were non-dioxine like PCBs: 3,3′-dichlorobiphenyl (PCB 11), 4,4′-dichlorobiphenyl (PCB 15), 2,4,4′-trichlorobiphenyl (PCB 28), 2,2′,5,5′-tetrachlorobiphenyl (PCB 52), 2,2′,4,5,5′-pentachlorobiphenyl (PCB 101), 2,2′,3,4,4′,5-hexachlorobiphenyl (PCB 138), 2,2′,4,4′,5,5′-hexachlorobiphenyl (PCB 153), 3,3′,4,4′,5,5′-hexachlorobiphenyl (PCB 169), 2,2′,3,4,4′,5,5′-heptachlorobiphenyl (PCB 180), 2,3,3′,4,4′,5,5′-heptachlorobiphenyl (PCB 189); and dioxine like PCBs: 3,4,4′,5-tetrachlorobiphenyl (PCB 81), 2,3′,4,4′,5-pentachlorobiphenyl (PCB 118), 2′,3,4,4′,5-pentachlorobiphenyl (PCB 123), 2,3′,4,4′,5,5′-hexachlorobiphenyl (PCB 167).

Hydrochloric acid (35% w/w, d = 1.187 g/mL) and NaOH (>98%) were from Carlo Erba (Milano, IT). NaCl, $MgSO_4 \cdot 7H_2O$ and H_2SO_4 (95–97%, d = 1.84 g/mL) were from Sigma-Aldrich. High-purity water (18.2 M Ω·cm resistivity at 25°C), produced by an Elix-Milli Q Academic system from Millipore (Vimodrone, MI, Italy) was used for standard and eluent preparation.

6.1.2.2 Preparation of sorbents

The synthesis procedures of the two sorbents were based on previous work concerning on the functionalization of SBA-15 silica [16, 17]. In a flask, 1 g of SBA-15, previously washed with about 50 mL of deionized water, was stirred with 200 mL of toluene for 30 min, at room temperature. Afterwards, 2 mL of functionalizing reagent ((3-aminopropyl)-triethoxysilane-APTES or N-[3-(trimethoxysilyl)propyl]aniline, Fig. 6.1B and 6.1C) was added dropwise. The flask was then connected to a water-refrigerated system and the solution heated to 110 ° C. The solution was kept under stirring for 24 hours. Afterwards, the powder was filtered and dried.

Hereafter the sample functionalized with APTES is denoted SBA-15-APTES and the sample functionalized with N-[3-(trimethoxysilyl)propyl]aniline is denoted SBA-15-AN.

6.1.2.3 Physico-chemical characterization

Nitrogen adsorption isotherms were measured using a Quantachrome AUTOSORB-1 (Boynton Beach, FL, USA) instrument. Prior to nitrogen adsorption, samples were outgassed at 393 K for 6 h. The BET specific surface areas (SSA) were calculated in the relative pressure range from 0.04 to 0.1 and the pore size distribution were determined through the NLDFT (Non Localized Density Functional Theory) method, using the equilibrium model for cylindrical pores.

For FTIR measurements, powders were pressed in self-supporting wafers and spectra were recorded at room temperature with a Bruker Tensor 27 (Bruker, Billerica, MA, USA) spectrometer operating at 2 cm^{-1} resolution, after outgassing the sample at room temperature (residual pressure of 0.1 Pa).

TG analyses were carried out between 298 K and 1073 K in air (flow rate 100 mL/min with a heating rate of 10 K/min) using a SETARAM 92 (Caluire, France) instrument.

Density functional theory (DFT) simulations were calculated by means of Gaussian 09W and Gaussian View (Gaussian Inc, Wallington, US).

6.1.2.4 Chromatographic analysis

The evaluation of sugar content was performed by ion-chromatography using an ICS-3000 gradient pump, Thermo Fisher Scientific, Waltham, MA, USA, coupled to pulsed amperometric detection. An AD40 Electrochemical Detector, Thermo Fisher Scientific, equipped with Ag/AgCl reference electrode and a gold working electrode was used. The detection potential was set at 0.1 V and maintained for 400 ms: the first 200 ms represents the delay time and the second 200 ms represents the determination time. The potential was then instantaneously set at -2 V and maintained for 10 ms and raised at 0.6 V and maintained for 10 ms to restore the gold oxide necessary to

maintain an active working electrode surface. The potential was finally set at -0.1V and maintained for 60 ms, to reduce the small amount of gold oxide previously formed. The waveform requires a total of 500 ms.

The sample (10 µL) was injected through a six-ways Rheodyne injection valve. The column used was a CarboPacPA10, 250x4 mm (100 µeq/column), Thermo Fisher Scientific which has a microporous substrate with particle size of 10 µm, 55% cross-linking functionalized with a difunctional quaternary ion latex (5% cross-linking).

After optimization, the eluent concentration was kept at 55 mM KOH (data available upon request). At these conditions, limits of detection (LODs) for glucose, fructose and sucrose, calculated as $s_m=s_m+3s_b$, with s_m=average signal of blank, s_b= standard deviation of blank on ten measurements, were respectively 69, 56 and 11 µg/L. Pump, detector settings, and data collection were managed by the Chromeleon v.6.80 software (Thermo Fisher Scientific).

For PAHs and PCBs analysis, a gas chromatographic-mass spectrometric (GC-MS) method was used, according to previous studies by our research group [2, 20], employing an Agilent (Santa Clara, CA,USA) 6980 series gas chromatograph coupled with an Agilent 5973 Network mass spectrometer detector.

The GC column was a (5%-Phenyl)-methylpolysiloxane column (HP 5ms, 30 m x 0.25 mm x 25 µm, Agilent), with He as gas carrier (1 mL/min). MS detection was performed in Single Ion Monitoring (SIM) mode, selecting for each analyte its proper m/z ratio (m/z ratio available upon request). 2 µL of each sample were injected using the Pulsed Splitless mode (pressure at 40 psi for 2.5 min). The oven ramp was: 90°C, hold for 2 min; ramp to 176 °C, 12 °C/min rate; ramp to 196°C, 5 °C/min rate, hold for 3 mins; ramp to 224°C, 12 °C/min rate; ramp to 244 °C, 5°C/min rate, hold for 3 min; ramp to 270 °C, 7°C/min rate, hold for 3 min; ramp to 300 °C, 5°C/min, hold for

10 min to completely clean and restore the GC column. The total run time for the complete separation of PAHs and PCBs is 52 min.

LODs, calculated as previously described for ion chromatography, were in the range from 0.06 µg/L (BaA) to 2.10 µg/L (DBA), while from 0.49 µg/L (PCB153) to 5.40 µg/L (PCB169).

GC-MS data were handled with OpenChrome software (Lablicate, Germany).

6.1.2.5 Adsorption tests

Tests to evaluate the effect of pH were performed on 0.25 g of sorbent. The sorbent was put in contact with 4 g solution containing 350 mg/g glucose, 350 mg/g fructose and 170 mg/g sucrose. These concentrations were chosen in order to match those contained in strawberry according to Kasperbauer [21]. Solutions were stirred at 1100 xg for 10 min. Experiments were performed at pH 2.1, 5.0 and 8.5.

6.1.2.6 Strawberry fruits

Commercial strawberry samples grown in Italy were used. *Fragaria x ananassa, Camarosa* cultivar was chosen as model plant, since it accounts for about 60% of the strawberry world's production and it adapts greatly to wide climate and growth conditions.

6.1.2.7 Extraction of PAHs and PCBs from strawberries by QuEChERS

Among organic micropollutants, PCBs and PAHs, present in the environment as a result of natural and anthropogenic processes, represent both point source and diffuse emissions [22].

PAHs and PCBs were extracted using a QuEChERS approach [8, 23]. Briefly, 5 g of homogenized strawberries were put in a vial containing 10 mL acetonitrile:H_2O pH 2.1 (70:30), 8.2 g $MgSO_4$ and 1 g NaCl. The tube was vigorously shaken and centrifuged at 1100 xg for 10 min. After extraction, a

4 mL aliquot of the supernatant was then transferred in a new vial containing 0.25 g of sorbent (PSA or SBA-15-APTES or SBA-15-AN) and 1.0 g $MgSO_4$ for the clean-up step. The tube was shaken and centrifuged (7870 xg, 10 min) and the supernatant was directly analysed by GC-MS. For each sorbent, the recovery was calculated spiking the fruit samples prior- (i) and post- (ii) extraction as follows:

- Pre-extraction spike: a cumulative batch of 50 g of homogenised strawberries was spiked with 6666 µL of a solution containing PAHs and PCBs at 300 µg/L each, to achieve a final concentration of 0.04 mg/kg. According to the extraction procedure above detailed, a theoretical final concentration of 20 µg/L is expected for each PAH and PCBs. The procedure was repeated in triplicate.
- Post-extraction spike: after the extraction and clean-up procedure, 187 µL of the extract is spiked with 13 µL of the solution containing PAHs and PCBs at 300 µg/L, so to obtain a final concentration of 20 µg/L for each PAH and PCBs. The procedure was repeated in triplicate.

For each analyte, extraction recovery percentage (ER%) was calculated from the peak areas obtained after the pre-extraction spike ($A_{pre\text{-}extraction}$) and post-extraction ($A_{post\text{-}extraction}$) according to the equation:

$$ER\% = 100 * A_{pre\text{-}extraction} / A_{post\text{-}extraction}$$

For each analyte and experimental conditions, signal-to-noise ratio (S/N) was derived from the software OpenChrome and was calculated from the height of the analyte chromatographic peak (H_{peak}) and that of the noise (h_{noise}), according to the 2015 United States Pharmacopeia definition [24]:

$$S/N = 2H_{peak}/h_{noise}$$

6.1.3 Results and discussion

6.1.3.1 Physico-chemical characterization

Table 6.1 reports textural features of SBA-15 as such and of functionalized SBA-15. For both SBA-15-APTES and SBA-15-AN, lower values of SSA, pore volume and pore diameter are observed with respect to the pristine SBA-15. These results reveal that grafting of organic moieties on the internal surface of silica mesopores occurred during functionalization.

Table 6.1 Textural features of SBA-15, SBA-15-APTES, SBA-15-AN and PSA

	SBA-15	SBA-15-APTES	SBA-15-AN	PSA
SSA (m^2/g)	490	323	298	384
Pore volume (cm^3/g)	0.92	0.53	0.54	0.70
Pore diameter (nm)	8.1	7.0	6.8	7.0

N_2 adsorption measurement was carried out also on PSA since no data for the commercial product were available. It is worth noting that the same features of PSA are in between those of SBA-15 and organically modified SBA-15, so that, as a whole, we can consider PSA, SBA-15-APTES and SBA-15-AN comparable systems for the proposed QuEChERS application.

Fig. 6.2 shows FT-IR spectra of SBA-15, SBA-15-APTES and SBA-15-AN after outgassing at room temperature.

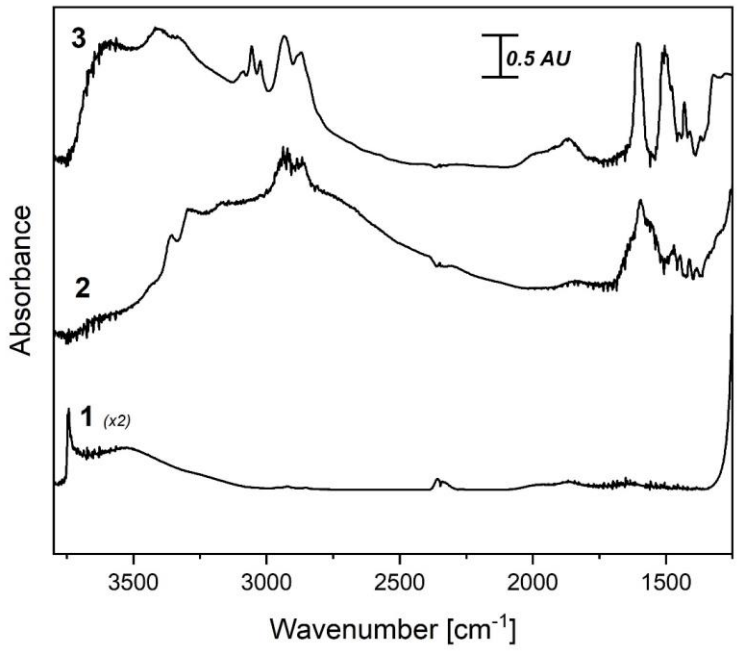

Fig. 6.2. FT-IR Spectra of SBA-15 (curve 1), SBA-15-APTES (curve 2) and SBA-15-AN (curve 3). The spectrum of SBA-15 was amplified by a factor 2 for sake of clarity.

The spectrum of SBA-15 (curve 1) reveals the typical features of an amorphous silica, i. e. the narrow band at 3743 cm^{-1}, due to the stretching mode of isolated silanols, and the broad band centred at 3530 cm^{-1}, due to H-bonded silanols.

In the spectrum of SBA-15-APTES (curve 2), bands due to the organic moieties are clearly observed, that are: i) two bands at 3355 cm^{-1} and 3295 cm^{-1} attributed to the stretching modes of $-NH_2$ groups; ii) two bands at 2930 cm^{-1} and 2875 cm^{-1} due to the stretching modes of aliphatic $-CH_2-$ groups; iii) a band at about 1595 cm^{-1} due to the bending mode of $-NH_2$ groups. As usually observed for amorphous silica modified with APTES, a broad and ill-

defined absorption is observed at about 3000 cm^{-1}, on which the previous mentioned bands are superimposed. This absorption is due to the residual silanols engaged in H-bonding with surface -NH_2 groups [25]. Indeed, in the spectrum, the stretching mode of isolated silanols is not present.

In the case of SBA-15-AN (curve 3), as for SBA-15-APTES, the bands due to the organic groups are visible in the spectrum, i.e. i) the band at 3330 cm^{-1} due to the stretching mode of -NH- species; ii) bands above and below 3000 cm^{-1} due to, respectively, aromatic -CH and aliphatic -CH_2- stretching modes; iii) bands below 1700 cm^{-1} due to ring modes of the aromatic moieties. Moreover, a broad absorption is observed at about 3600 cm^{-1} which is tentatively ascribed to the residual silanols engaged in H-bonding with aromatic rings [26].

In summary, the set of IR data reveal that amine species in modified SBA-15 are located and exposed on the silica surface, in agreement with textural features (Table 6.1) discussed above.

From TG curves (not reported), the amount of amino groups was estimated and it is 4.41 mmol/g for SBA-15-APTES and 2.23 mmol/g for SBA-15-AN.

According to data found for commercially available PSA in the market, capacity for PSA ranges from 0.65 to 1.22 mmol/g [27, 28]. The above-mentioned capacity data suggest, per se, a competitive performance of functionalized SBA-15 in respect to PSA, and supports the study herein proposed.

6.1.3.2 Adsorption measurements

The following experiments were performed in order to optimize the pH conditions to be used in QuEChERS application. Furthermore, the results may be useful in formulating possible interactions acting between adsorbents and sugars during retention.

Results are represented in Fig. 6.3A, 6.3B, 6.3C. According to the acidic dissociation constants of the sugars considered (pK_a=12.2 for glucose, 12.0 for fructose and 12.6 for sucrose), the concentration of dissociated sugars may be considered negligible at pH values studied (2.1, 5.0 and 8.5).

Organically modified mesoporous silicas show better removal performance than commercial PSA for all the pH values. It is worth noting that textural properties such as SSA and pore volume of SBA-15-APTES and SBA-15-AN are comparable to those of PSA (see Table 6.1), therefore the better adsorption performance of organically modified mesoporous silica has to be ascribed to the functional groups acting as adsorption sites, the amount of which is larger in SBA-15-APTES and SBA-15-AN than in PSA. Nevertheless, a role of different surface chemical properties of the two silica supports, cannot be ruled out.

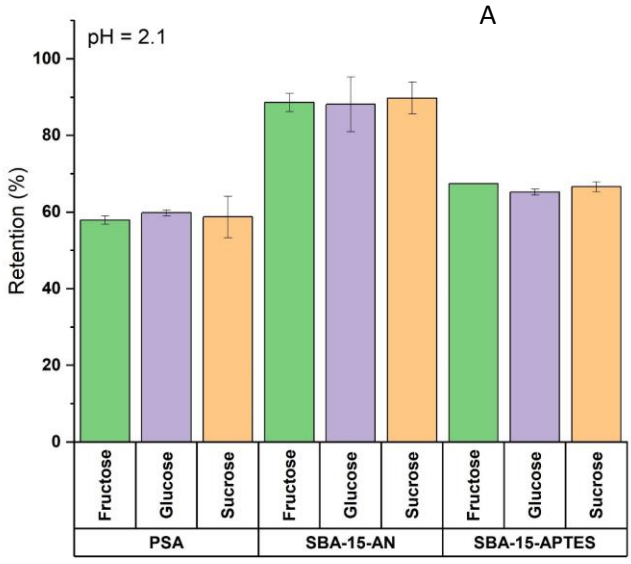

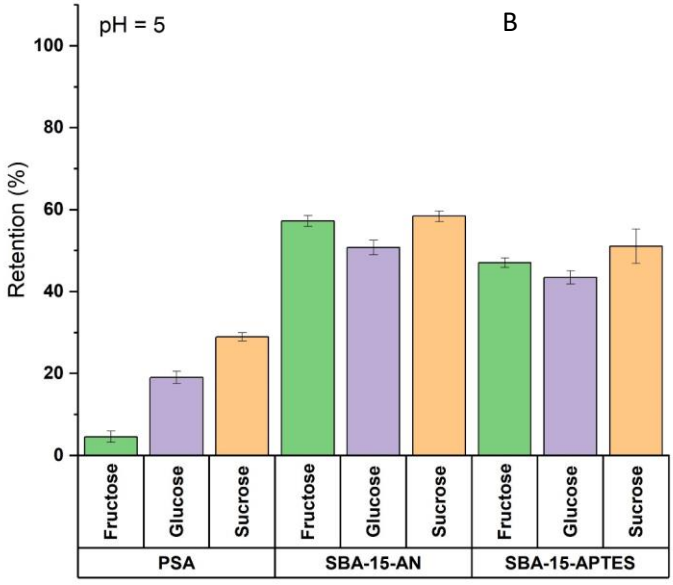
B
pH = 5
Retention (%)
100
80
60
40
20
0
Fructose
Glucose
Sucrose
Fructose
Glucose
Sucrose
Fructose
Glucose
Sucrose
PSA
SBA-15-AN
SBA-15-APTES

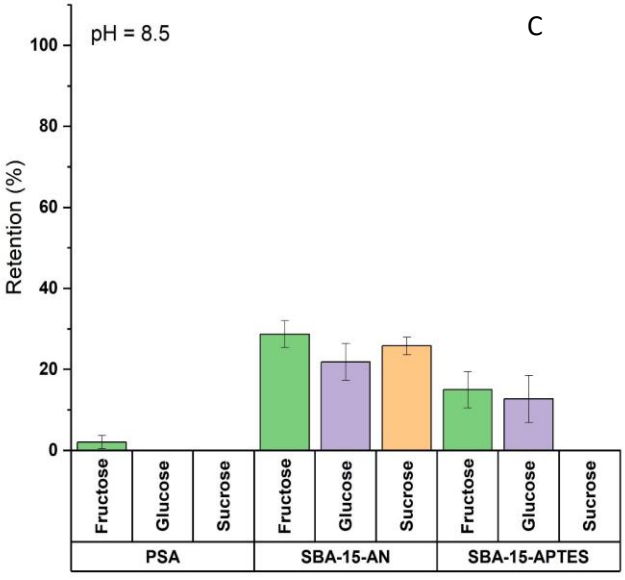
C
pH = 8.5
Retention (%)
100
80
60
40
20
0
Fructose
Glucose
Sucrose
Fructose
Glucose
Sucrose
Fructose
Glucose
Sucrose
PSA
SBA-15-AN
SBA-15-APTES

Fig. 3. Adsorption of glucose, fructose, sucrose on PSA, SBA-15-APTES and SBA-15-AN at pH 2.1 (A), 5.0 (B) and 8.5 (C). For experimental details, see text.

Firstly, the retention properties of aminopropyl-modified silica and PSA towards sugars has been ascribed mainly to H-bonding [29]. The role of H-bonding of protonated ethylenediamine based materials, structurally similar to PSA, in the retention of uncharged compounds is supported by many authors [30, 31], who also speculated on possible leading retention mechanisms via H-bonding as a function of pH and on the abundancy of NH_3^+/NH_2 and NH_3^+/NH groups [31].

As shown in Fig. 6.3, for all the adsorbents, retention capabilities decrease at increasing pH. This may be ascribed to a change of the relative population of protonated and deprotonated amine groups and to their involvement in H-bonding. At increasing pH, the population of protonated amines decreases. Since protonated amines are stronger Brønsted acids than amines, they may be considered also stronger H donor in H-bonding.

Data in Fig. 3A-3B-3C show that SBA-15-AN has higher retention abilities than SBA-15-APTES at all the pH values tested (SBA-15-AN > SBA-15-APTES > PSA). Indeed, if we consider that aniline (pK_b 8.9) is a weaker base than propylamine (pK_b 3.5), the decrease of protonated amine population upon increasing pH is expected to be relatively larger in SBA-15-AN than SBA-15-APTES. Thus, it may be proposed that H-bonding between protonated amines and sugar molecules, where the former act as proton donor and the latter as proton acceptor, does not play the only role in the adsorption.

Therefore, the better performance of SBA-15-AN compared to that of SBA-15-APTES can be ascribed to a higher hydrophobicity of the material due to the more hydrophobic functional group, which is usually desired in case of organic molecules adsorption from water solution. Moreover, the electron-

withdrawing effect of the aromatic ring enhances the positive charge of the ammonium group, increasing the strength of H-bonding with sugar molecules.

Experimental tests indicated that pH 2.1 is the optimal pH value to achieve the highest sugars adsorption in a QuEChERS application.

6.1.3.3 Organically modified mesoporous silicas in the d-SPE cleanup of QuEChERS

In a QuEChERS procedure, after extraction with acetonitrile, a clean-up step performed in *d*-SPE is necessary to remove coextracted interferents without losing analytes of interest.

To this purpose, the capabilities of SBA-15-APTES and SBA-15-AN as *d*-SPE sorbents were investigated in the determination of persistent pollutants (PAHs and PCBs, included dioxine-like congeners) in strawberries, using the QuEChERS extraction approach.

Performances of the modified silicas were studied and compared with those of PSA, measuring both signal-to-noise ratio (S/N) and extraction recovery (ER) of PAHs and PCBs after the application of the QuEChERS protocol.

S/N is a parameter characteristic of the chromatogram and indicates the quantification accuracy of the components during the analytical separation. The higher the S/N, the better recognized the analyte and the lower the detection limits obtainable. Due to this intrinsic property, S/N is considered a primary standard for comparison of chromatographic performances [32] and it is therefore frequently used as response in analytical design optimizations [32-34]. In a complex matrix, such as strawberry rich in sugars, anthocyanins and polyphenols [35], S/N is indicative of the efficiency of matrix removal.

Additionally, ER was also measured, since it is indicative of the efficiency of the whole method (extraction and clean-up) to extract analytes of interest, without losing them by adsorption during the clean-up step.

Results obtained by our study for S/N are reported in Fig. 6.4 (PAHs) and 6.5 (PCBs) while ER values are shown in Fig. 6.6 (PAHs) and 6.7 (PCBs). Data obtained in the absence of the *d*-SPE treatment were also considered.

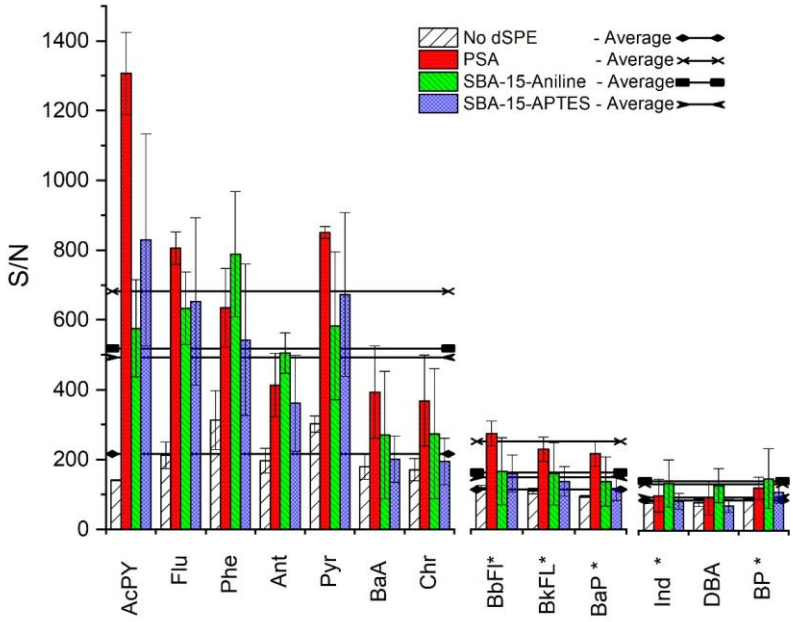

Fig. 6.4. Signal-to-noise ratio (S/N) obtained after the QuEChERS extraction of PAHs from strawberry, without and with the d-SPE clean-up by PSA, SBA-15-APTES and SBA-15-AN. For QuEChERS extraction conditions, see text

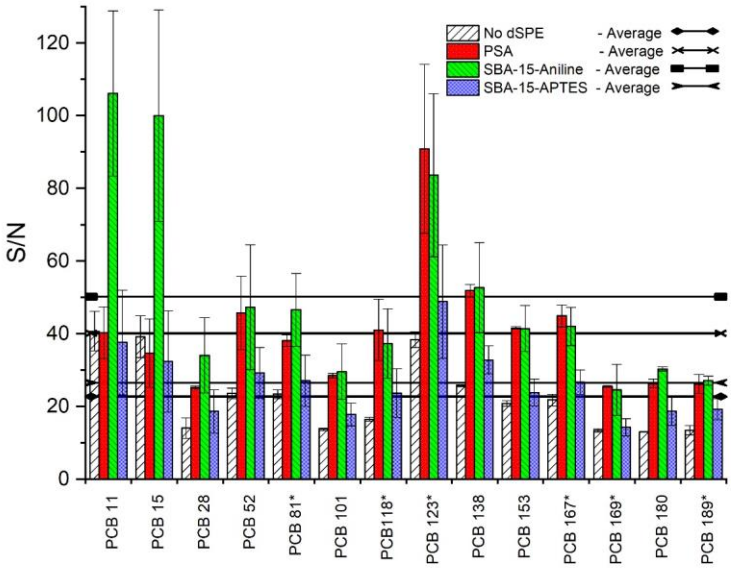

Fig. 6.5. Signal-to-noise ratio (S/N) obtained after the QuEChERS extraction of PCBs from strawberry, without and with the *d*-SPE clean-up by PSA, SBA-15-APTES and SBA-15-AN. For QuEChERS extraction conditions, see text.

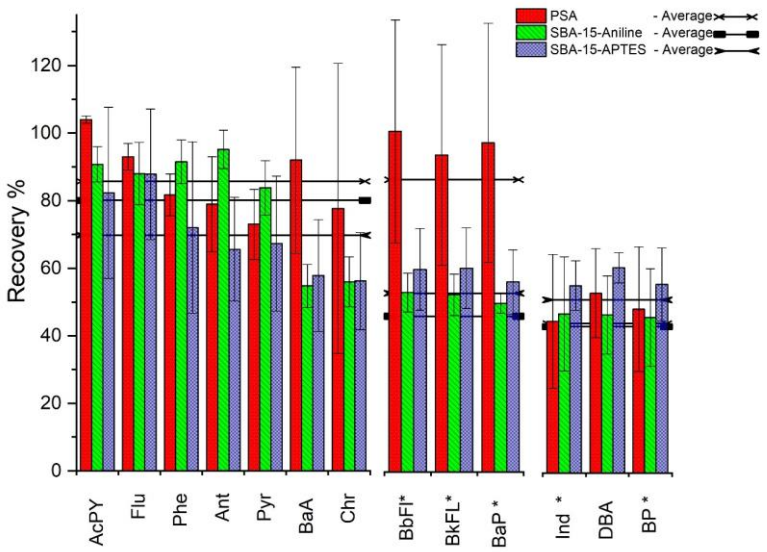

Fig. 6.6. Extraction recovery percentage obtained after the QuEChERS extraction of PAHs from strawberry and the *d*-SPE clean-up by PSA, SBA-15-APTES and SBA-15-AN. For QuEChERS extraction conditions, see text.

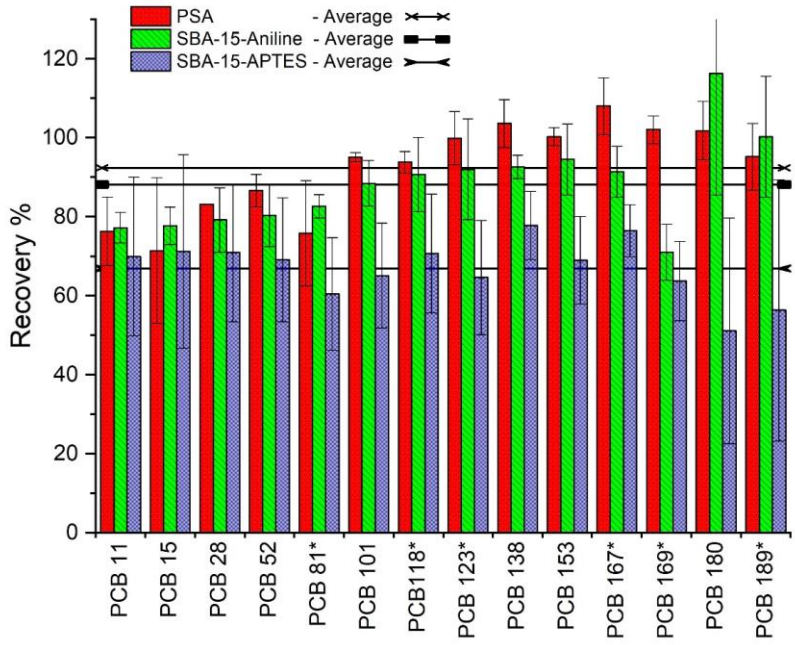

Fig. 6.7. Extraction recovery percentage obtained after the QuEChERS extraction of PCBs from strawberry and the *d*-SPE clean-up by PSA, SBA-15-APTES and SBA-15-AN. For QuEChERS extraction conditions, see text.

For an easier interpretation, for each sorbent, experimental results for PAHs are shown, in Fig. 6.4 and 6.6, as single value or as average for compounds: up to four benzene rings (acenaphthylene, the isomers: phenanthrene/anthracene; fluorene/pyrene; benzo[a]anthracene/chrysene); four benzene rings around a 5-membered ring and five benzene rings (the isomers: benzo[b]fluoranthene/benzo[k]fluoranthene/benzo[a]pyrene);

five benzene rings or five benzene rings around a 5-membered ring (dibenzo[a,h]anthracene and the isomers indeno[1,2,3-cd]pyrene/benzo[ghi]perylene). For PCBs, for each sorbent, experimental results were shown, in Fig. 6.5 and 6.7, as single value or as average for the 14 congeners tested.

As regards S/N values, for all the analytes (Fig. 6.4 and 6.5), the values obtained without a *d*-SPE treatment are the lowest, indicating a poor quality of the analytical method. The increase of S/N values in the presence of the *d*-SPE treatment indicates a better detectability, essentially due to the removal of coextracted matrix compounds, and the consequent improvement of the baseline. In this regard, both the organically modified mesoporous silica are effective in improving the analytical method.

For PAHs (Fig. 6.4), S/N obtained with PSA are higher than those obtained with SBA-15-APTES and SBA-15-AN for all the hydrocarbons, except for the last three heaviest compounds for which SBA-15-AN is the best performing d-SPE sorbent. The improvement of S/N for these last compounds (about 30%) turns to be important in the enhancement of the detection limits in real matrices, since the heaviest compounds are affected by poor detectability.

For PCBs (Fig. 6.5), the highest S/N is observed for SBA-15-AN, for which, on average, an improvement of S/N values of about 20% in respect to PSA is observed.

Extraction recovery ER% as a function of the d-SPE sorbent used is shown in Fig. 6.6 for PAHs and in Fig. 6.7 for PCBs.

For the 13 PAHs, average ER% follows the order PSA (76±19 %) > SBA-15-AN (63±7 %) > SBA-15-APTES (61±14 %), even though comparable performances are observed for PSA and SBA-15-AN for lower molecular weight PAHs. Differently, ER% obtained without any d-SPE sorbent are significantly lower, ranging from 14±3 to 25±2% (data not shown).

According to the Anova test (p=0.0001, 95% confidence interval), the average ER for PSA is statistically different from SBA-15-AN and SBA-15-APTES, whereas average ER for the two organically modified mesoporous silica do not show statistical difference. Despite the higher ER obtained for PSA, the lower standard deviation observed for SBA-15-AN indicates that the d-SPE cleanup with SBA-15-AN is more reliable than the one performed with PSA. Statistic variability of ER% values for each sorbent was also evaluated through Horwtiz equation (Thompson modification [36]), calculating at first the concentration of each PAH, according to its extraction yields, and finally the maximum acceptable RSD%. Since the maximum acceptable RSD% value calculated was 22%, the average RSD% values observed for PAHs with each sorbent (26.2% for PSA and 14.2% for SBA-15-AN) indicate that the use of PSA provided recoveries falling outside the range of acceptability. Differently, the reliability of SBA-15-AN is confirmed since average RSD% is far below the Horwitz value.

Data shows that for all the *d*-SPE sorbents, a decrease of ER% is observed with the increase of molecular weight introduced by the aromatic rings. This behaviour was verified for PSA also by Sadowska-Rociek et al [37] in the analysis of PAHs in tea.

Even if, overall, PSA is the best performing sorbent for all PAHs, SBA-15-APTES provides higher ER% for higher molecular weight PAHs.

For PCBs, average ER% follows the order PSA (92±6 %) > SBA-15-AN (88±9 %) > SBA-15-APTES (67±17 %). Again, poor recovery is observed without any d-SPE step (ER% ranging from 36±6 to 44±7%, data not shown). The average ER values obtained for PSA and SBA-15-AN are not statistically different (Anova test, p=0.0001, 95% confidence interval), whereas average ER values obtained with SBA-15-APTES statistically differ from those obtained by PSA and SBA-15-AN. Again, the application of the Horwitz equation (calculated RSD%=22%), confirmed the statistical acceptability for

recoveries obtained with PSA and SBA-15-AN (RSD%=7.2% and 10.2%, respectively), but not with SBA-15-APTES (RSD%=25.8%).

Presuming that the extraction recovery calculation used compensates for any matrix effect, it is reasonable to assume that differences in extraction recovery values observed among the three d-SPE materials is due to the different extent of adsorption of PAHs and PCBs by each sorbent, being the extraction procedure the same for the three tests.

For each sorbent, PCBs exhibit higher ER% values than PAHs. For each d-SPE sorbent, for PAHs an increase of ER% is observed upon decreasing molecular weight (MW), showing a partial anticorrelation (the higher the MW, the lower the ER%) for SBA-15-AN (ER% = -1.9 MW + 346, r^2= 0.919) and for SBA-15-APTES (ER% = -3.3 MW + 424, r^2= 0.840), while for PSA this behaviour is not well evidenced (ER% = -1.5 MW + 340, r^2= 0.429). This suggests that at variance with what hypothesized by Dachs and Bayona [38] for silica based octadecyl substrates, in this case, steric hindrance and shape selectivity do not play a crucial role in the extraction. To explain the higher extent of adsorption observed for higher molecular weight PAHs, density functional theory (DFT) simulations were calculated by the software Gaussview 6.0 in order to estimate the potential and charge density distribution for each PAH tested [39].

Results obtained (Fig. 6.8) show that the centre of each ring on both sides of the PAH molecular plane is negatively charged and corresponds with delocalized π electrons.

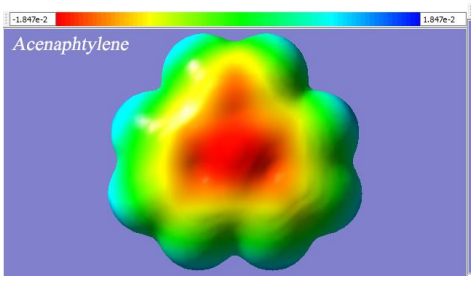
-1.847e-2
1.847e-2
Acenaphtylene

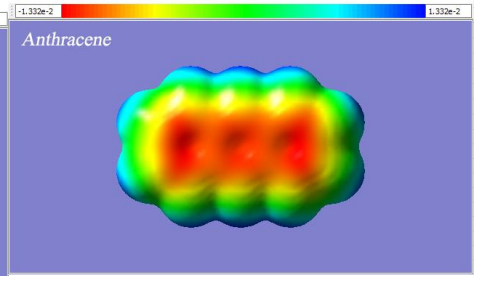
-1.332e-2
1.332e-2
Anthracene

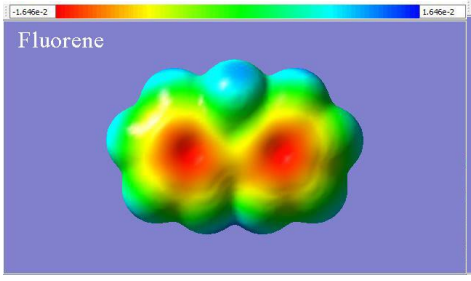
-1.646e-2
1.646e-2
Fluorene

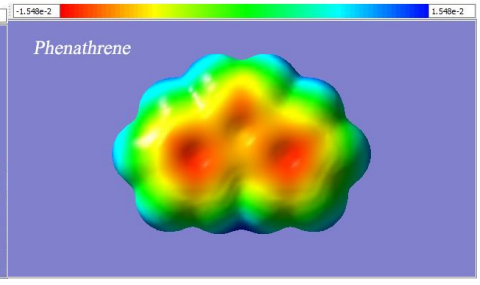
-1.548e-2
1.548e-2
Phenathrene

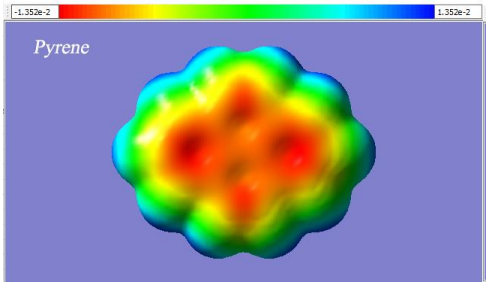
-1.352e-2
1.352e-2
Pyrene

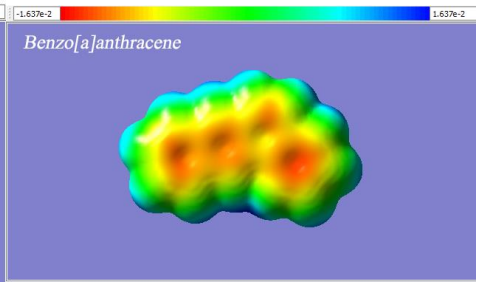
-1.637e-2
1.637e-2
Benzo[a]anthracene

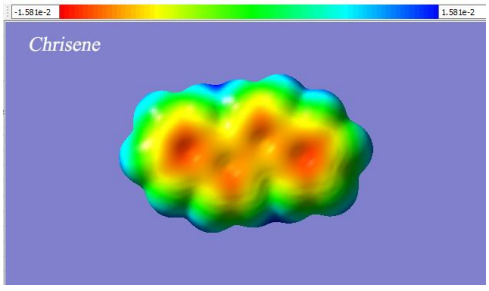
-1.581e-2
1.581e-2
Chrisene

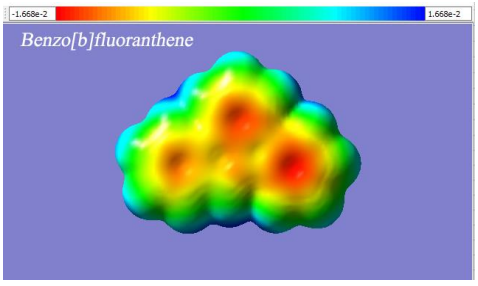
-1.668e-2
1.668e-2
Benzo[b]fluoranthene

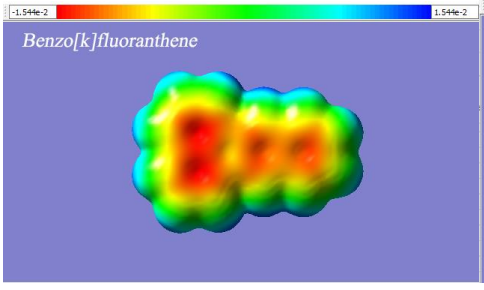
-1.544e-2
1.544e-2
Benzo[k]fluoranthene

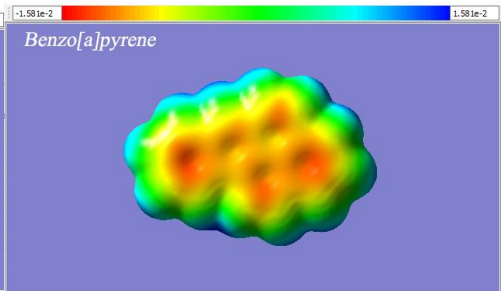
-1.581e-2
1.581e-2
Benzo[a]pyrene

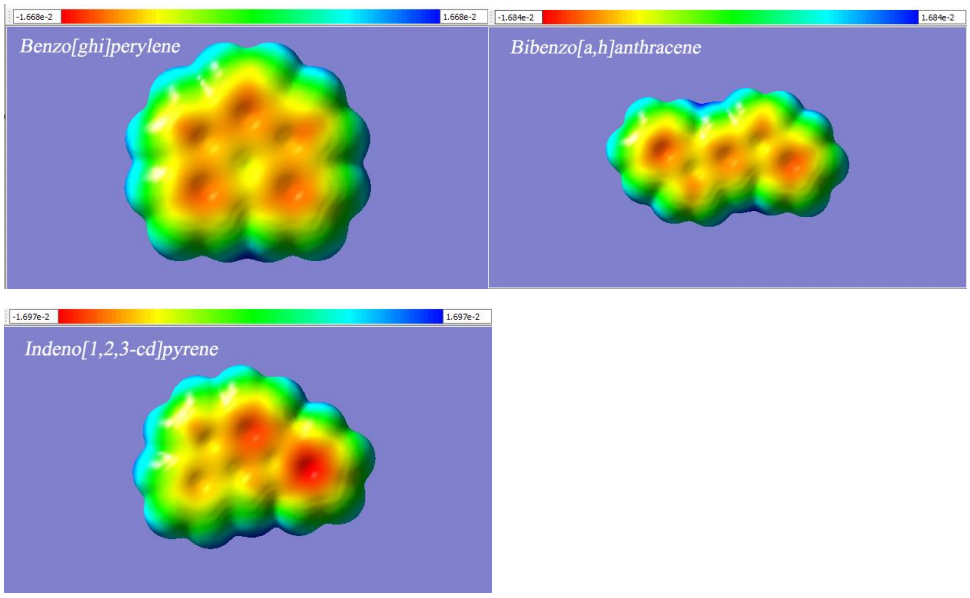

Fig. 8: Electrostatic potential and charge density distribution results of target PAHs, listed following the classes described in paragraph 3.3 (ring classification). At the top of each structure, the colour scale of electrostatic potential distribution (unique for each PAH) is represented, with the blue (red) portion representing the most positive (negative) potential.

Indeed, the area of the π-electron plane spatially increases when the number of rings increased, as demonstrated also by Yang and co-workers [40]. Hence, the heavier molecular weight of the PAHs offers higher surface availability for interaction with positively charged amino groups. Moreover, such behaviour is also in agreement with stronger Van der Waals interactions. Conversely, for PCBs, the addition of chlorine atoms on the biphenyl structure enhances steric hindrance, in agreement with observations of Dachs and Bayona [38]. In Fig. 6.9, as an example, the different behaviour of PAHs (Fig. 6.9A) and PCBs (Fig. 6.9B) is compared for SBA-15-AN.

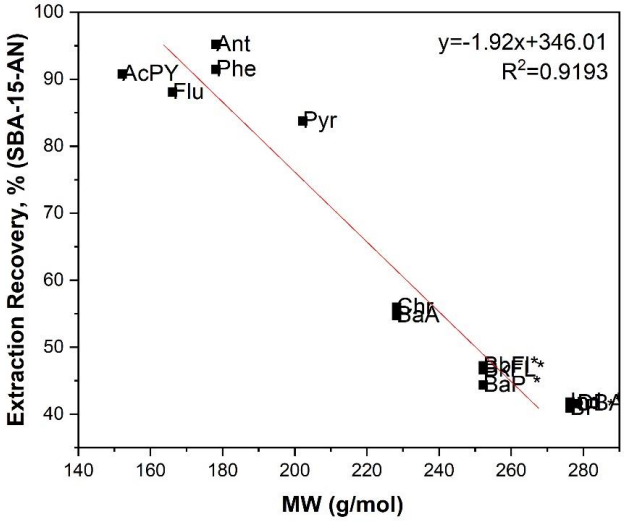

A

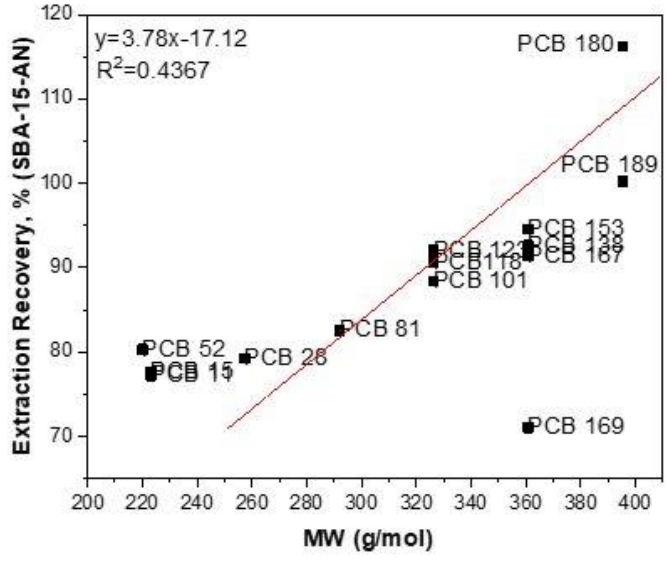

B

Fig. 6.9. Dependence of PAH (A) and PCB (B) extraction recovery percentage on molecular weight (MW) using SBA-15-AN as *d*-SPE sorbent within the QuEChERS protocol in strawberry.

Eventually the polarity of micropollutants was also considered. Variations in logP does not significantly influence the extraction performance of the

QuEChERS method when SBA-15-APTES or SBA-15-AN are used as d-SPE sorbents. Instead, an apparent correlation of ER% with log P for both PAHs and PCBs classes is observed only for PSA (ER% = 10.36 logP + 0.49, r^2=0.653), highlighting possible limitations in its use of this d-SPE sorbent for more polar analytes. This observation agrees with what found by Scordo et al. [1] in the extraction of perfluoroalkyl acids from strawberry.

6.1.4. Conclusions

SBA-15 mesoporous silica were functionalized with (3-aminopropyl)-triethoxysilane (SBA-15-APTES) and N-[3-(Trimethoxysilyl)propyl]aniline (SBA-15-AN) and used for the first time as d-SPE sorbents in the removal of coextracted compounds (e.g. sugars) in the QuEChERS protocol applied for the determination of micropollutants (PAHs and PCBs) in strawberry. SBA-15-APTES and SBA-15-AN were physico-chemically characterized and compared with PSA, the d-SPE sorbent usually employed in QuEChERS application. The removal capabilities of SBA-15-APTES and SBA-15-AN towards glucose, sucrose and fructose, chosen as model sugars present in strawberry was observed to be higher than that of PSA, due to the higher amount of adsorption active sites. A thorough study of the effect of pH on removal of sugars allowed to propose an interaction mechanism between amines and sugar molecules mainly based on H-bonding.

The suitability of SBA-15-APTES and SBA-15-AN as *d*-SPE sorbents were confirmed including these sorbents in the clean-up step of a QuEChERS protocol for the determination of PAHs and PCBs in intentionally contaminated strawberries. Signal-to-noise ratio for PCBs can be significantly reduced by SBA-15-AN, indicating even a more efficient cleanup if compared to PSA. It is worth remembering that the reduction of signal-to-noise ratio is important to determine lower concentrations of micropollutants in food. Overall, QuEChERS protocol performed by SBA-15-AN provides slightly lower or

comparable extraction recoveries than PSA (63±7 % vs 76±19 % for PAHs, respectively and 92±6 % vs 88±9 % for PCBs) and better reproducibility of the method. Molecular weight of the target micropollutants, but not log P, seem to influence the overall QuEChERS extraction recovery in the organically modified SBA-15.

6.2. Encapsulation of the glyphosate herbicide in mesoporous and soil-affine sorbents for its prolonged release

L. Rivoira, S. Frassati, S. Cordola, M. Castiglioni, B. Onida, S. Ronchetti, I. Ingrando, M.C. Bruzzoniti,
"Encapsulation of the glyphosate herbicide in mesoporous
and soil-affine sorbents for its prolonged release"
Chemical Engineering Journal, Submitted

6.2.1 Introduction

Weed control is the botanical component of pest control that is used to prevent weeds from reaching a matured crop which is ready for cultivation [41]. Both physical and chemical methods are exploited to reduce weeds that are harmful to agricultural plants and fodder. Among them, herbicides are the dominant tool used for weed control in modern agriculture.

Nowadays, it is recognized that, to ensure the effectiveness of crop production, herbicides are often applied at exceeding dosages [42] and that current formulations generally release the compound into the environment practically instantaneously [43].

In the light of the information described above, a wide use of herbicides is evident, thus leading all the countries of the world to face different problems, such as the rapid evolution of herbicide-resistant weeds [44, 45], the environmental impact of these compounds, [46], and the impact on human health, with particular attention to worker exposure [47, 48], with 170,000 workers worldwide employed in the agricultural died every year. On these incidences, a correlation between deaths and exposure to toxic pesticides through spray, drift and direct contact cannot be excluded [49].

In order to prevent the above-mentioned issues and given the public pressure to reduce the overall pesticide use, new integrated weed management strategies are now strongly encouraged [50, 51]. Among these, an important part is devoted to the development of new methods for the application of herbicides on soils.

Among the several herbicide formulations that are applied, glyphosate is probably the most used in the world (about 720k tons production in 2012)

[52]. Glyphosate (N-(phosphonomethyl)glycine) is a broadspectrum post-emergence herbicide used both in agriculture and for the conservation of green spaces, such as parks and gardens [53]. The more common methods of glyphosate use include broadcast, aerial, spot, and directed spray applications [54]. It should be remarked that despite glyphosate is typically spread on leaves, its absorption through roots has been clearly assessed [55] and application to soils are also reported, i.e. for fungicidal aims [56].

Despite its huge consumption, glyphosate has been the subject of controversial discussions over its impact on the environment and human health in recent years, with IARC (International Agency for Research on Cancer) classifying glyphosate as *a probable human carcinogen compound* (class 2A), oppositely to EFSA (European Food Safety Authority) stating that this herbicide *is unlikely to pose a carcinogenic hazard to humans*.

Despite this still-open discussion, on December 12, 2019 European Union renewed the licence for the sale of glyphosate for five years [57], even if some countries (for example Italy) has already introduced some restrictions on the use of this herbicide [58].

The impact of glyphosate on the environment has been extensively studied, as traces of glyphosate and its metabolites could be found both in water basins, in soils and even in the atmosphere [59]. Therefore, selected approaches are nowadays exploited to face the emergency caused by the use of glyphosate. Most of them are post-use remedies, and are mainly based on the development of new technologies for the removal of the herbicide from the environmental compartments [16, 17]. However, it is also appropriate to evaluate some approaches defined "a priori" which, on the contrary, are based on the reduction of the quantity of glyphosate released into the environment.

The incorporation of active formulations inside specific carriers to obtain a controlled release in the environment has been extensively explored for

agricultural applications, in order to set-up the concentration of the active principle within a range spanning from the minimum effective concentration to the maximum concentration safe for the operator [60]. Applications reporting the encapsulation of fungicides [61], herbicides [62], insecticides [63], acaricides [64], as well as of compounds intended for the stimulation of plant growth and productivity [65] are frequently presented in the scientific literature. Conversely, research concerning glyphosate is under-investigated and light controlled [66] and supramolecular [67] systems are the only solutions proposed.

Mesoporous silica and clay based materials exhibit adsorption properties that were exploited for the preparation of sorptive substrates [14, 68] and in water remediation technologies [69, 70]. In particular, the removal of herbicides using both types of supports through selective bonds between silica or clay supports with the active compounds is demonstrated [71].

Hence, this work aimed at the innovative encapsulation of glyphosate into selected silica- and clay- based supports. The encapsulation of the herbicide allows the application of the loaded support, promoting both a punctual application and the controlled release of glyphosate, thus limiting human exposure to glyphosate, during application. To the best of our knowledge, this work represents the first study specifically devoted to the encapsulation of glyphosate into mesoporous sorbents, which indeed have a structure affine to the composition of the soil.

For this study, three different types of environmental-friendly mesoporous silica and clay-based supports were selected, namely: SBA-15, montmorillonite (MMT) and Al pillared montmorillonite (Al-MMT). MMT and Al-MMT can be also considered low cost and then their use appears feasible in the proposed application. After physicochemical characterization of the pre- and post-impregnated supports, tests on the release of glyphosate were performed simulating different environmental conditions, such as acid rains

or soil leaching. Data obtained within release tests were fitted to kinetics models typically used to describe desorption of active principles from mesoporous supports. Finally, the sorbent showing the best releasing performances was chosen for a real sample application, in a water/soil bench-scaled system.

6.2.2 Experimental

6.2.2.1 Materials and reagents

A highly stable mesoporous silica sieve (Santa Barbara Amorphous, hereafter called SBA-15), montmorillonite K-10 (MMT) and Al pillared montmorillonite (Al-MMT) were purchased from Sigma-Aldrich (Darmstadt, Germany).

Glyphosate, sodium hydroxide solution (grade >98%), ethanol, hydrochloride acid (40%), oxalic acid (98%) and calcium chloride were from Sigma-Aldrich (Darmstadt, Germany).

High purity water (18.2 MΩ cm resistivity at 25 °C), produced by an Elix Milli Q Academic system (Millipore, Vimodrone, MI, Italy) was used for standard and eluent preparation.

6.2.2.2 Instrumental setup and calibration

The release profiles of glyphosate from the tested substrates were evaluated by means of suppressed ion chromatography as recently optimized by our research group [17]. A DX-100 ion chromatograph (25-µL injection loop) from Dionex, Thermo Scientific, (Sunnyvale, CA, USA) equipped with a conductivity detector was used. An IonPac AG16 (50 × 4 mm) and IonPac AS16 (250 × 4 mm) were used as guard and analytical columns, respectively. Mobile phase was 35 mM NaOH at a flow rate of 1.0 mL/min. Detection was performed by electrochemical suppressed conductivity (100mA current set-up) using a 4-

mm ESRS-300 membrane suppressor. Chromatographic data were collected by PeakNet 2.8 software.

For calibration curve, a 100 mg/L glyphosate stock solution was used to prepare standard solutions (six levels, from 0.5 to 15 mg/L). Each level was injected in triplicate and a new calibration curve was run, weekly. Limits of detection and limits of quantifications of the chromatographic method were calculated according to Shrivastava and Gupta and were 0.1 mg/L and 0.3 mg/L, respectively [72].

6.2.2.3 Impregnation of the supports with glyphosate

The impregnation of supports with glyphosate was achieved using water as solvent through the incipient wetness impregnation technique [73], by which a volume of a solution containing the active ingredient to be incorporated is put in contact with the support itself. Consequently, the solution is forced to spread by capillary within the available pores, by means of a manual or a mechanical mixing. Finally, the impregnated material is dried as to evaporate the excess of solvent and to allow the deposition of the desired molecules inside the support.

In detail, a saturated solution of glyphosate was prepared by dissolving 0.4 g of glyphosate in 33 mL of water (solubility=12 g/L, at room temperature [74]). Subsequently, 1 mL of such solution was added dropwise to 0.6 g of each support, thus obtaining a homogenous slurry, which was finally oven dried at 60°C for 24 hours. The impregnation procedure was performed at room temperature and was repeated until the glyphosate saturated solution was totally consumed. The procedure allowed to obtain 40% glyphosate impregnation in respect to the total weight of the support.

6.2.2.4 Physicochemical characterization of the supports pre- and post-impregnation

X-ray diffraction (XRD) patterns were obtained using a PANalytical X'Pert Powder (Cu Kα radiation) diffractometer. The measurements were performed by means of a circular sample holder with diameter of 30 mm and thickness of 2 mm. Nitrogen adsorption isotherms were measured using a Quantachrome (FL, USA) AUTOSORB-1 instrument. Prior to nitrogen adsorption, samples were outgassed (393 K, 5 h). BET specific surface areas (SSA) were calculated in the relative pressure range 0.04–0.1.

6.2.2.5 Release of glyphosate from supports in aqueous solutions

The release of encapsulated glyphosate from the different tested supports in aqueous solutions, was evaluated simulating different environmental conditions. In detail, 0.25 g of each impregnated material was put in contact with 15 mL of the following aqueous solutions: i) ultrapure water, pH 6.5; ii) 0.02 M oxalic acid (pH 3), to simulate acid rains; iii) 0.01 M $CaCl_2$ solution, to simulate soil salinity (experiments were performed both at neutral and acidic pH). The suspension was stirred in an orbital shaker up to 7 days at room temperature, withdrawing 100 µL-aliquots from each solution at scheduled times, namely: 0 and 30 seconds, 1, 2, 5, 10, 30, 60, 1140 (1 day), 2880 (2 days), 4320 (3 days), 8640 (6 days) and 10080 minutes (7 days). The cumulative sampled volume was less than 5% of the initial volume (15 mL), thus it can be assumed that the influence of the volume change on the release pattern is negligible. Release tests were performed separately for each support, in order to avoid any competitive equilibrium, and were repeated in triplicates.

Each sampled solution was then diluted 1:1000 with ultrapure water prior to IC analysis. The concentration of the glyphosate released (C_r) was derived through the calibration curve previously commented. The percentage of

glyphosate released (*Release %*) was calculated according to the following equation:

$$Release\% = \left(\frac{1000 * Cr}{Cmax}\right) * 100$$

where C_{max} is the maximum concentration that could be released from each support, according to the encapsulation procedure and the nominal glyphosate content (i.e. 40 % w/w), namely 6400 mg/L. This concentration was chosen to match the content of glyphosate in commercial formulations (e.g. 64-66% for granular RoundUp product) in consideration of the amount of commercial product to be applied in real applications (about 10 g of granules per liter, according to the manufacturer indications).

6.2.2.6 Mathematical modelling of glyphosate release

The profiles of glyphosate release from the studied supports were mathematically modelled to better understand the dissolution profile. Within this work, several models were evaluated, as hereafter listed. Even if all models were originally developed for drug delivery from polymeric and non-polymeric supports, they are commonly applied for the release of herbicides [75, 76] as well.

Zero-order model (*Release %* vs. time) [77]

The release rate is supposed to be independent from the concentration of herbicide, And the same amount of compound is expected to be released per unit of time, according to eq. 1.

$$C_t = C_0 + K_0 t \qquad (1)$$

where C_t is the amount of herbicide (mg/L) dissolved at the time t (expressed in hours), C_0 is the initial amount of the herbicide dissolved in the solution and K_0 is the zero-order release constant, expressed as mg/L/h.

Pseudo first-order model (log of *Release %* vs. time) [78]

Differently to the zero-order model, in the first-order kinetic, the release rate depends on the concentration. The linearized model is expressed by eq. 2:

$$log\ Ct = log\ C_0 - Kt/2.303 \quad (2)$$

where Ct is the concentration of herbicide (mg/L) released at t time (expressed in hours), C_0 (mg/L) is the initial dissolved concentration of herbicide in the media and K is first order constant (1/hour).

Korsmeyer and Peppas model (log of *Release %* vs. log of time) [79]

The Korsmeyer-Peppas model (eq. 4) can be used to discriminate between Fickian diffusion or non-Fickian (anomalous) diffusion [80]. The linear relation is expressed by eq. 3

$$logCt = logK + n\ logt \quad (3)$$

where Ct is the concentration of drug released at time t (mg/L), K ($hour^{-n}$) is the release rate constant and n is the diffusional exponent (adimensional). This kinetic equation is claimed valid only for the first 60% of the released active principle [79].

For a dispersed, non-swellable system, the value of n gives an indication of the release mechanism, as hereafter listed [81]: i) $n < 0.5$, quasi-Fickian diffusion, ii) $n = 0.5$, Fickian diffusion mechanism, iii) $0.5 < n < 1$, non-Fickian diffusion, iv) $n = 1$, case II transport (zero-order release), v) $n > 1$, super case II transport.

It should be noted that for n=0.5, a Fickian diffusion is present. Accordingly, eq. 3 simplifies into the Higuchi's equation (eq.4):

$$C_t = K_H\ t^{0.5} \quad (4)$$

where C_t is the amount of drug released (mg/L) at time t (expressed in hours) and K_H is the release rate constant of H ($hour^{-1/2}$).

6.2.2.7 Water/soil bench-scaled system

The release of glyphosate from the most promising support among the four tested (Al-MMT) was evaluated in a real soil/water system and compared in parallel with the release of glyphosate from a commercial formulation. Soil was collected from a public garden in the town of Torino (Valentino Park) and was chosen to have the representative composition of typical soils intended for horticulture uses [82], where glyphosate is mostly employed. In detail, 0.25 g of each formulation was added to 15 g soil/15 ml tap water dispersion in a glass bottle. pH of the suspension was measured and was equal to 6.8. At selected times after herbicide application (from 0 min to 7 days, as for the water release studies), the bottles were hand-shaken, the contents were allowed to settle, and 100 µL of the supernatant solution were filtered and analysed by IC to determine the glyphosate concentration released. The periodic sampling of such a small amount of supernatant was assumed not to have any influence on the release pattern. Release kinetics were evaluated in triplicate.

6.2.3. Results and Discussions

6.2.3.1 Physicochemical characterization

The Incipient Wetness Impregnation technique is a protocol frequently exploited for the encapsulation of active principles in supporting materials, since it does not require specific reagents or procedures, and since it guarantees quantitative impregnation of the supports [6].

To investigate how glyphosate was encapsulated in the tested materials, physicochemical characterization of SBA-15, MMT and Al-MMT was performed.

Specific surface area (SSA_{BET}) and pore volume of each substrate, obtained by nitrogen sorption analysis before and after impregnation (Figure S1, S2 and S3 in the Supplementary Material) are reported in Table 6.2.

***Table 6.2**. Specific surface area (SSA) and pore volume of the four tested materials, before and after the encapsulation of glyphosate. Brunauer–Emmett–Teller (BET) model was used for calculations.*

	SSA_{BET} (m^2/g)	**Pore volume (m^3/g)**
SBA-15	701	0.99
SBA-15 impregnated	492	0.74
MMT	279	0.42
MMT impregnated	83	0.15
Al-MMT	250	0.26
Al-MMT impregnated	6	0.017

The three sorbents cover a wide range of porosity (from 0.26 to 0.99 m^3/g pore volume and from 250 to 700 m^2/g SSA).

The impregnation with glyphosate resulted, for all the supports, in a significant modification of nitrogen adsorption-desorption isotherms (Figure S1, S2 and S3 in the Supplementary Material) and a reduction of SSA and pore volume (Table 1). These results indicate the location of glyphosate molecules inside the mesopores of the materials. This evidence is dramatic for Al-MMT (around 98% and 96% reduction of SSA and pore volume,

respectively), suggesting that in this case the original mesoporous structure has been fully occupied by the herbicide. Indeed, the adsorption-desorption isotherms of N_2 on Al-MMT (Figure S1) reveal that the hysteresis loop, typical of disordered mesoporous materials, almost disappeared after the inclusion of glyphosate (red-triangled line).

The almost complete filling of pore volume for Al-MMT by glyphosate, at variance with SBA-15 and MMT, is in agreement with the lowest pore volume measured for Al-MMT (0.26 m^3/g) when compared to those of SBA-15 (0.99 m^3/g) and MMT (0.42 m^3/g), considering that the same amount of glyphosate (0,40 g) per gram of support is present in the three impregnated materials.

In order to characterize the glyphosate in SBA-15, MMT and Al-MMT, XRD measurements were also performed (Figure 6.10).

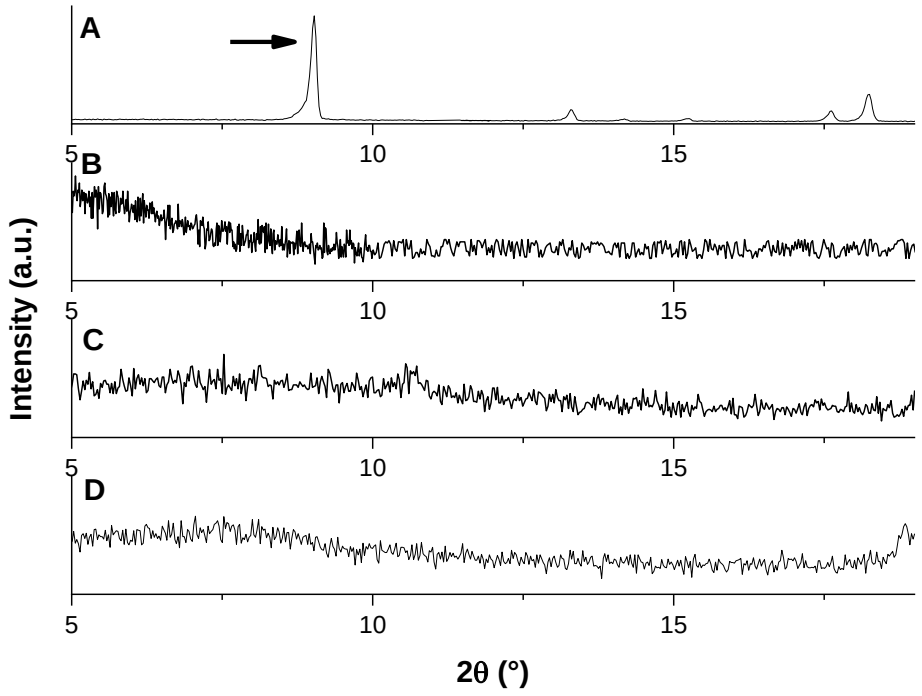

***Figure 6.10**. XRD patterns of glyphosate (A) and post-impregnated support: B - SBA-15, C- MMT, D- Al-MT. Black arrow points the main peak of crystalline glyphosate (2θ = 8.9°)*

Results showed that the main peak of crystalline glyphosate (2θ = 8.9°, Fig.6.10A) is absent for all sorbents (6.10B, 6.10C, 6.10D). The lack of crystalline glyphosate signal is indicative for a complete amorphization of glyphosate. This is ascribed to the location of molecules inside materials mesopores, preventing crystallization [83] , and to their interaction with the surface sorbents.

The location of glyphosate molecules inside mesopores was confirmed by small angle XRD patterns (see Supplementary Material). In details, to what concern SBA-15 a decrease of the intensity of the peak (100) is observed, being indicative of the pore filling, in agreement with the decrease of the scattering contrast between the pores and the walls [84]. As far as MMT and Al-MMT are concerned, the location of glyphosate molecules in the interlayer spacing of the clays is evidenced by the vanishing of the typical basal peak (related to d001), indicating that the interlayer has expanded due to the inclusion of glyphosate [83].

6.2.3.2 Desorption tests in ultrapure water

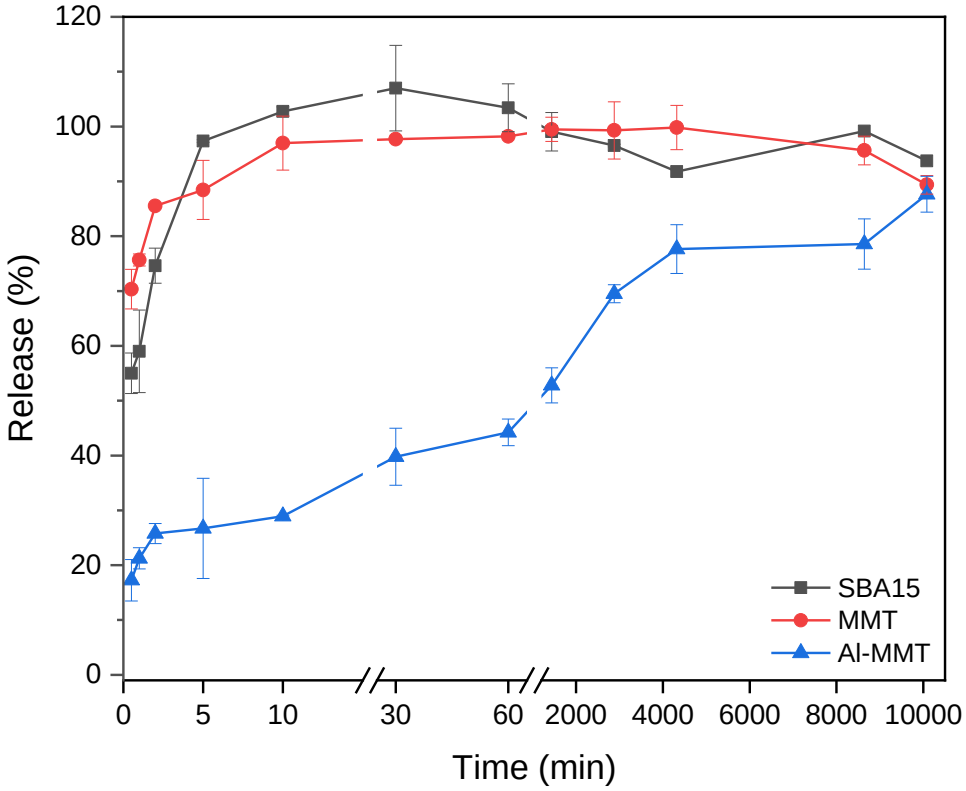

***Figure 6.11**. Desorption kinetics of glyphosate in ultrapure water from impregnated supports SBA-15, MMT and Al-MMT. For an easier comprehension, sampling time is expressed both as minutes and hours in the lower and upper X axis, respectively. Experimental conditions are detailed in Experimental Section.*

Ultrapure water (pH 6.5) was chosen as the first aqueous medium to be tested in order to avoid any competition of external species which could affect the release of glyphosate from supports.

The dissolution profiles of glyphosate in ultrapure water from SBA-15, MMT and Al-MMT are shown in Figure 6.11. The values on the left y-axis are given as percentages of the total amounts of glyphosate present in the dissolution vessel and, for all release curves, a 100% release corresponds to 6400 mg/L glyphosate concentration (for more details, see Experimental Section, 6.2.2). When focusing on the short sampling times, it is observed that more than 50% of the glyphosate is released from both SBA-15 and MMT after only 30 seconds, reaching a quantitative release after 10 minutes. Hence, no prolonged release of the herbicide was observed for such sorbents. For SBA-15, less than 10% of the herbicide is still retained after 5 minutes and a complete released is observed after 10 minutes of contact with water, suggesting that weak interactions occur between glyphosate molecules and SBA-15 surface. This behaviour is in agreement with adsorption results previously obtained [17], showing negligible interactions between glyphosate and SBA-15 at neutral pH, whereas partial adsorption was observed only at acidic pH (see next paragraph).

A similar behaviour was observed also for MMT (96.9% release after 10 minutes). Despite several works report that selective interactions between glyphosate and MMT can occur, in particular at acidic pH (< 4) [85, 86], desorption tests here presented are performed at a neutral pH, which is higher than the point of zero charge (PZC) of MMT (about 3.4). In such conditions, the clay mineral surface is negative [85] and the negatively charged glyphosate [17] could hardly be retained by the negatively charged surface adsorption sites due to electrostatic repulsion. Such behavior is responsible for the fast and quantitative release rate of glyphosate within the short sampling time.

Differently to what previously discussed for MMT and SBA-15, the trend of Al-MMT indicate a slower kinetic release. Indeed, after 2 minutes only 28% (of impregnated glyphosate was released in the solution from Al-MMT,

suggesting that the interactions between the herbicide and the support are stronger than those occurring in SBA-15 and MMT. To explain this behavior, it should be mentioned that Al-MMT is characterized by the presence of Al^{3+} ions that could be complexed with glyphosate, mainly through phosphate-Al interaction [87], forming monomeric and dimeric complexes [88]. This interaction is, therefore, proposed to be responsible for the slower release of the herbicide from Al-MMT.As regards the releasing mechanism, it should be mentioned that the complexation constants of Al-glyphosate are lower than Al-H_2O constants [88]. Hence, a competition of water molecules, interacting with aluminium, could occur.

Al-MMT system exhibits a prolonged release of glyphosate which appears appealing for the proposed application. The slow release observed for Al-MMT is ascribed to strong interactions between glyphosate molecules and internal surface of the support. Moreover, the diffusion of glyphosate molecules from the internal pore structure may at same extent control the release. The location of glyphosate molecules in the interlayer spacing of the pillared clay is evidenced by the XRD pattern at small angles (Figure S6 in the Supplementary Material), as previously discussed. The release of glyphosate by Al-MMT is in agreement with the work of Siepmann and co-workers, in which the drug release was shown to be kinetically longer for supports in which the active principle was encapsulated in the material core [89].

The performances of Al-MMT (20% of the herbicide still inside the support after 7 days) were compared with those reported in the only two literature papers on the release of glyphosate. Data show that Al-MMT exhibits better or at least similar prolonged release performances (i.e. slower dissolution profiles) than biochar-attapulgite (quantitative glyphosate release of glyphosate after 2 hours) [66], and supramolecular organic guest intercalated layered double hydroxides (40% release after 24 hours) [67] systems, respectively.

6.2.3.3 Desorption tests in simulated acid rain solution

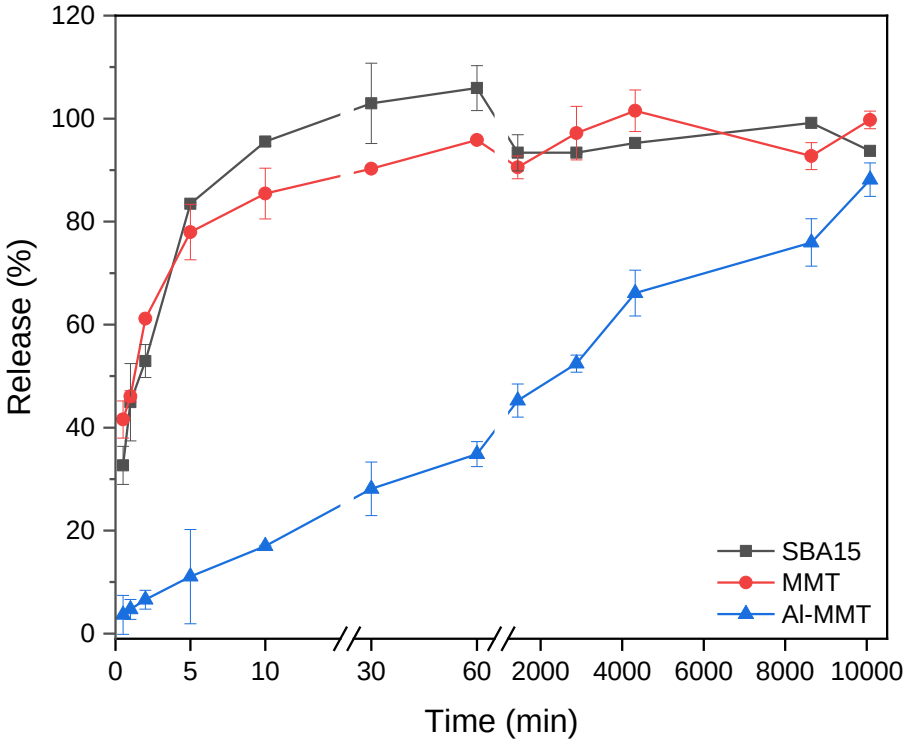

***Figure 6.12**. Desorption kinetics of glyphosate in 0.02M oxalic acid (pH=3) from SBA-15, MMT and Al-MMT. For an easier comprehension, sampling time is expressed both as minutes and hours in the lower and upper X axis, respectively. Experimental conditions are detailed in Experimental Section.*

Once assessed the desorption behaviours in ultrapure water, the same tests were replicated at pH 3, simulating worst conditions of rain acidity [90] (Figure 6.12).

The dissolution profiles of Figure 3 showed that, also at acidic conditions, Al-MMT was the only support characterized by a prolonged release of glyphosate (about 13% still retained after 7 days), with a partial slowdown of the kinetic in comparison to the one obtained in ultrapure water (Table 6.3, column A vs B). A slowdown was also observed for pure MMT (Table 6.3, column C vs D), despite this support quantitatively release glyphosate after 60 minutes.

Table 6.3. Comparison of glyphosate release up to 3 days between ultrapure water medium (UP) and 0.02M oxalic acid, pH3 (pH3). Gray cells show sampling times in which quantitative release of glyphosate is reached.

Glyphosate release (%)				
	Al-MMT		**MMT**	
	pH3 (A)	**UP (B)**	**pH3 (C)**	**UP (D)**
0.5 min	3.6	17.3	41.6	70.3
1 min	4.7	21.2	46.1	75.7
2min	6.6	25.8	61.2	85.5
5min	11.1	26.7	78.0	88.4
10min	17.0	28.9	85.4	97.0
30min	28.1	39.8	90.3	97.7
60 min	34.9	44.2	95.9	98.2

1 day	45.3	52.8	90.5	99.5
2 days	52.4	69.5	97.2	99.3
3 gg	66.1	77.6	101.5	99.8

To explain the slowdown of Al-MMT and MMT kinetics, both acid-base equilibrium of glyphosate and surface properties of montmorillonite should be considered. Indeed, at pH 3 glyphosate is present with a protonated carboxylic, and a monovalent phosphonic group (Figure 6.13A).

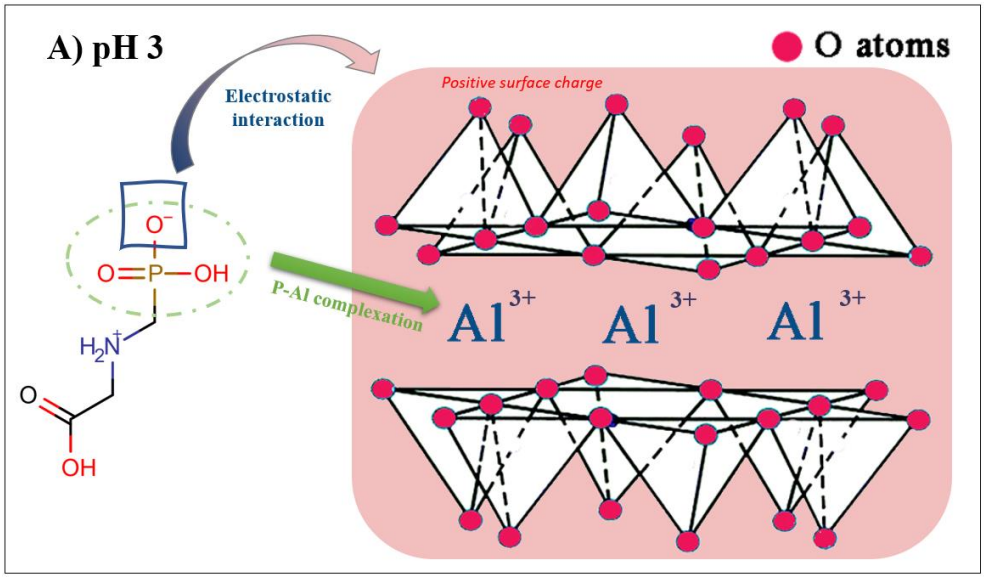

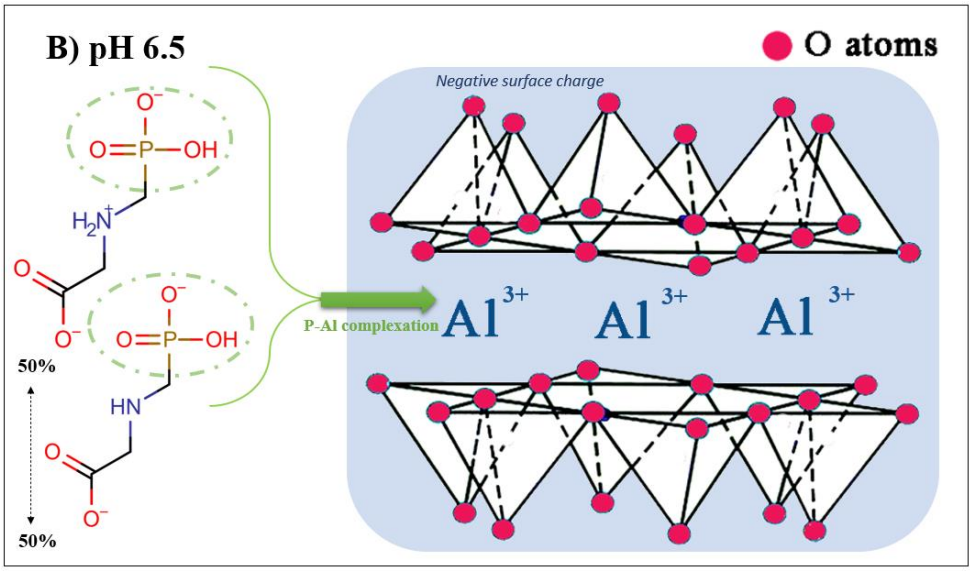

***Figure 6.13**. Surface charge of Al-MMT and chemical dissociation of glyphosate at pH 3 (A) and pH 6.5 (B). Main interaction occurring at both pH values are also highlighted.*

Since pH conditions are lower than Al-MMT PZC (about 4.3 [91]), the surface of montmorillonite has to be considered positively charged (Figure 6.13A). Conversely, in ultrapure water (pH around 6.5) glyphosate is present with the same monovalent phosphonic group but with the deprotonated carboxylic, (Figure 6.13B) and the surface of montmorillonite has to be considered negatively charged, being above its PZC. Therefore, electrostatic repulsions occur in ultrapure water, which instead are not present at pH 3.

Summarizing, for Al-MMT at pH values close to neutrality, the effect of both P-Al interactions and electrostatic repulsion influence the release of glyphosate, thus justifying the lower retention of glyphosate, and hence the faster kinetic release, observed in respect to acidic pH conditions where only P-Al interactions occur. Moreover, despite the zwitterionic form of glyphosate

at pH3, electrostatic attractive interactions between the negative phosphonic group and the positive surface of Al-MMT may give a further contribution to the retention, besides the complexation of Al^{3+} ions by glyphosate.
A fast release was observed for SBA-15 since more than 85% of glyphosate is released after 5 minutes. However, after 30 seconds about 35% release was observed at pH 3, against 55% in ultrapure water, thus supporting the role of surface charge also in the interaction between SBA-15 and negatively charged glyphosate. Indeed, pH 3 may be considered below the PZC of SBA-15 PZC (5.2), whereas at pH around 6.5 the surface of SBA-15 has to be considered mainly negatively charged [92].

6.2.3.4 Desorption tests in simulated soil conditions

Previous tests were performed without considering any competing species. However, the presence of the soil matrix can affect the release of glyphosate from encapsulating support. Competitive interactions between surface moieties and soil salts, such as calcium chloride [93], can be established, with charged species potentially promoting a faster release of the herbicide.
Experiments were performed on Al-MMT only, since MMT and SBA-15 were shown to exhibit a fast release, not compatible with prolonged applications. Glyphosate desorption from Al-MMT in 0.01M $CaCl_2$ solution was studied, roughly simulating the ionic strength of soil solutions [93].
Dissolution profiles obtained in 0.01M $CaCl_2$ at pH conditions acidic (pH=3) and close to neutrality (pH=6.7) are reported in Figure 6.14 (triangled blue- and squared black- lines, respectively), together with desorption profiles obtained in ultrapure water and oxalic acid solution (starred green- and pointed red- lines, respectively) for a better comparison.

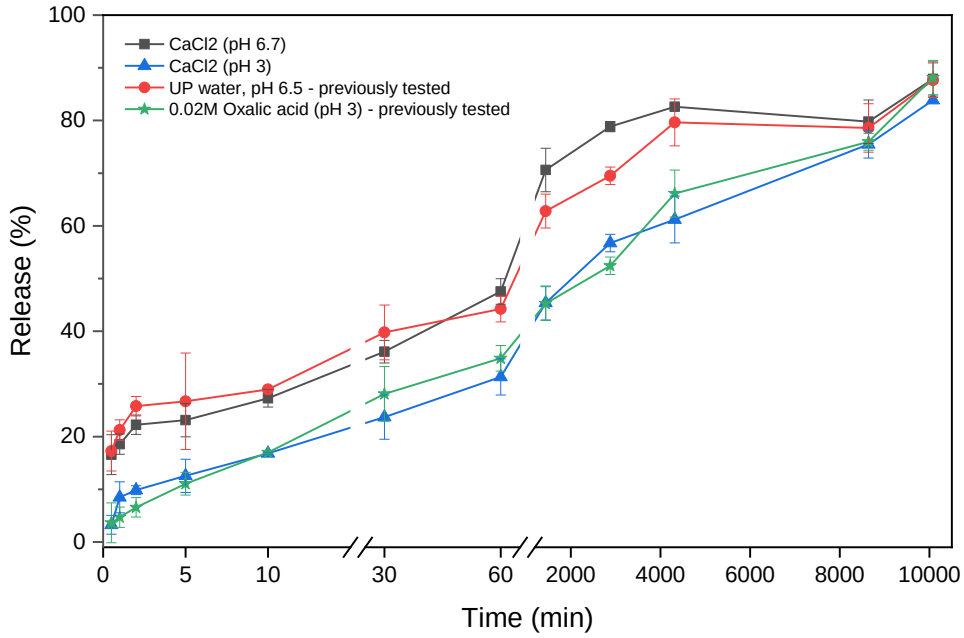

***Figure 6.14**. Desorption profiles of glyphosate 0.01M $CaCl_2$ solution, at acidic (pH 3) and almost neural (pH 6.7) conditions. Release percentage in ultrapure water (UP water) and 0.02 oxalic acid solution are overlaid. For an easier comprehension, sampling time is expressed both as minutes and hours in the lower and upper X axis, respectively. Experimental conditions are detailed in Experimental Section.*

Results confirmed that, within the standard deviation of the measurements, glyphosate release is not affected by $CaCl_2$, thus suggesting the absence of significant competitive interactions between Al-MMT and $CaCl_2$. It is important to highlight that after 7 days, about 10-15% of the herbicide is still adsorbed on the support and that the prolonged release of Al-MMT is confirmed also when simulating soil salinity conditions. Furthermore, the slower kinetic in acidic conditions (as discussed in the "Desorption tests in simulated acid rain solution" paragraph) is still confirmed in $CaCl_2$ solution (green and blue lines

-obtained in 0.02M oxalic acid solution and in $CaCl_2$, pH3 respectively- have a similar trend and are well separated from red and black ones -obtained at neutral conditions-).

6.2.3.5 Computational treatment of release data through kinetic models

The release data of glyphosate from Al-MMT in soil simulating conditions (at both neutral and acid conditions) were fitted to different kinetic models, namely zero-order, first order and Korsmeyer–Peppas models described in Paragraph "Mathematical modelling of glyphosate release" (Experimental section). For each of the above-mentioned model, fitting equation, R^2 values and release constants were determined (Table 6.4).

***Table 6.4**. Modelling of glyphosate release data from Al-MMT in 0.01 $CaCl_2$, at pH 6.7 and pH 3*

Kinetic model	Test conditions	Linearized fitting equation	R^2	K
Zero-order	$CaCl_2$, pH 6.7	$C_t=34.61 + 0.39t$	0.6526	0.39
	$CaCl_2$, pH3	$C_t=19.45 + 0.43t$	0.8362	0.43
Pseudo first-order	$CaCl_2$, pH 6.7	$logC_t = 1.80 - 0.005t$	0.6764	0.12

	$CaCl_2$, pH3	$logC_t = 1.90 - 0.004t$	0.8398	0.09
Korsmeyer–Peppas	$CaCl_2$, pH 6.7	$logC_t = 1.61 + 0.21logt$	0.9902	0.94
	$CaCl_2$, pH3	$logC_t = 1.48 + 0.32logt$	0.9947	0.33

Results clearly show that glyphosate released from Al-MMT follows the Korsmeyer–Peppas kinetic equation. Indeed, for both neutral and acidic pH conditions, R^2 for zero-order and first-order model ranges from 0.65 to 0.84, while the first seven datapoints (representing release of up to approximately 60% of the loaded glyphosate) showed a R^2 value higher than 0.99 when computed by Korsmeyer–Peppas model.

Korsmeyer–Peppas *n* diffusional exponent was consequently calculated, obtaining n=0.21 and 0.32 for neutral and acidic pH conditions, respectively. Accordingly, the release of glyphosate from Al-MMT support appears to be diffusion controlled, following a quasi-Fickian model.

Finally, the release rate constant (K) is equal to 0.94 $hours^{-0.21}$ and 0.33$hours^{-0.32}$ for neutral and acid pH, respectively. The kinetic parameters obtained were used to calculate release of glyphosate according to the Korsmeyer and Peppas model (Figure 6.15) which was in satisfactory agreement with the experimental data.

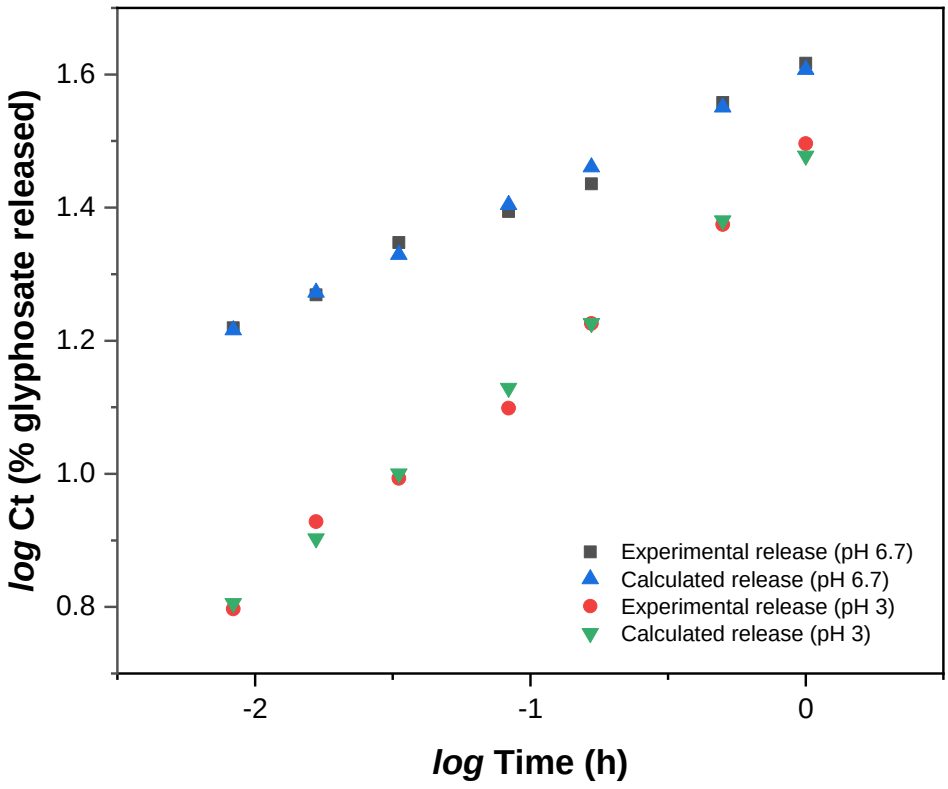

***Figure 6.15**. Release kinetics for glyphosate from Al-MMT. Experimental and calculated values according to linearized Korsmeyer and Peppas model.*

To the best of our knowledge, no other studies investigating the kinetic models describing the release of glyphosate in controlled release applications are nowadays present in literature.

6.2.3.6 Real sample application

The efficacy of Al-MMT in the controlled release of glyphosate was finally tested in a bench scale plant. A laboratory self-made system was setup with a glass bottle filled with a known aliquot of tap water (typically used for

irrigation) and soil according to the procedure previously described (see "Water/soil bench-scaled system" paragraph in Materials and Method Section, §2.7). Through this apparatus, the release of the herbicide was assessed considering not only the dissolution in water medium, but also the competitive adsorption equilibrium of soil, thus simulating a real application in field or in a flowerpot. Releasing performances of impregnated Al-MMT were compared with those of a glyphosate commercial formulation and both kinetic plots are represented in Figure 6.16:

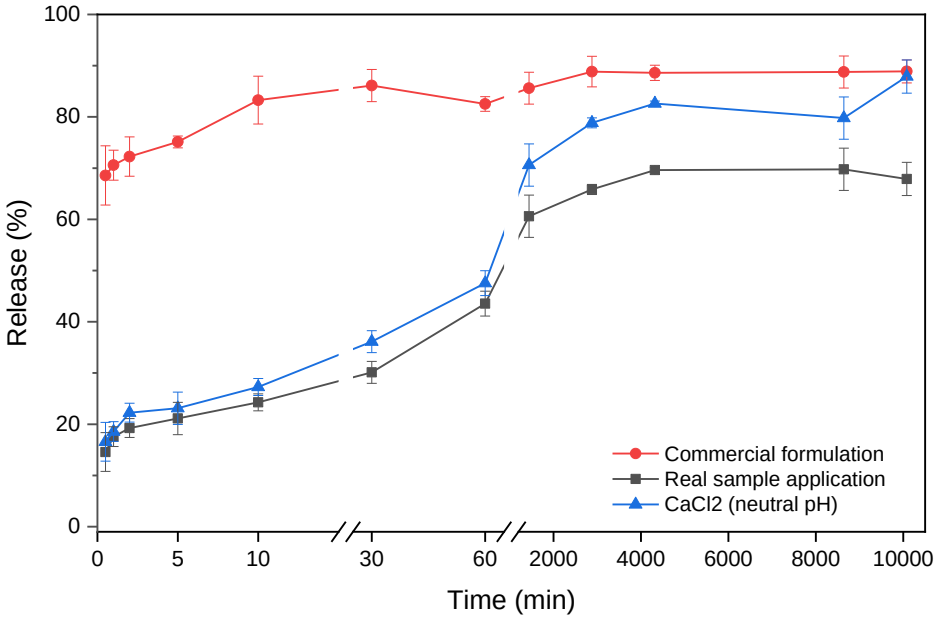

***Figure 6.16**: Desorption profile of glyphosate in bench scaled system (tap water/soil suspension, pH 6.8) from Al-MMT. Releases from glyphosate commercial formulation and from Al-MMT in $CaCl_2$ media, at pH 6.7 were compared. For an easier comprehension, sampling time is expressed both as minutes and hours in the lower and upper X axis, respectively. Experimental conditions are detailed in Experimental Section.*

As shown by the dissolution curves, the bench system confirmed the good performances of Al-MMT as support for the prolonged release of glyphosate, with about 40% of the herbicide still retained after 3 days. The presence of a complex matrix such as real soil particles does not significantly affect the release trend. Moreover, the releasing kinetic of Al-MMT is clearly slower than the one obtained with the commercial formulation, which was almost quantitatively dissolved within 30 seconds after its application (89%). It should be remarked how, in the presence of soil particles, the observed final release of glyphosate applied as commercial formulation is less than 100%, probably due to the herbicide adsorption by the soil particles [94].

6.2.4. Conclusions

Mesoporous silica and clay supports were innovatively presented as releasing systems of glyphosate for application in soils. This practice has the advantage to avoid air-dispersion pollution and worker exposure to glyphosate. This study highlighted that the enhancement of interactions between the support and glyphosate is of paramount importance to achieve a prolonged release of the herbicide. In this regard, the Al-MMT system proved to be the most promising encapsulating support due to: i) Al-glyphosate complexation (through phosphorous moiety); ii) electrostatic interactions bewteen glyphosate and clay surface. Release performances of Al-MMT support (about 10-20% of glyphosate still retained on the support after 7 days) were confirmed both in ultrapure water, and in experimental conditions simulating acid rains and soil composition and was poorly affected by any competitive interaction between the Al-MMT surface and other species. The non-uniform particle size distribution of Al-MMT promoted a semi-Fickian diffusion mechanism which is responsible for the release of glyphosate from the support, as described by the Korsmeyer–Peppas equation (n diffusion exponential < 0.5). The bench scale application of Al-MMT in a tap water/

soil suspension system fully demonstrated the applicability of Al-MMT in the prolonged release of glyphosate in real world applications.

6.3 References

1. Scordo, C.V.A., et al., *Optimization and validation of a method based on QuEChERS extraction and liquid chromatographic–tandem mass spectrometric analysis for the determination of perfluoroalkyl acids in strawberry and olive fruits, as model crops with different matrix characteristics.* Journal of Chromatography A, 2020. **1621**: p. 461038.
2. Rivoira, L., et al., *Impact of effluents from wastewater treatments reused for irrigation: Strawberry as case study.* Environmental Engineering and Management Journal, 2019. **18**(10): p. 2133-2143.
3. Grob, K., et al., *Food contamination with organic materials in perspective: packaging materials as the largest and least controlled source? A view focusing on the European situation.* Critical reviews in food science and nutrition, 2006. **46**(7): p. 529-535.
4. Sung-Jin, L., et al., *Persistent organic pollutants (POPs) residues in greenhouse soil and strawberry organochlorine pesticides.* Korean Journal of Environmental Agriculture, 2016. **35**(1): p. 6-14.
5. European Commission, *2014/663/EU: Commission Recommendation of 11 September 2014 amending the Annex to Recommendation 2013/711/EU on the reduction of the presence of dioxins, furans and PCBs in feed and food Text with EEA relevance.* 2014.
6. Anastassiades, M., et al., *Fast and easy multiresidue method employing acetonitrile extraction/partitioning and "dispersive solid-phase extraction" for the determination of pesticide residues in produce.* J AOAC Int, 2003. **86**(2): p. 412-31.
7. Rossini, D., et al., *Innovative combination of QuEChERS extraction with on-line solid-phase extract purification and pre-concentration, followed by liquid chromatography-tandem mass spectrometry for the determination of non-steroidal anti-inflammatory drugs and their metabolites in sewage sludge.* Analytica Chimica Acta, 2016. **935**: p. 269-281.
8. Bruzzoniti, M.C., et al., *QuEChERS sample preparation for the determination of pesticides and other organic residues in environmental matrices: a critical review.* Analytical and Bioanalytical Chemistry, 2014. **406**(17): p. 4089-4116.
9. Oshita, D. and I.C.S.F. Jardim, *Comparison of Different Sorbents in the QuEChERS Method for the Determination of Pesticide Residues in Strawberries by LC–MS/MS.* Chromatographia, 2014. **77**(19): p. 1291-1298.
10. He, Y. and Y.-H. Liu, *Assessment of primary and secondary amine adsorbents and elution solvents with or without graphitized carbon for the SPE clean-up of food extracts in pesticide residue analysis.* Chromatographia, 2007. **65**(9-10): p. 581-590.
11. Wu, Z. and D. Zhao, *Ordered mesoporous materials as adsorbents.* Chemical Communications, 2011. **47**(12): p. 3332-3338.
12. Li, C.M., et al., *Functionalized Porous Silica-Based Nano/Micro Particles for Environmental Remediation of Hazard Ions.* Nanomaterials, 2019. **9**(2): p. 247.
13. Kumar, P. and V.V. Guliants, *Periodic mesoporous organic–inorganic hybrid materials: applications in membrane separations and adsorption.* Microporous and Mesoporous Materials, 2010. **132**(1-2): p. 1-14.
14. Bruzzoniti, M.C., et al., *Retention properties of mesoporous silica-based materials.* Analytica Chimica Acta, 2000. **422**(2): p. 231-238.
15. Casado, N., et al., *Current development and applications of ordered mesoporous silicas and other sol–gel silica-based materials in food sample preparation for xenobiotics analysis.* TrAC Trends in Analytical Chemistry, 2017. **88**: p. 167-184.

16. Fiorilli, S., et al., *Iron oxide inside SBA-15 modified with amino groups as reusable adsorbent for highly efficient removal of glyphosate from water.* Applied Surface Science, 2017. **411**: p. 457-465.
17. Rivoira, L., et al., *Functionalized iron oxide/SBA-15 sorbent: investigation of adsorption performance towards glyphosate herbicide.* Environmental Science and Pollution Research, 2016. **23**(21): p. 21682-21691.
18. Paris, A., et al., *Polycyclic aromatic hydrocarbons in fruits and vegetables: Origin, analysis, and occurrence.* Environmental Pollution, 2018. **234**: p. 96-106.
19. Lovett, A.A., et al., *PCB and PCDD/DF congeners in locally grown fruit and vegetable samples in Wales and England.* Chemosphere, 1997. **34**(5): p. 1421-1436.
20. Bruzzoniti, M.C., et al., *Extraction of polycyclic aromatic hydrocarbons and polychlorinated biphenyls from urban and olive mill wastewaters intended for reuse in agricultural irrigation.* Journal of AOAC International, 2020. **103**(2): p. 382-391.
21. Kasperbauer, M.J., J.H. Loughrin, and S.Y. Wang, *Light Reflected from Red Mulch to Ripening Strawberries Affects Aroma, Sugar and Organic Acid Concentrations.* Photochemistry and photobiology, 2001. **74**(1): p. 103-107.
22. Vane, C.H., et al., *Polycyclic aromatic hydrocarbons (PAH) and polychlorinated biphenyls (PCB) in urban soils of Greater London, UK.* Applied Geochemistry, 2014. **51**: p. 303-314.
23. De Carlo, R.M., et al., *Evaluation of different QuEChERS procedures for the recovery of selected drugs and herbicides from soil using LC coupled with UV and pulsed amperometry for their detection.* Analytical and Bioanalytical Chemistry, 2015. **407**(4): p. 1217-1229.
24. United States of Pharmacopoeia 38 NF 33, *United States Pharmacopeial Convention,General chapter <621>, Chromatography*. 2015. p. 424-434.
25. Brunel, D., et al., *Spectroscopic studies on aminopropyl-containing micelle templated silicas. Comparison of grafted and co-condensation routes*, in *Studies in Surface Science and Catalysis*, R. Aiello, G. Giordano, and F. Testa, Editors. 2002, Elsevier. p. 1395-1402.
26. Onida, B., et al., *The surface of ordered mesoporous benzene - Silica hybrid material: An infrared and ab initio molecular modeling study.* Journal of Physical Chemistry B, 2005. **109**(24): p. 11961-11966.
27. Ye M., Y.Y., Trinh A., *Analysis of Multi-Pesticide Residues in Vegetables, Food, and Fruits by SPE/GC-MS.* available at https://www.sigmaaldrich.com/content/dam/sigma-aldrich/docs/Supelco/Posters/t405020h.pdf last accessed September 2020.
28. Shimelis, O., et al., *Evaluation of a solid-phase extraction dual-layer carbon/primary secondary amine for clean-up of fatty acid matrix components from food extracts in multiresidue pesticide analysis.* Journal of Chromatography A, 2007. **1165**(1): p. 18-25.
29. Plössl, F., M. Giera, and F. Bracher, *Multiresidue analytical method using dispersive solid-phase extraction and gas chromatography/ion trap mass spectrometry to determine pharmaceuticals in whole blood.* Journal of Chromatography A, 2006. **1135**(1): p. 19-26.
30. Orso, D., et al., *Multiresidue Determination of Pesticide Residues in Honey by Modified QuEChERS Method and Gas Chromatography with Electron Capture Detection.* Journal of the Brazilian Chemical Society, 2014. **25**.
31. Ling, C., et al., *High adsorption of sulfamethoxazole by an amine-modified polystyrene–divinylbenzene resin and its mechanistic insight.* Environmental science & technology, 2016. **50**(18): p. 10015-10023.
32. Wells, G., H. Prest, and C.W. Russ IV, *Why use signal-to-noise as a measure of MS performance when it is often meaningless? .* Technical Overview, Agilent

Technologies, 2011: p. available at https://www.google.com/url?sa=t&rct=j&q=&esrc=s&source=web&cd=&cad=rja&uact=8&ved=2ahUKEwiN_76uuJPuAhVPCuwKHY_cDTUQFjABegQIBxAC&url=https%3A%2F%2Fwww.agilent.com%2Fcs%2Flibrary%2Ftechnicaloverviews%2Fpublic%2F5990-8341EN.pdf&usg=AOvVaw35pJ2yCwYqtgeugpe9ySZj.

33. Bérubé, J. and C. Wu, *Signal-to-noise ratio and related measures in parameter design optimization: an overview.* Sankhyā: The Indian Journal of Statistics, Series B, 2000: p. 417-432.
34. Rivoira, L., et al., *Simple SPE–HPLC determination of some common drugs and herbicides of environmental concern by pulsed amperometry.* Talanta, 2015. **131**: p. 205-212.
35. Renai, L., et al., *Productivity and nutritional and nutraceutical value of strawberry fruits (Fragaria x ananassa Duch.) cultivated under irrigation with treated wastewaters.* Journal of the Science of Food and Agriculture, 2020. **in press**.
36. Rivera, C. and R. Rodríguez, *Horwitz equation as quality benchmark in ISO/IEC 17025 testing laboratory.* Private communication, 2014.
37. Sadowska-Rociek, A., M. Surma, and E. Cieślik, *Comparison of different modifications on QuEChERS sample preparation method for PAHs determination in black, green, red and white tea.* Environmental Science and Pollution Research, 2014. **21**(2): p. 1326-1338.
38. Dachs, J. and J.M. Bayona, *Large volume preconcentration of dissolved hydrocarbons and polychlorinated biphenyls from seawater. Intercomparison between C18 disks and XAD-2 column.* Chemosphere, 1997. **35**(8): p. 1669-1679.
39. Sato, T., T. Tsuneda, and K. Hirao, *A density-functional study on π-aromatic interaction: Benzene dimer and naphthalene dimer.* The Journal of chemical physics, 2005. **123**(10): p. 104307.
40. Yang, X., et al., *Molecular simulation of naphthalene, phenanthrene, and pyrene adsorption on MCM-41.* International journal of molecular sciences, 2019. **20**(3): p. 665.
41. Harker, K.N. and J.T. O'Donovan, *Recent weed control, weed management, and integrated weed management.* Weed Technology, 2013. **27**(1): p. 1-11.
42. Carvalho, F.P., *Pesticides, environment, and food safety.* Food and Energy Security, 2017. **6**(2): p. 48-60.
43. Huang, B., et al., *Advances in targeted pesticides with environmentally responsive controlled release by nanotechnology.* Nanomaterials, 2018. **8**(2): p. 102.
44. Egan, J.F., et al., *2, 4-dichlorophenoxyacetic acid (2, 4-D)–resistant crops and the potential for evolution of 2, 4-D–resistant weeds.* Proceedings of the National Academy of Sciences, 2011. **108**(11): p. E37-E37.
45. Powles, S.B. and J.M. Matthews, *Multiple herbicide resistance in annual ryegrass (Lolium rigidum): a driving force for the adoption of integrated weed management*, in *Resistance'91: Achievements and Developments in Combating Pesticide Resistance*. 1992, Springer. p. 75-87.
46. Rose, M.T., et al., *Impact of herbicides on soil biology and function.* Advances in agronomy, 2016. **136**: p. 133-220.
47. Korres, N.E., *Herbicide effects on humans: exposure, short and long-term effects and occupational hygiene.* Weed control: sustainability, hazards, and risks in cropping systems worldwide. CRC Press, Taylor Francis Group, Boca Raton, FL, 2018. **14**.
48. Da Silva Pinto, B.G., et al., *Occupational exposure to pesticides: Genetic danger to farmworkers and manufacturing workers–A meta-analytical review.* Science of The Total Environment, 2020: p. 141382.
49. International Labour Organization (ILO) *Agriculture: a hazardous work*. 2015.

50. Bajwa, A.A., G. Mahajan, and B.S. Chauhan, *Nonconventional weed management strategies for modern agriculture.* Weed science, 2015. **63**(4): p. 723-747.
51. Chauhan, B.S., *Weed ecology and weed management strategies for dry-seeded rice in Asia.* Weed Technology, 2012. **26**(1): p. 1-13.
52. Wang, X.-x., et al., *The feasible study on the reclamation of the glyphosate neutralization liquor by bipolar membrane electrodialysis.* Desalination, 2012. **300**: p. 58-63.
53. Duke, S.O. and S.B. Powles, *Glyphosate: a once-in-a-century herbicide.* Pest Management Science: formerly Pesticide Science, 2008. **64**(4): p. 319-325.
54. International Agency for Research on Cancer (IARC), *IARC Monographs Volume 112: evaluation of five organophosphate insecticides and herbicides*. 2015.
55. Saunders, L.E. and R. Pezeshki, *Glyphosate in runoff waters and in the root-zone: a review.* Toxics, 2015. **3**(4): p. 462-480.
56. Zaller, J.G., et al., *Glyphosate herbicide affects belowground interactions between earthworms and symbiotic mycorrhizal fungi in a model ecosystem.* Scientific reports, 2014. **4**(1): p. 1-8.
57. European Commission, *Glyphosate report. Available at: https://ec.europa.eu/food/plant/pesticides/glyphosate_en*. 2019.
58. Ministero della Salute (Italia), *Decreto 9 agosto 2016: Revoca di autorizzazioni all'immissione in commercio e modifica delle condizioni d'impiego di prodotti fitosanitari contenenti la sostanza attiva «glifosate», in attuazione del regolamento di esecuzione (UE) 2016/1313 della Commissione del 1° agosto 2016*. 2016.
59. Istituto Superiore per la Protezione e la Ricerca Ambientale (ISPRA), *Rapporto nazionale pesticidi nelle acque. Dati 2017 - 2018*. 2020.
60. Campos, E.V.R., J.L. de Oliveira, and L.F. Fraceto, *Applications of controlled release systems for fungicides, herbicides, acaricides, nutrients, and plant growth hormones: a review.* Advanced Science, Engineering and Medicine, 2014. **6**(4): p. 373-387.
61. Qian, K., et al., *Release kinetics of tebuconazole from porous hollow silica nanospheres prepared by miniemulsion method.* Microporous and mesoporous materials, 2013. **169**: p. 1-6.
62. Grillo, R., et al., *Poly (ε-caprolactone) nanocapsules as carrier systems for herbicides: Physico-chemical characterization and genotoxicity evaluation.* Journal of hazardous materials, 2012. **231**: p. 1-9.
63. Paradelo, M., et al., *Influence of pore water velocity on the release of carbofuran and fenamiphos from commercial granulates embedded in a porous matrix.* Journal of contaminant hydrology, 2012. **142**: p. 75-81.
64. Zhao, J., et al., *Water dispersible avermectin-layered double hydroxide nanocomposites modified with sodium dodecyl sulfate.* Applied clay science, 2011. **51**(4): p. 460-466.
65. de Campos Bernardi, A.C., et al., *Brazilian sedimentary zeolite use in agriculture.* Microporous and Mesoporous Materials, 2013. **167**: p. 16-21.
66. Chen, C., et al., *Fabrication of light-responsively controlled-release herbicide using a nanocomposite.* Chemical Engineering Journal, 2018. **349**: p. 101-110.
67. Meng, J., et al., *Novel layered pesticide slow/controlled release materials—supramolecular structure and slow release property of glyphosate intercalated layered double hydroxides.* Chinese Science Bulletin, 2005. **50**(8): p. 745-751.
68. Kowalska, M., H. Güler, and D.L. Cocke, *Interactions of clay minerals with organic pollutants.* Science of the total environment, 1994. **141**(1-3): p. 223-240.
69. Bruzzoniti, M.C., et al., *Novel insights in Al-MCM-41 precursor as adsorbent for regulated haloacetic acids and nitrate from water.* Environmental Science and Pollution Research, 2012. **19**(9): p. 4176-4183.

70. Biswas, B., J. Labille, and B. Prelot, *Clays and modified clays in remediating environmental pollutants*. 2020, Springer.
71. Bruzzoniti, M.C., et al., *Adsorption of bentazone herbicide onto mesoporous silica: application to environmental water purification.* Environmental Science and Pollution Research, 2016. **23**(6): p. 5399-5409.
72. Shrivastava, A. and V. Gupta, *Methods for the determination of limit of detection and limit of quantitation of the analytical methods.* Chronicles of young scientists, 2011. **2**(1): p. 21-21.
73. Krijn de Jong, *Synthesis of solid catalysts*. 2009: John Wiley & Sons.
74. Kim, S., et al., *PubChem in 2021: new data content and improved web interfaces.* Nucleic Acids Research, 2021. **49**(D1): p. D1388-D1395.
75. Huayao, C., et al., *Highly efficient alginate sodium encapsulated chlorpyrifos/copper (II) Schiff base mesoporous silica sustained release system with pH and ion response for pesticide delivery.* RSC advances, 2016. **6**(115): p. 114714-114721.
76. Lin, G., et al., *Preparation of pH-responsive avermectin/feather keratin-hyaluronic acid with anti-UV and sustained-release properties.* Colloids and Surfaces B: Biointerfaces, 2019. **175**: p. 291-299.
77. Baveja, S., K.R. Rao, and K.P. Devi, *Zero-order release hydrophilic matrix tablets of β-adrenergic blockers.* International journal of pharmaceutics, 1987. **39**(1-2): p. 39-45.
78. Lagergren, S.K., *About the theory of so-called adsorption of soluble substances.* Sven. Vetenskapsakad. Handingarl, 1898. **24**: p. 1-39.
79. Ritger, P.L. and N.A. Peppas, *A simple equation for description of solute release I. Fickian and non-fickian release from non-swellable devices in the form of slabs, spheres, cylinders or discs.* Journal of controlled release, 1987. **5**(1): p. 23-36.
80. Zhang, P., et al., *Diffusion-controlled drug release from the mesoporous magnesium carbonate Upsalite®.* Journal of pharmaceutical sciences, 2016. **105**(2): p. 657-663.
81. Olejnik, A., et al., *Physico-chemical characterization of formulations containing endomorphin-2 derivatives.* Amino acids, 2017. **49**(10): p. 1719-1731.
82. Schulten, H.R., P. Leinweber, and C. Sorge, *Composition of organic matter in particle-size fractions of an agricultural soil.* Journal of soil science, 1993. **44**(4): p. 677-691.
83. Gurikov, P. and I. Smirnova, *Amorphization of drugs by adsorptive precipitation from supercritical solutions: A review.* The Journal of Supercritical Fluids, 2018. **132**: p. 105-125.
84. Gu, J., et al., *A new strategy to incorporate high density gold nanowires into the channels of mesoporous silica thin films by electroless deposition.* Solid state sciences, 2004. **6**(7): p. 747-752.
85. Khoury, G.A., et al., *Glyphosate adsorption on montmorillonite: An experimental and theoretical study of surface complexes.* Applied Clay Science, 2010. **50**(2): p. 167-175.
86. Morillo, E., T. Undabeytia, and C. Maqueda, *Adsorption of glyphosate on the clay mineral montmorillonite: effect of Cu (II) in solution and adsorbed on the mineral.* Environmental science & technology, 1997. **31**(12): p. 3588-3592.
87. Gérard, F., *Clay minerals, iron/aluminum oxides, and their contribution to phosphate sorption in soils—A myth revisited.* Geoderma, 2016. **262**: p. 213-226.
88. Purgel, M., et al., *Glyphosate complexation to aluminium (III). An equilibrium and structural study in solution using potentiometry, multinuclear NMR, ATR–FTIR, ESI-MS and DFT calculations.* Journal of Inorganic Biochemistry, 2009. **103**(11): p. 1426-1438.
89. Siepmann, J., R.A. Siegel, and M.J. Rathbone, *Fundamentals and applications of controlled release drug delivery*. Vol. 3. 2012: Springer.

90. Casiday, R. and R. Frey. *Acid Rain: Inorganic Reactions Experiment*. 1998; Available from: http://www.chemistry.wustl.edu/~edudev/LabTutorials/Water/FreshWater/acidrain.html.
91. Sakurai, K., A. Teshima, and K. Kyuma, *Changes in zero point of charge (ZPC), specific surface area (SSA), and cation exchange capacity (CEC) of kaolinite and montmorillonite, and strongly weathered soils caused by Fe and Al coatings.* Soil science and plant nutrition, 1990. **36**(1): p. 73-81.
92. Kokunešoski, M., et al., *Synthesis and surface characterization of ordered mesoporous silica SBA-15.* Materials Chemistry and Physics, 2010. **124**(2-3): p. 1248-1252.
93. Houba, V., et al., *Soil analysis procedures using 0.01 M calcium chloride as extraction reagent.* Communications in soil science and plant analysis, 2000. **31**(9-10): p. 1299-1396.
94. Celis, R., et al., *Inorganic and organic clays as carriers for controlled release of the herbicide hexazinone.* Journal of Agricultural and Food Chemistry, 2002. **50**(8): p. 2324-2330.

Ringraziamenti

Il mio primo ringraziamento va alla professoressa Bruzzoniti per l'aiuto, il sostegno e l'incoraggiamento che mi hanno permesso di crescere sia in ambito scientifico che personale. Ringrazio Luca, che è stato un importante compagno di viaggio e un amico in questi anni trascorsi insieme a confrontarci e a collaborare al meglio per tutti i traguardi che abbiamo raggiunto insieme. Senza di voi non avrei mai avuto la possibilità di migliorare, crescere e diventare una persona migliore. Siete e sarete sempre la mia seconda famiglia.

Il grazie più grande ai miei genitori, mia sorella e la nonna per avermi sopportato e supportato in tutti questi anni di studio. A mamma che, nonostante le difficoltà di questi anni, mi ha sempre incoraggiato a dare il meglio; a papà e Stefania, che oggi ci guardano da lassù, ma che sono sicuro che siano sempre con me e che mi spronino ad essere una persona migliore.

Un ringraziamento a tutte le persone del secondo piano, Mery, Agnese, Ornella, Paolo con cui ho trascorso tante giornate, con cui mi sono confrontato e divertito, e che, non in ultimo, mi sono stati sempre vicino nelle difficoltà. Ringrazio anche tutti i tesisti e i colleghi per l'amicizia e per i momenti trascorsi insieme che mi hanno allietato le giornate.

Ringrazio infine con affetto tutti i miei amici che mi sono stati vicino e che mi hanno supportato ed ascoltato nei momenti difficili.